IntechOpen

Smart Microgrids

Edited by Majid Nayeripour, Eberhard Waffenschmidt and Mostafa Kheshti

SMART MICROGRIDS

Edited by **Majid Nayeripour, Eberhard Waffenschmidt** and **Mostafa Kheshti**

Smart Microgrids
http://dx.doi.org/10.5772/intechopen.72092
Edited by Majid Nayeripour, Eberhard Waffenschmidt and Mostafa Kheshti

Contributors

Ibrahim Aldaouab, Nowshad Amin, Mohammad Shakeri, Lucian Pîslaru-Dănescu, Laurentiu Constantin Lipan, Bharath Kumar T, Ramamoorty M, Chandra Sekhar O, Andreea El-Leathey, Andrea Schroeder, Christoph Kahlen, Mariapia Martino, Antonis Papanikolaou, César Angeles-Camacho, Fernanda Alvarez-Mendoza, Peder Bacher, Henrik Madsen

Notice

First published in London, United Kingdom, 2018 by IntechOpen
eBook (PDF) Published by IntechOpen, 2019
IntechOpen is the global imprint of INTECHOPEN LIMITED, registered in England and Wales, registration number: 11086078, The Shard, 25th floor, 32 London Bridge Street
London, SE19SG – United Kingdom
Printed in Croatia

British Library Cataloguing-in-Publication Data
A catalogue record for this book is available from the British Library

Additional hard and PDF copies can be obtained from orders@intechopen.com

Smart Microgrids
Edited by Majid Nayeripour, Eberhard Waffenschmidt and Mostafa Kheshti

p. cm.

Print ISBN 978-1-78923-458-9

Online ISBN 978-1-78923-459-6

eBook (PDF) ISBN 978-1-83881-653-7

Meet the editors

Majid Nayeripour: After an 8-year industrial experience and academic working in electrical engineering and renewable energy field, Majid Nayeripour was promoted to a full professor in the area of microgrid in 2016. He received the Sabbatical Award from the Shiraz University of Technology, Iran, and was invited to the Cologne University of Applied Science, Germany, in January 2016. During his research at this university, he gained new experiences about the problems relating to the high-penetration level of distributed generations and 100% renewable energy in Germany, and he received the Fellowship Program Award for an experienced researcher from the Alexander von Humboldt (AvH) Foundation in 2017. Currently, he is working at the Cologne University of Applied Science and is involved in the research on control and dynamic investigation of interconnected microgrids. He has published more than 120 journal and conference papers and 4 books and supervised more than 10 research projects.

Eberhard Waffenschmidt studied Electrical Engineering at the Technical University (RWTH) in Aachen, where he received his PhD degree. Between 1995 and 2011, he was employed at the Philips Research as a senior scientist. Since 2011, he has been a professor of Electrical Power Grids at TH-Köln (Cologne University of Applied Science). Furthermore, he is a chairman of the Solarenergie Förderverein Deutschland e.V. (SFV, German Association for the Promotion of Solar Power). His special interest is identifying and removing the obstacles on the way to a 100% use of renewable energy.

Mostafa Kheshti, born in Iran, received his BSc degree in Control Engineering from the Shiraz University of Technology, Iran, and worked at the Regional Dispatching Center of Fars Regional Electric Company. As a distinguished elite engineer, he was invited to join the School of Electrical Engineering at the Xi'an Jiaotong University, China, in 2011 where he received his MSc and PhD degrees with highest honors and full scholarships in 2013 and 2017, respectively. He joined the Shandong University afterward where he currently works as an associate professor. His research interests include stability control and optimization of the renewable energy integrated power grid with intelligent methods. He is a book editor of IntechOpen publications as well as the advisory panel of Elsevier.

Contents

Preface

Emerging from a conventional power system to a more evolving dynamical system in which renewable energy sources play major roles, comes with benefits of sustainable and clean power generation in the form of smart grids. However, the intermittency of these resources imposes uncertainty and complexity to different layers of the system. As the continuity of power supply to the end-users is of significant importance, plenty of research related to the design of microgrids, energy management, and strategies is required to achieve a reliable power supply.

This book aims to present the recent materials related to the smart microgrids and the management of intermittent renewable energy sources that organized into seven chapters.

Chapter 1 studies the optimal sizing and management of different microgrid configurations, including solar panels, wind turbines, and battery energy storage systems.

Chapter 2 presents an energy management system with several approaches to overcome intermittency and create a semi-dispatchable generation supply in a power system with a small wind turbine, solar panels, fuel cells, and a hydrogen storage system.

Chapter 3 develops a LabVIEW design and testing of an energy management system for the interconnected or islanded operation of a microgrid to the public electric grid.

Chapter 4 works on a new strategy of a home energy management system in a smart grid environment to transform ordinary premises to a smart house to be energy efficient by simply rescheduling operation time of the appliances at home.

Chapter 5 presents the unconventional backup structures in low-voltage smart microgrids and switching to a backup power supply to maintain the continuous power supply to the loads.

Chapter 6 focuses on composite system reliability assessment where reliability modeling of power system components is analyzed by the node elimination method and modified minimal cutset method that would be useful in the planning and operation of larger power systems.

Chapter 7 introduces the European research project called PLANET, which will aid different energy networks to leverage innovative energy conversion in alternative carriers and storage technologies to explore, identify, evaluate, and quantitatively assess optimal grid planning and management strategies for future energy scenarios that target full energy system decarbonization.

In the call for the chapters in this book, we were overwhelmed with several high-quality manuscripts. However, to make the quality and clarity of the book easy to follow for different readers, only a handful was selected to briefly present the recent research on the smart

microgrids. We therefore would like to thank all the authors who participated in writing this book and sharing their latest findings to the readers and researchers.

We would also like to thank the team at IntechOpen for their continuous support on this book, and special thanks go to Ms. Iva Lipović, the Publishing Process Manager, for her kind support and patience to coordinate the publishing process of this book.

Prof. Majid Nayeripour and Prof. Eberhard Waffenschmidt
Cologne University of Applied Science
Cologne, Germany

Assoc. Prof. Mostafa Kheshti
School of Electrical Engineering
Shandong University, China

Chapter 1

Renewable Energy Microgrid Design for Shared Loads

Ibrahim Aldaouab and Malcolm Daniels

Additional information is available at the end of the chapter

http://dx.doi.org/10.5772/intechopen.75980

Abstract

Renewable energy resource (RER) energy systems are becoming more cost-effective and this work investigates the effect of shared load on the optimal sizing of a renewable energy resource (RER) microgrid. The RER system consists of solar panels, wind turbines, battery storage, and a backup diesel generator, and it is isolated from conventional grid power. The building contains a restaurant and 12 residential apartments. Historical meter readings and restaurant modeling represent the apartments and restaurant, respectively. Weather data determines hourly RER power, and a dispatching algorithm predicts power flows between system elements. A genetic algorithm approach minimizes total annual cost over the number of PV and turbines, battery capacity, and generator size, with a constraint on the renewable penetration. Results indicate that load-mixing serves to reduce cost, and the reduction is largest if the diesel backup is removed from the system. This cost is optimized with a combination of particle swarm optimization with genetic-algorithm approach minimizes total annual cost over the number of solar panels and micro-turbines, battery capacity, and diesel generator size, with a constraint on the renewable penetration. Results indicate that load-mixing serves to reduce cost, and the reduction is largest if the diesel backup is removed from the system.

Keywords: renewable energy system, load profile, PV, wind turbine, battery, loads shared

1. Introduction

1.1. Distributed electricity generation

Electrical power is historically generated at a few large power stations and transmitted over long distances to end users. However, in recent years, there is an increase in decentralized or distributed electric power generation, where the power is produced and used at the same

location [1]. Often, this decentralized power is produced with renewable energy technologies, such as wind and solar, due to the decreasing costs of these technologies [1].

There are many advantages to a power distribution system that relies on many small generation facilities rather than a few large power plants. Transmitting power over long distances is inefficient and requires expensive infrastructure. Smaller facilities that are close to where the power is used can provide higher quality power, with fewer blackouts and a more steady voltage. Since many of the small generating stations are natural gas powered or powered with renewable sources, there is less pollution than large plants that often run on coal. Finally, a distributed energy generation model is more secure than a centralized model.

The challenge to expanding distributed electricity generation is partly economic and partly technical. The capital costs for building a small-scale facility is large relative to the power it can produce. Many renewable technologies produce irregular power that varies with the weather, and this power is difficult to incorporate into the grid [2].

1.2. Motivation for expanding distributed generation

Increasing attention is given to designs for integrating renewable energy with traditional power to satisfy electrical loads from individual or multiple buildings. Research in this area is driven by several factors. First, costs for photovoltaic (PV) panels and wind micro-turbines (MT) are steadily dropping, along with battery energy storage systems (BESS). For example, the reported cost of installed solar PV systems fell by an average of 6–12% per year from 1998 to 2014, depending on the scale of the system [3]. Similarly, the price of wind power is dropping significantly, as more turbines are brought online, and currently about 5% of the energy requirements for the United States is supplied through wind power. In the previous decade, more than two-thirds of all wind installations in the United States have been small- or mid-sized wind turbines [4]. Battery storage has also dropped to a level of about $100 per kWh of capacity [5]. Another motivating factor is the various grid-pricing structures available, which often create an incentive for using less power at certain times of the day or making the overall electrical demand more uniform. Microgrids can achieve this, reducing the cost of grid electrical power.

In addition to economic motivation, there is increased recognition of the damage to the environment due to CO_2 emission from traditional power generation. The benefit of using RER microgrids for buildings is the potential reduction in carbon and other pollutants because buildings consume over 40% of end-use energy worldwide [6]. In order to address the problem of efficient building energy use and to reduce pollution in buildings, the United States has set a zero net energy target on 50% of commercial buildings by 2040 and on all commercial buildings by 2050 [6]. A zero net energy building is one that produces some renewable energy on-site, such that the building sometimes uses grid power and at other times produces extra renewable power. The average amount of renewable power produced annually is the same as the building's average annual consumption.

Finally, another advantage for microgrids is the improved reliability that they offer. There are multiple sources of power in a microgrid, such that there is less chance of a complete power outage.

1.3. Problem statement

Several studies consider the optimal design and sizing of the RER system for residential or commercial building individually [7, 8]. The RER microgrid design in this work is applied to a mixed commercial and residential building. Residential loads peak in the evening and early morning times, whereas commercial loads peak in the daytime. A shared residential and commercial load therefore has the potential to be more uniform than one or the other alone. A uniform load is easier to efficiently match to the RER supply, and it may also help lower the grid power costs. This chapter studies the effect of combining loads for an RER microgrid on the full cost of the microgrid. The size of the RER system partly depends on the shape of the load profile, such that irregular profiles require larger RER systems than smooth profiles. For example, an irregular load profile requires more energy storage to satisfy peak loads. The concept explored in this work is the benefit of combining different realistic load profiles in order to develop a total profile that is smoother and less costly to satisfy with an RER microgrid.

2. Building energy demand model

The residential load profile used for this work is generated from measured aggregate hourly consumption data for 12 apartments in a residential building in Columbus, Ohio [8]. The apartments are on the third floor of a three-story building, which means that they will have higher heating loads in the winter and cooling loads in the summer. This choice represents a worst-case scenario in terms of the peaks in the residential load. One year of hourly metered power use for these apartments is available, starting at 12 am on Sunday, June 9, 2013. These apartments use electricity for hot water, heating, and cooling. The hourly commercial load profile is synthesized from typical load profiles for commercial kitchens [9]. The average demand from the commercial load is selected to be nearly the same as the average demand from the 12 residential apartments.

2.1. Historical residential demand

Figure 1 illustrates the weekly average for the aggregate residential load data. Each day of the week, there is a peak in the morning at about 8 am, representing the electricity consumption as residents prepare for the workday. At the end of the day, at about 8 pm, there is a larger peak as residents return home for dinner and other electricity-consuming activities.

To determine the temperature-dependent component of the residential data, a piecewise linear regression is used. Each week, aggregate residential consumption data are averaged to create 52 single values. The same is done for the temperature. **Figure 2** shows a plot of the average weekly power versus average weekly outdoor temperature. The fit shown in **Figure 2** has five parameters as follows: a heating slope (HS), cooling slope (CS), heating temperature (HT), cooling temperature (CT), and baseline (B) [8]. The baseline component defines the hourly expected weather independent demand. The heating and cooling slopes KW per Fahrenheit degree (kW/°F) enable respective prediction of the hourly heating and cooling demand for a typical weather year.

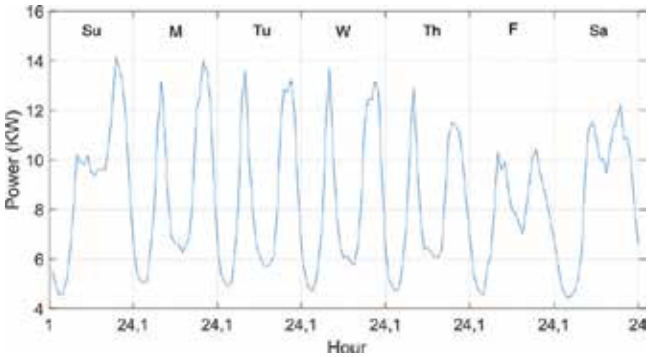

Figure 1. Weekly average aggregate residential load.

The threshold temperatures and heating/cooling slopes depend on many factors, such as building construction and size. Values for the temperature-dependent five-parameter model were calculated to be: HS = 0.16 kW/°F., CS = 0.12kW/F°, HT = 57 F°, and CT = 48 F°.

2.2. Commercial kitchen demand model

Figure 3 illustrates the weekly average baseline consumption for the commercial kitchen. The same basic profile shape is used for each day, scaled to represent the different amounts of customer traffic for each day of the week. The peak consumption occurs at 8 pm as the kitchen serves dinner, and there is also a peak at 1 pm for lunch. The kitchen uses power more consistently than the residential load through the afternoon hours.

2.3. Controlling load profile characteristics

In order to compare the three individual loads, the load factor (LF) is used. LF is defined as the ratio of the average per-month consumption to the peak hourly consumption for that month.

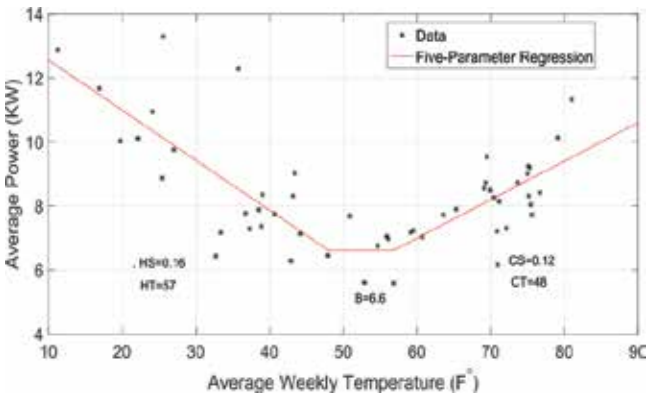

Figure 2. Temperature dependence for residential data, along with a five-parameter fit.

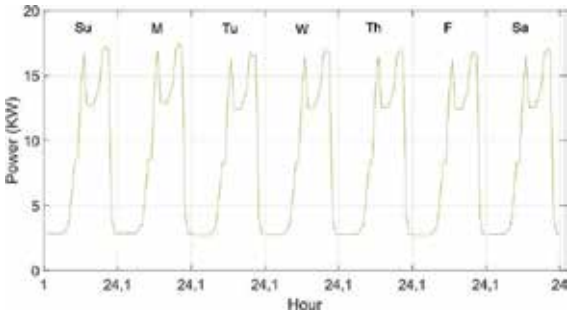

Figure 3. Weekly average commercial load (baseline).

For the data used in this study, an average yearly LF is found by averaging the 12 monthly LF values. **Figures 4** and **5** show the comparison of the monthly LF values for the three types of loads considered: residential, commercial, and combined. **Figure 4** shows the effect of combining the residential load with only the baseline commercial load. In this case, the load factor of the combined is between the residential and commercial load factors each month. **Figure 5**

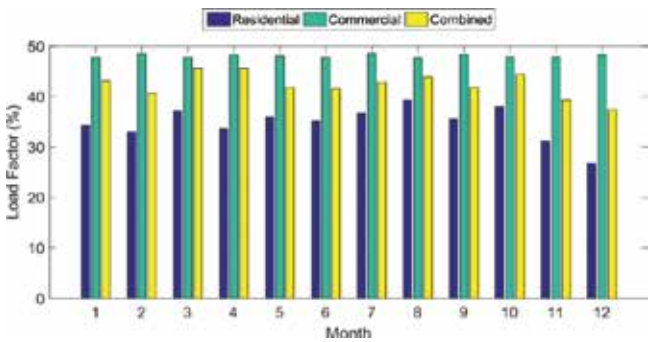

Figure 4. Comparison of monthly load factors for the three loads with no weather-dependent component.

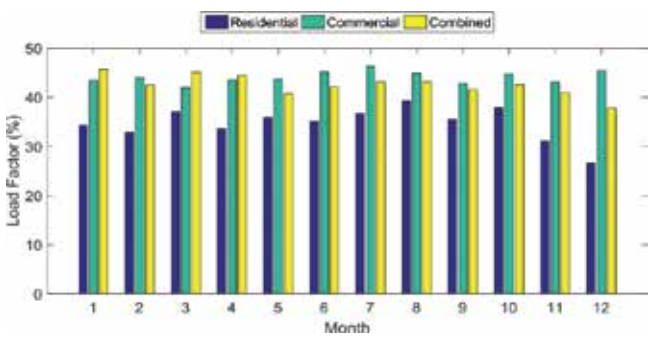

Figure 5. Comparison of monthly load factors for the three loads with weather-dependent component.

shows the effect of combining the residential load with the commercial load, where the weather-dependent load is included with the commercial load. The load factor behavior varies more in this case. The LF for the combined load is still between the LF for the residential and commercial loads, except for January, March, and April.

3. Proposed microgrid structure

The main components of the renewable energy resource (RER) microgrid examined here are solar photovoltaics (PV), micro-wind turbines (MT), and a battery energy storage system (BESS). These are utilized for electricity generation and energy storage, and they supply energy to a load that is normally satisfied with grid power alone. The microgrid is studied for two types of operating conditions. First is an isolated RER which provides all of the load power. The second system is an RER with a diesel generator backup in which the generator is activated if the RER cannot supply the full load.

For each system, the hourly power flow to or from each element of the microgrid is simulated. The capacity of each RER component is chosen to minimize the overall cost.

3.1. Isolated RER

The first type of microgrid is the isolated RER, which is shown in **Figure 6**. The RER operates independently from the local utility grid to provide all of the electricity to residential and commercial building. This system requires large battery storage to use during low wind and solar output times. The RER for the isolated mode must be large enough to produce energy to cover 100% of the building's energy needs.

3.2. RER and diesel generator

Figure 7 illustrates the second configuration and RER with a diesel generator backup. The diesel generator has the option of charging the battery, which is significantly different from the other scenarios.

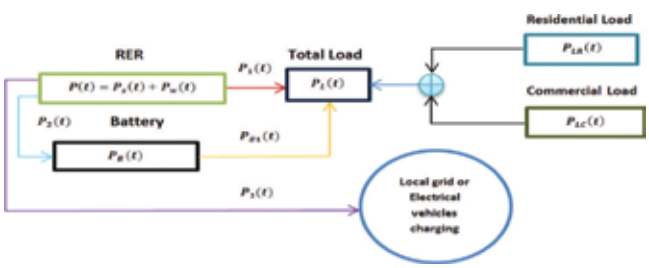

Figure 6. Isolated grid model.

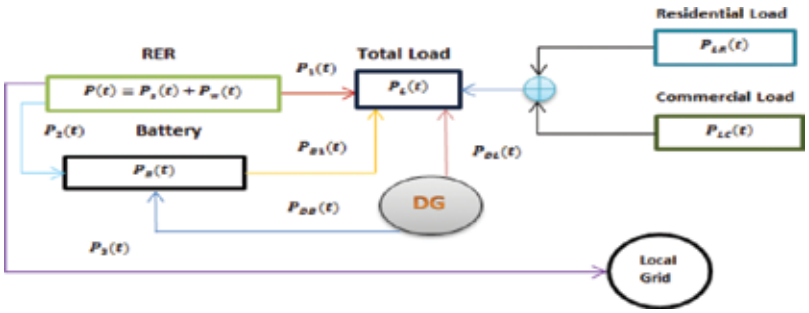

Figure 7. RER and diesel generator model.

3.3. RER and battery modeling

3.3.1. Photovoltaic model

The power generated by a photovoltaic panel depends on two fundamental parameters: the solar irradiation and the ambient temperature. In order to simplify the model, the power produced by a PV panel, the following equation is used [8].

$$P_s(t) = \eta_s A_s G(t) \tag{1}$$

where η_s: Energy conversion efficiency (%), A_s: PV panel area (m^2), $G(t)$: Solar irradiation (W/m^2), and $P_s(t)$: Power generated by solar PV (W).

The solar irradiation, sampled hourly, is found from typical meteorological year (TMY) data, for Columbus, Ohio [10]. The number of solar PV panels is N_s.

3.3.2. Micro-wind turbine model

The electrical power generated by a micro-wind turbine depends on the wind speed, air density, area swept by the turbine blades, and an efficiency factor called the Betz coefficient [9]. A constant air density of 1.225 $k_g/m^3$is used, and the Betz coefficient is taken to be 59%.

$$P_w(t) = 0.5\rho A_w C_p V_w^3(t) \tag{2}$$

where ρ: Air density (k_g/m^3), A_w: Micro-turbine swept area (m^2), C_p: Betz coefficient, $V_w(t)$: Wind speed (m/s), and $P_w(t)$: Power generated by micro-turbine (W)

The wind speed, sampled hourly, is found from typical meteorological year (TMY) data, for Columbus, Ohio [10]. The number of micro-turbines is N_w.

3.3.3. Battery energy storage model

Whenever the RER output exceeds the load demand, the extra power is stored in a battery. This power is then used whenever the RER is unable to supply the load demand. The charge level of the battery is $P_B(t)$, which is restricted to be in the range of 20–80% of the battery capacity, B_{cap}(kWh).

$$0.2\,B_{cap} \le P_B(t) \le 0.8\,B_{cap} \tag{3}$$

When charging or discharging the battery, the maximum amount of energy that can be removed during a 1-hour interval is B_{HR}. This limit is expressed by the following inequality.

$$\left|P_B(t) - P_B(t-1)\right| \le B_{HR} \tag{4}$$

Both the battery capacity and the hourly charge/discharge limit are parameters for the microgrid.

For every hour in the simulation of the microgrid, there is a decision made to charge or discharge the battery. This decision is determined in part by the charge level of the battery. If the current charge level is in the range of 20–80% of B_{CAP}, then the battery can be charged or discharged. If the current charge level is less than 20% of B_{CAP}, the battery can only be charged. If the current charge level is more than 80% of B_{CAP}, the battery can only be discharged.

3.4. Diesel generator model

The diesel generator supports the microgrid by supplying power $P_{DL}(t)$ directly to the load and power $P_{DB}(t)$ to the battery. The sum of these two must be less than the maximum power output D_{max} from the generator, such that.

$$0 \le P_{DB}(t) + P_{DL}(t) \le D_{max} \tag{5}$$

The conditions for activating the generator at each hour are determined by the current load and RER output, the state of the battery's charge, and whether or not the generator was running the previous hour. If the RER and battery cannot meet the load, the generator is activated. If the generator was running the previous hour and the battery can take more charge, then the generator is allowed to run during the current hour.

4. Dynamic microgrid modeling

4.1. Isolated RER dispatch algorithm

At each hour of the simulation for the grid-isolated system illustrated in **Figure 6**, the RER power $P(t)$ is determined using the TMY data. In addition, the load $P_L(t)$ and the charge level of the battery at the previous hour $P_B(t-1)$ are known. From this information, the graph in **Figure 8** is used to determine all other quantities. The graph illustrates the process of updating these quantities each hour. The following characteristics are implemented in this graph.

- If the RER output is less than the load at a given hour, then all of the available RER output is sent to the load (i.e., no battery charging at this hour), and the battery satisfies the remainder of the load.

- If the RER output is greater than the load, then the load is completely satisfied by the RER, and no battery power is used for the load. As much charging power as possible is transmitted to the battery, if its charge level is less than the upper threshold. Any remaining power from the RER is sent back to local grid.
- There is a possibility of power outage if the combined RER and battery outputs cannot meet the load. Increasing the size of the system reduces this possibility.

4.2. Diesel generator RER dispatch algorithm

At each hour of the simulation for the RER with distributed generation (DG) system illustrated in **Figure 7**, the RER power $P(t)$ is determined using the TMY data. In addition, the load $P_L(t)$ and the charge level of the battery at the previous hour $P_B(t-1)$ are known. From this information, the graph in **Figure 9** is used to determine all other quantities and to determine when the DG is turned on/off. The graph illustrates the process of updating these quantities each hour. The following characteristics are implemented in this graph.

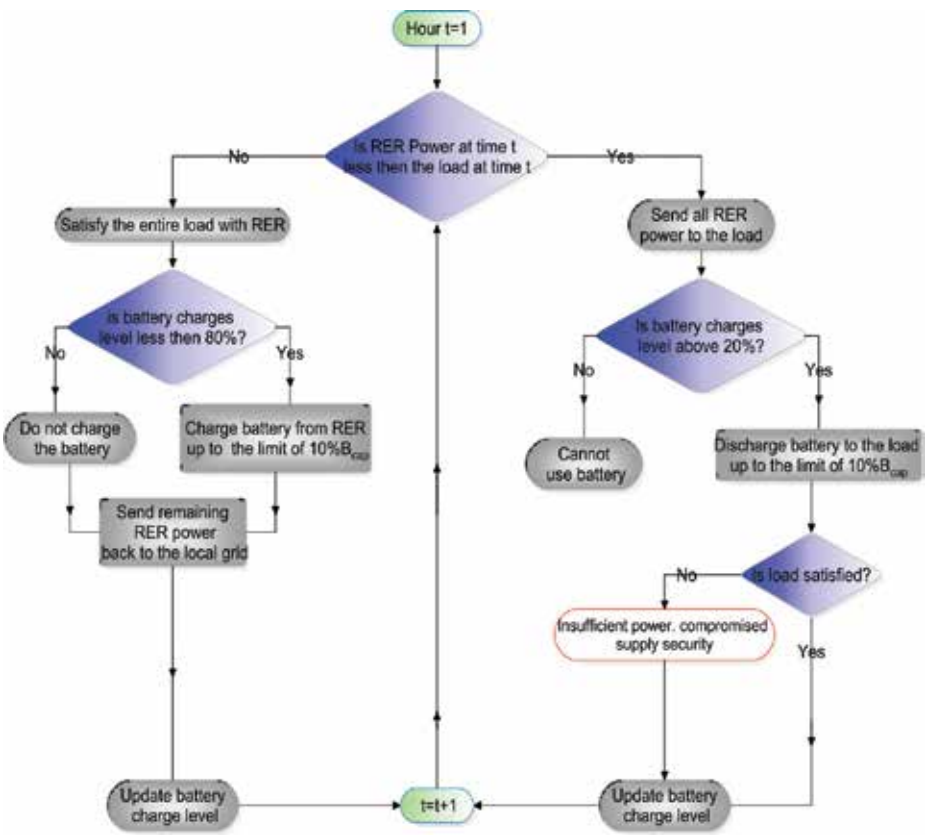

Figure 8. Isolated RER dispatch algorithm.

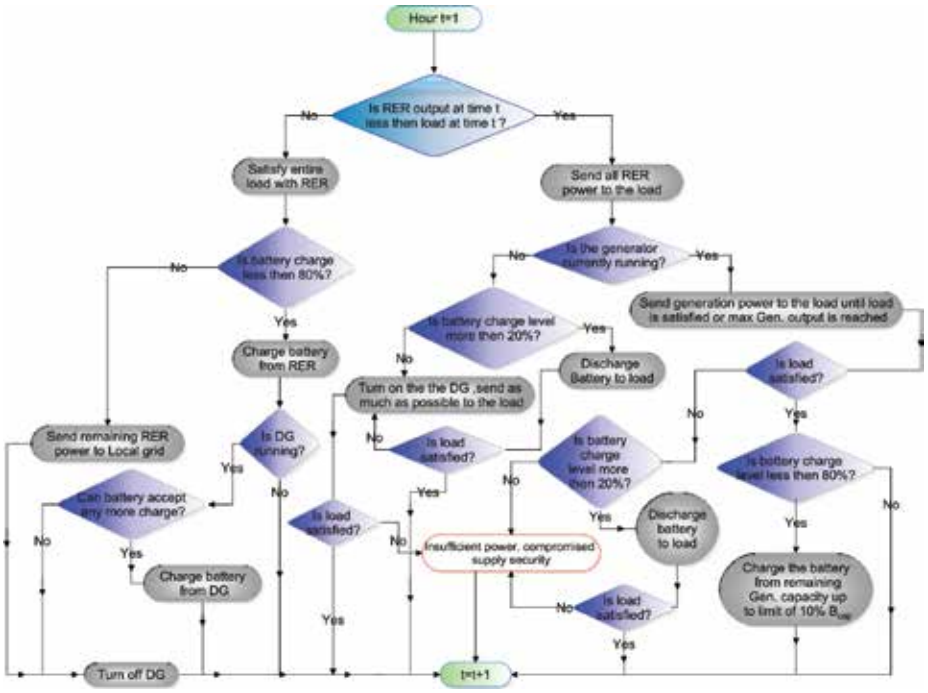

Figure 9. Diesel generator RER dispatch algorithm.

- If the RER output is less than the load at a given hour, then all of the available RER output is sent to the load (i.e., no battery charging at this hour), and as much power as possible from the battery is used to meet the load if its charge level is above the minimum threshold. If this is not sufficient to meet the load, the generator is used to make up the difference.
- If the RER output is greater than the load, then the load is completely satisfied by the RER and no battery power is used for the load. As much charging power as possible is transmitted to the battery if its charge level is less than the upper threshold. Any remaining power from the RER is sent back to the local grid.
- The generator is turned on if the combined RER and battery power cannot meet the load. If it is already running, then it will remain on until the battery is fully charged.
- There is a possibility of power outage if the combined RER, battery, and DG outputs cannot meet the load. Increasing the size of the system reduces this possibility.

5. Annual cost model

The annual cost of the system, A_{CS}, is found with the following equation.

$$A_{CS} = A_{CC} + A_{RC} + A_{OC} + A_{GC} \tag{6}$$

where A_{CC} = capital cost, A_{RC} = replacement costs, A_{FC} = fuel cost, and A_{OC} = operating costs.

Each of these categories is described in the following subsections.

5.1. Annual capital cost

The capital cost is found from the initial costs for the PV array, MT units, BESS, and DG. The PV capital cost is \$1.8 per peak watt of PV power. It is assumed that each solar panel in the array is 2 m^2 with a 20% efficiency, and that the peak radiation intensity is 1000 W/m^2. This leads to a per-panel capital cost of \$720, with N_s panels in the entire array. Each MT unit has an up-front cost, including installation, of \$22,000 (about \$2 per peak watt of wind power) [11, 12]. There are N_W of these units installed. Each kWh of BESS capacity has a cost of \$300 [11, 12], and the DG cost is approximated by a linear function of the capacity D_{max}, from \$7000 for a 5 kW capacity to \$14,000 for a 40 kW capacity, based on advertised prices [12]. The DG cost formula is therefore

$$C_{DG} = (D_{max} - 5\ \text{kW})\left(\frac{\$7000}{35\ \text{kW}}\right) + \$7000 \tag{7}$$

The total up-front capital cost is then the sum of all four terms.

$$C_{CAP} = \$720 \cdot N_s + \$22{,}000 \cdot N_W + \$300 \cdot B_{Cap} + C_{DG} \tag{8}$$

Standard amortization is applied to this capital cost, using an interest rate of $i = 6\%$and a project lifetime of $N = 20$ years. The amortization factor is.

$$CRF = \frac{i(1+i)^N}{(1+i)^N - 1} \tag{9}$$

This factor is applied to the capital cost to find the annual capital cost as.

$$A_{CC} = CRF \cdot C_{CAP} \tag{10}$$

5.2. Annual replacement cost

The PV and MT components last the full lifetime of the system, but the BESS and DG have shorter lifetimes and therefore need periodic replacement. Replacement costs are found with a sinking fund factor, which computes the amount of money that needs to be annually set aside to pay for periodic replacement of the BESS and DG. The formula for the sinking fund factor is.

$$SFF(N_L) = \frac{i}{(1+i)^{N_L} - 1} \tag{11}$$

The lifetime of the component in question is N_L and the interest rate i is the same as that used in the capital recovery factor. The BESS lifetime is 7 years, and the DG lifetime is 15 years. The annual replacement cost is therefore given by.

$$A_{RC} = \$300 \cdot B_{Cap} \cdot SFF(7) + C_{DG} \cdot SFF(15) \tag{12}$$

5.3. Annual operating costs

The only component that has significant operating costs is the DG, which requires fuel, oil for lubrication, and periodic maintenance. Each kWh of output from the DG requires 0.13 gallons of diesel fuel at a cost of $2 per gallon, with an additional maintenance cost of $0.05/kWh. The simulation produces the hourly output from the DG as $P_D(t)$, and summing this quantity gives the yearly energy output. For the entire plant lifetime, the total operating cost T_{OC} can therefore be given as follows.

$$T_{OC} = N\sum P_D(t)\left(0.13\,\frac{\text{gal}}{\text{KWh}}\,2\,\frac{\$}{\text{gal}} + 0.05\,\frac{\$}{\text{KWh}}\right) \tag{13}$$

This quantity can be amortized using the same amortization factor that was applied to the capital cost. This gives an annual operating cost of.

$$A_{OC} = T_{OC} \cdot CRF \tag{14}$$

6. Optimization problem formulation

In this section, the objective function is the total annual microgrid cost A_{CS} as described in the previous section. This total annual cost is a nonlinear function of the parameters N_s, N_w, and B_{CAP}, and evaluating this function requires execution of the dynamic model.

The nonlinear minimization is achieved with either the particle-swarm optimization (PSO) algorithm or the genetic algorithm (GA). PSO is used in situations in which no nonlinear constraints are needed, while GA is used if there are constraints.

Some of the constraints are simply bounds on the variables. The minimum values for each number cannot be negative, for example, and the upper bounds are chosen to be large enough for the RER to meet a required percentage of the load. The percentage of the annual load that is met by the wind and solar energy is called the renewable energy penetration formed with the following equation:

$$PEN = \frac{\sum\left[P_1(t) + P_2(t)\right]}{\sum L(t)} \times 100\% \tag{15}$$

where P_1 is Power from RER sources, P_2 is Power from battery, and L is total load.

The system with DG backup has its own dispatch algorithm, which behaves differently than the grid-connected. This is because the DG on/off cycling incurs a maintenance cost. To avoid this, the rules for determining when to turn on and off the DG are designed to minimize the number of DG cycles. To ensure that there are no power losses, the minimum DG size is restricted to be equal to the peak load, such that the DG is capable of supplying the entire load with no RER assistance, if necessary. A nonlinear constraint is used to enforce a minimum RER penetration. The optimization requires the GA, and it is summarized as follows:

$$\begin{gathered}\min_{N_s, N_w, B_{CAP}, D_{MAX}} A_{CS} \\ LB_S \le N_s \le UB_S \\ LB_W \le N_w \le UB_W \\ LB_B \le B_{CAP} \le UB_B \\ LB_{DG} \le D_{MAX} \le UB_{DG} \\ PEN \ge PEN_{MAX}\end{gathered} \tag{16}$$

where N_s is the number of solar panels, N_W is number of wind turbines, and B_{CAP} is battery capacity and diesel generation capacity.

The grid-isolated system with no backup is similarly optimized, except that the renewable energy penetration is naturally 100% for this system, since there is no diesel generator backup power used. A modified version of the backup code is used to model the grid-isolated system with no backup. To ensure that there are no power losses, the cost function includes a large cost penalty for each hour of power shortage. With this arrangement, there is no nonlinear constraint function, such that the PSO algorithm can be used. The optimization algorithm chooses a sufficiently large RER system in order to avoid the high cost penalty on the power losses.

7. Simulation results

The MATLAB simulation results for the optimization are presented in this section, for two versions of the microgrid: grid-isolated with no backup, and grid-isolated with diesel backup. The hourly RER power is generated in the same way for two cases, using hourly TMY profiles for solar radiation and wind speed. **Figure 10** shows an example of the RER power, for 10 wind turbines and 100 solar panels, relative to the combined commercial and residential load. The upper plot in this figure shows hourly RER power produced for the entire year, and the lower figure compares the RER power to the load for 1 week. When RER power output is greater than the load, the excess production can be passed to the battery. When the RER power is less than the load, the battery must make up the deficit completely for the grid-isolated with no backup scenario. If the backup is available, then these elements can be used in addition to the battery.

7.1. Isolated microgrid with no backup

The dynamic modeling results for the isolated microgrid with no backup are illustrated in **Figure 11**. This figure shows the hourly flows of power from the RER directly to the load, along with the power from the battery to the load. The RER and battery sizes must be large enough to meet the load each hour, and the figure illustrates that the combined RER and battery flows are equal to the load. This constraint forces the RER and battery sizes to be large enough to meet the highest demand in the year, which means that during most of the year the battery is not fully utilized. This fact is demonstrated by **Figure 12**, which shows the battery

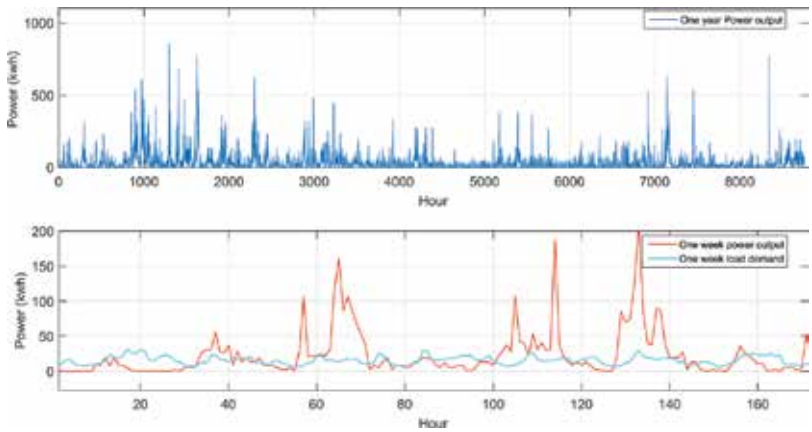

Figure 10. Combined PV and MT output for N s = 100 and N w = 10 (top). Comparison between total PV and MT output and the combined load for 1 week (bottom).

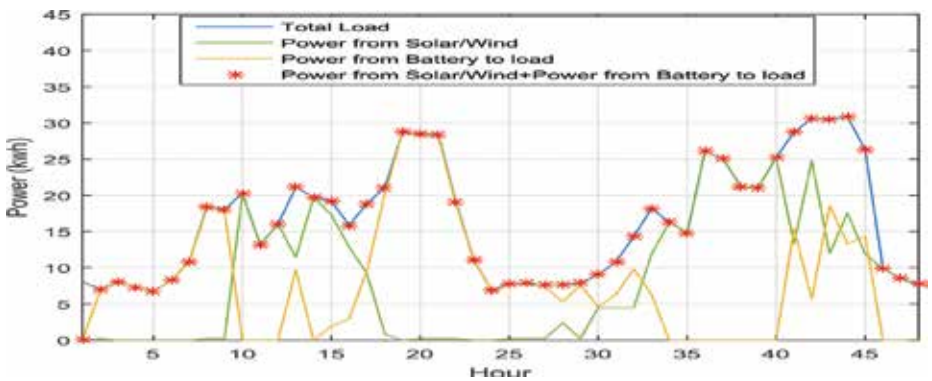

Figure 11. Power dispatching for 48 h in January (grid-isolated no backup).

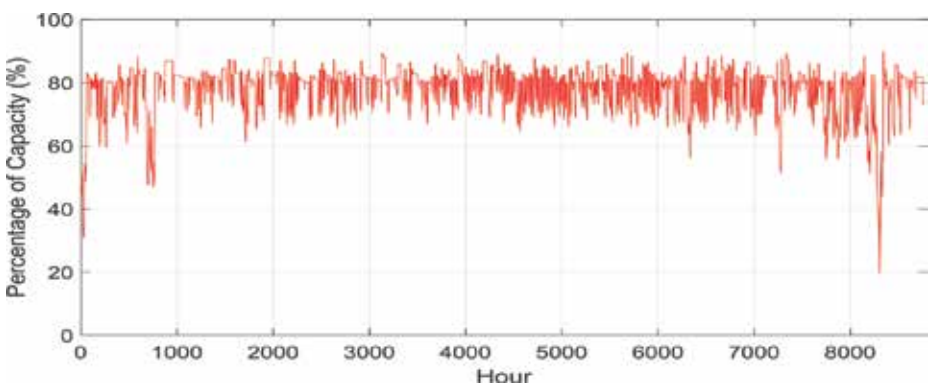

Figure 12. Battery storage level for isolated microgrid without backup.

charge level. The charge level remains high for most of the year, dipping down to low values only during a few times of peak demand.

Table 1 summarizes the results that optimize total microgrid annual cost for the residential load alone, the commercial load alone, and the mixture of the two. For comparison, the sum of the results for the residential and commercial loads is included.

When added separately, the sum of the residential and commercial load annual costs is $91,320. If these loads are mixed, however, and are satisfied by a single, larger microgrid, then the annual cost decreases to $86,000. This illustrates the cost advantage of combining the two loads into a single mixed load. Separately supplying the two loads would require more solar panels and a significantly larger battery capacity than supplying the mixed load, although the number of MTs remains the same. Because this simulation does not have diesel generator backup, the RER penetration is 100%. For each case, only about 25% of the RER output is transmitted to the load. This low percentage is due to the fact that the RER size must be chosen significantly large to meet peak yearly demand. This means that there will be many hours of energy overproduction that cannot be utilized.

7.2. Microgrid with diesel generator backup

When the grid-isolated microgrid is augmented with a DG backup system, this allows the relatively few hours of peak demand to be partially met with DG power. When the system is cost optimized, this leads to several interesting features. The size of the RER shrinks significantly, the usage of the battery becomes more regular throughout the year, and the percentage of RER power that makes it to the load nearly doubles. The trade-off for these improvements is a reduced RER penetration.

Figure 13 illustrates the power dispatching for a one-week period in January, showing the intermittent operation of the DG. The DG operates during unusually high loads, which can be seen to occur as shown in **Figure 14** when the battery energy level dips to low levels.

The DG removes the burden of meeting the peak loads from the battery, such that the energy levels in the battery can swing more uniformly over its full range throughout the year. This is illustrated in **Figure 14**, which shows the battery energy level together with the DG operation for the entire year of the simulation. The pattern in the DG clearly shows a seasonal component, such that it operates more frequently during the heating and cooling seasons.

Load		N_s	N_w	B_{CAP} **(kWh)**	**cost (×1000 $)**	**%RER output to the load**	**%RER Pen.**
No backup	Residential	388	6	621	46.20	28	100
	Commercial	428	7	487	45.12	24	100
	Sum	816	13	1108	91.32	26	100
	Mixed	790	13	959	86.00	27	100

Table 1. Optimization results for the isolated microgrid with no backup power.

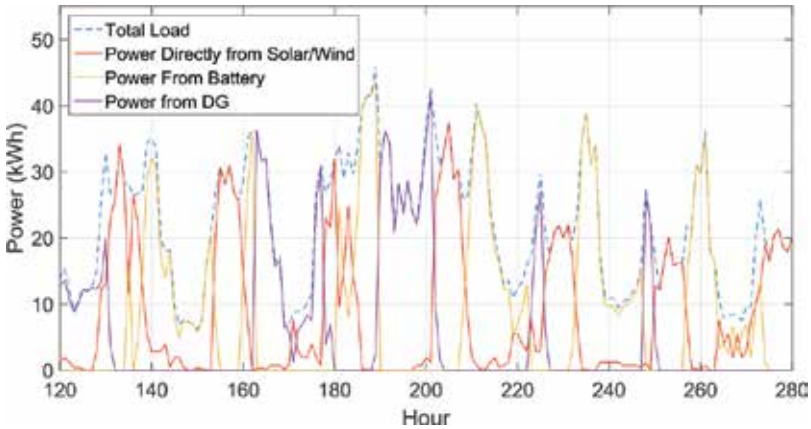

Figure 13. Power dispatching for 160 h in January (grid-isolated with DG backup).

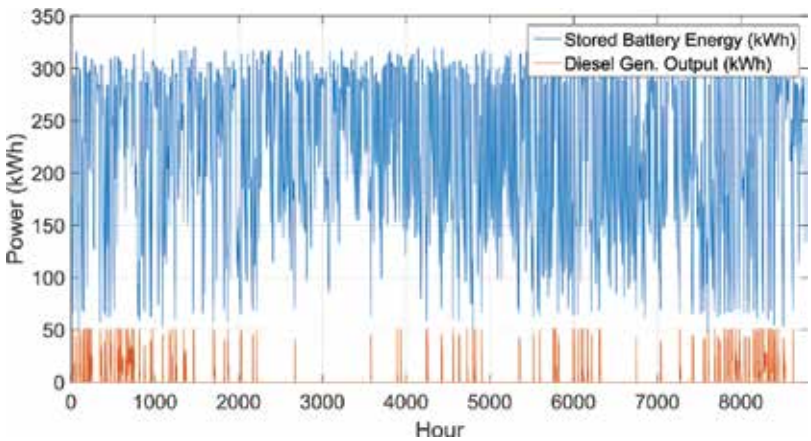

Figure 14. Battery and DG operation for microgrid with backup.

Table 2 summarizes the results that optimize total microgrid annual cost for the residential load alone, the commercial load alone, and the mixture of the two. The sum of the individual results for the residential and commercial loads is included as before, for comparison with the mixed-load results.

The largest effect of adding the DG backup to the microgrid is with the costs, which are about a fourth of the costs for the no-backup case. The optimization was made with the constraint of greater than 80% RER penetration, and it should be mentioned that the costs can be further reduced by lowering this constraint. Another large benefit in having the DG is the increase in the amount of RER power that makes it to the load, which doubles from roughly 25–50%. When comparing the sum of the costs of the residential and commercial loads to the cost of the mixed load, there is less of a difference than with the no-backup case. This indicates that the DG is reducing some of the benefit of mixing the loads.

Load	N_s	N_w	B_{CAP} (kWh)	D_{MAX} (kW)	DG on time (hr)	DG Starts	cost (×1000 $)	% RER output to the load	% RER Pen.
Residential	214	2	228	35	588	67	21.00	49	82
Commercial	244	1	215	24	756	50	20.13	47	84
Sum	458	3	443	59	1344	117	41.13	48	83
Mixed	404	1	356	50	602	83	39.68	52	82

Table 2. Optimization results for the isolated microgrid with DG backup power.

8. Summary and discussion

To illustrate the effect of renewable energy penetration, the cost optimization is constrained to produce a result with a fixed penetration. This applies to the isolated grid with diesel backup. **Figure 15** shows a plot of cost per kWh versus penetration, under the assumption that the microgrid's non-renewable power component has a price of $0.2/kWh. Plots of the average cost per kWh for all three loads (residential, commercial, and mixed) are shown, where the average cost is computed by dividing the annual cost by the total annual load. As the renewable energy penetration approaches 100%, the cost of power from the microgrid becomes rapidly more expensive, approaching the case 1 result. As the renewable energy penetration decreases to zero, the cost of power approaches the price of nonrenewable energy, $0.2/kWh. The minimum cost per kWh occurs in the range of 30–40% of penetration.

Figure 15 also shows the interaction between load mixing and renewable energy penetration. Below 70% penetration, the mixed load cost is between the residential and commercial costs. Above this threshold, however, the mixed load cost is below both the residential and commercial costs.

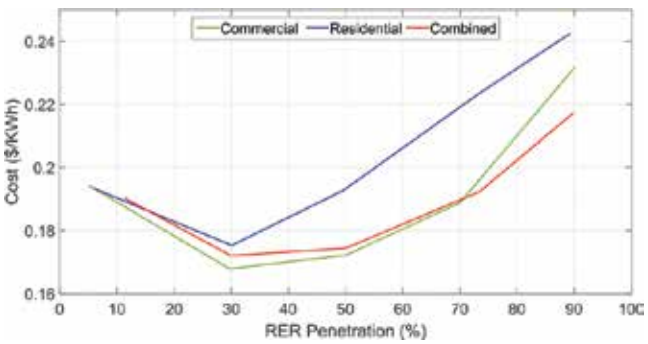

Figure 15. Average cost per kWh versus RER penetration.

9. Conclusion

The simulation results confirm that using a backup power source to support renewable energy reduces overall microgrid costs. For example, using a DG backup lowers the renewable energy penetration from 100 to 82%, but cuts the overall cost by more than a factor of two. However, the simulation results also indicate a clear benefit to mixing residential and commercial loads, such that the cost for satisfying the mixed load is less than the sum of the costs for the loads individually. Depending on the configuration, the cost for the mixed load is 3–8% less than the sum of the individual costs.

Microgrid designs for building applications involve determining the best mix of building loads for optimizing energy delivery. The result of the modeling work presented here is that combining loads allow for a measure of control over the microgrid costs. This concept is important for moving toward 100% renewable energy penetration.

Author details

Ibrahim Aldaouab* and Malcolm Daniels

*Address all correspondence to: aldaouabi1@udayton.edu

University of Dayton, Dayton, OH, USA

References

[1] Distributed Generation. Definitions, benefits, technologies & challenges. International Journal of Science and Research (IJSR). 2016;**5**(7):1941-1948

[2] How Electricity Is Delivered To Consumers. Available from: https://www.eia.gov/energyexplained/index.cfm?page=electricity_delivery [Accessed: November 7, 2017]

[3] Obi M, Bass R. Trends and challenges of grid-connected photovoltaic systems—A review. Renewable and Sustainable Energy Reviews. 2016;**58**:1082-1094

[4] Kumar Y, Ringenberg J, Depuru S, Devabhaktuni V, Lee J, Nikolaidis E, Andersen B, Afjeh A. Wind energy: Trends and enabling technologies. Renewable and Sustainable Energy Reviews. 2016;**53**:209-224

[5] Diouf B, Pode R. Potential of lithium-ion batteries in renewable energy. Renewable Energy. 2015;**76**:375-380

[6] Erdinc O, Uzunoglu M. Optimum design of hybrid renewable energy systems: Overview of different approaches. Renewable and Sustainable Energy Reviews. 2012; **16**(3):1412-1425

[7] Shaahid SM, Elhadidy MA. Technical and economic assessment of grid-independent hybrid photovoltaic–diesel–battery power systems for commercial loads in desert environments. Renewable and Sustainable Energy Reviews. 2007;**11**(8):1794-1810

[8] Aldaouab I, Daniels M, Hallinan K. Microgrid Cost Optimization for a Mixed-Use Building. In: 2017 IEEE Texas Power and Energy Conference (TPEC). 2017

[9] Aldaouab I, Daniels M. Microgrid battery and thermal storage for improved renewable penetration and curtailment. In: IEEE International Energy & Sustainability Conference (IESC). 2017

[10] NSRDB Update—TMY3: Alphabetical List by State and City. Available from: http://rredc.nrel.gov/solar/old_data/nsrdb/1991-2005/tmy3/ [Accessed: December 1, 2017]

[11] Aldaouab I, Daniels M. Renewable energy dispatch control algorithms for a mixed-use building. In: 2017 IEEE Green Energy and Smart Systems Conference IGESSC. 2017

[12] Find Quality Manufacturers, Suppliers, Exporters, Importers, Buyers, Wholesalers, Products and Trade Leads from OurAward-winning International. Available from: http://https://www.alibaba.com [Accessed: February 2, 2017]

Chapter 2

A Proposed Energy Management System to Overcome Intermittence of Hybrid Systems Based on Wind, Solar, and Fuel Cells

Maria Fernanda Alvarez Mendoza,
César Angeles-Camacho, Peder Bacher and
Henrik Madsen

Additional information is available at the end of the chapter

http://dx.doi.org/10.5772/intechopen.76760

Abstract

Distributed resource (DR) impacts voltage and frequency, and deviations out of tolerance limits are financial damage to the customers. This chapter presents an energy management system (EMS) with several approaches to overcome intermittency and create a semi-dispatchable generation supply. The EMS will work as a prosumer considering its level of dispatchability, without disturbing the frequency of the network. The power generation model is based on a small wind turbine, solar panels, PEMFC, and a hydrogen storage system. Probabilistic information concerning short-term forecast applied to wind speed and radiation is provided by individual stochastic models. The prosumer is modeled by applying time series analysis through the root mean square algorithm with forgetting factor and by using model predictive control to integrate the system. A case is presented using historic wind speed and radiation data from Mexico City and loads curves based on average households and mini-store on a daily basis.

Keywords: distributed generation, forecast, energy intermittence, model predictive control, energy storage

1. Introduction

Renewable energies are increasingly being used to generate electricity. Integration to the network, however, requires adjusting the new technologies in order to meet the established norms. Wind and photovoltaic renewable energy generation technologies are up to now the

most developed technologies, and, in both, intermittence is the major issue to attend for connection to the grid.

Studies concerning non-dispatchable generation combined with storage which focus on isolated networks are [1–3] where a DC configuration is proposed for the renewable energy integration and storage is implemented to increase the use of wind power and reduce the operation of backup systems. For stand-alone systems employing two or more technologies to generate electricity is common. Another way to deal with intermittence is by combining the wind power with forecast, which leads to focusing on ways to accurately plan how to use the generated power and how to participate in market regulation [4, 5]. The wind power uncertainty has been another research topic as in [6] where wind power forecasting uncertainty is investigated in the unit commitment. The study of levelized costs of grid-connected wind turbines with ESD [7, 8] or renewable sources implemented as DG [9], as well as the analysis of the wind energy in Germany [10], is an example of the many studies in the implementation of renewable energies.

The issue with intermittence in wind power can be decreased when a forecast model is implemented. The approach suggested in this study used an energy storage device (ESD) to stabilize the inherent variations and to balance the deviations of the actual wind power to better meet the planned network infeed. The purpose of the ESD is to reduce the intermittence with the implementation of a filter and to be able to meet the short-term planned production of the hybrid system (HS) at the distribution level. To keep a stable frequency in the network, what matters for the operation of the transmission system is not so much the variation in production but the unpredictability of the production which is the study in this work.

The major contribution, as shown in the following sections, is the ability to change the output power of the HS from a non-dispatchable to a semi-dispatchable generation giving the capability to inform the system operator to program the network dispatch. The flexibility of power dispatch depends greatly on the short-term prediction and the storage characteristics to reduce the variations of the power generated by the wind turbine.

Unlike other studies, we propose an energy management system (EMS) to overcome the frequency affectation when the hybrid system is connected as DG, by means of solely clean energies without depending in fossil power plants.

2. Implemented model philosophy

The interaction between the HS elements described in Section 4 is done through a developed model predictive control (MPC) algorithm. In consequence, the development of a wind and solar radiation forecast algorithm, alongside the modeling of the different implemented generation devices, is presented.

2.1. Forecast model

Energy forecasting is particularly meaningful when considering wind power because of dispatch planning and market operations [11]; the focus in this chapter is dispatch planning.

There are two approaches for wind speed forecasting, namely, weather-based and time series-based approaches. While the former uses hydrodynamic atmospheric models which incorporate physical phenomena such as frictional, thermal, and convective effects, the latter uses only historical wind speed data recorded at the site to build statistical models from which forecasts are derived [12].

The sample data used for the forecast was a 3-month data with a 10-min resolution (12,960 measurements) from a 1-year data recollected from Mexico City; the complete study was made for a whole year. Even though the collected measurement data covers a year, in this study only the first week of results was shown so the reader can truthfully see the behavior of the hybrid system and the output power in a clear way.

2.1.1. Autoregressive (AR) model

A stochastic model that can be extremely useful in the representation of certain practically occurring series is the autoregressive model. In this model, the current value of the process is expressed as a finite, linear aggregate of previous values of the process and a random shock a_t [13].

In this model, the current value of the process was expressed as a finite, linear aggregate of previous values of the process. The AR model is a classic forecast model implemented in time series analysis. An AR(ρ) model relates ρ historic observations to the value Y_{t+1}:

$$Y_{t+1} = \mu + \sum_{i=0}^{\rho-1} \Theta_i Y_{t-i} + \varepsilon_{t+1} \tag{1}$$

$$Y_{t+1} = \widehat{Y}_{(t+1|t)} + \varepsilon_{t+1} \tag{2}$$

From Eq. (1), μ is a term correcting the mean value, Θ_i is the coefficient of each past observation Y_{t-i} is describing its influence on the next value Y_{t+1}, and finally ε_t is assumed to be white noise [13, 14]. This is an iterative process, meaning that a six-steps-ahead forecast is required to calculate Eq. (2), to upgrade Y_t plugging in the last forecast value generated, and to repeat the process:

$$\widehat{Y}_{t+k|t} = \mu + \sum_{i=0}^{\rho-1} \widehat{\theta}_i \widehat{Y}_{t+k-(i+1)|t} \tag{3}$$

$\widehat{Y}_{t+k-(i+1)|t}$ is equal to the observation if the observation exists; otherwise, it is equal to the prediction. An AR process is a linear process characterized by a finite number of terms.

2.1.2. Recursive least square with forgetting factor

Notice that the k-step AR(ρ) model can be written as [15]

$$Y_{t+k} = \left(Y_t, Y_{t-1}, \ldots, Y_{t-\rho+1}\right) \begin{pmatrix} \Theta_0 \\ \vdots \\ \Theta_{\rho-1} \end{pmatrix} + \varepsilon_{t+k} \tag{4}$$

which, by introducing the standard notation using X as the regressor vector, becomes

$$Y_{t+k} = X_t^T \widehat{\theta}_t + \varepsilon_{t+k} \tag{5}$$

Recursive least square (RLS) with forgetting factor is based on the AR process and allows the parameter vector θ to change over time. For the weighted least squares estimator, the weighted estimation is calculated as

$$\widehat{\theta}_t = \widehat{\theta}_{t-1} + R_t^{-1} X_{t-k} \left[Y_t - X_{t-k}^T \widehat{\theta}_{t-1} \right] \tag{6}$$

where

$$R_t = \lambda R_{t-1} + X_{t-k} X_{t-k}^T \tag{7}$$

This is a recursive implementation of a weighted least squares estimation, where the weights are exponentially decaying over time. With X_t as the regressor vector, θ_t as the coefficient vector and Y_t as the dependent variable (observation at time t), the k-step prediction at t is

$$\widehat{Y}_{t+k|t} = X_t^T \widehat{\theta}_t \tag{8}$$

The parameter λ is the forgetting factor, describing how fast historical data are down-weighted. The weights are equal to

$$\omega(\Delta t) = \lambda^{\Delta t} \tag{9}$$

Δt is the age of the data [16]. If $\lambda(t)$ is constant $\lambda(t) = \lambda$, then the memory is of the form

$$T_0 = \frac{1}{1-\lambda}. \tag{10}$$

Typical values for λ are in the range from 0.90 to 0.995. The forgetting factor can be chosen based on assumptions of the dynamics, or it can be a part of the global optimization [15].

2.1.3. Electrolyzer model

Hydrogen production through water electrolysis is a method of storing wind energy, and it is of great importance to understand that the hydrogen is fundamental to the implementation of this hybrid system, since it is the energy carrier that allows the hybrid system to work autonomously for long periods of time. The hydrogen can be stored and distributed to be used a posteriori to generate electricity via the fuel cell (FC); the only by-product of this combustion is water, so no additional pollution is generated [17].

The hydrogen production by electrolysis of water is reached by the decomposition of water into oxygen and hydrogen gas, thanks to an electric current passed through the water. The reaction has a standard potential of 1.23 V, meaning it ideally requires a potential difference of 1.23 V to split water. The chemical representation is given by

$$2H_2O \rightarrow 2H_2 + O_2. \tag{11}$$

The basic operation of the electrolyzer can be demonstrated by a small experiment, which is shown in **Figure 1** [18]. The water is electrolyzed into hydrogen and oxygen by passing an electric current through it.

The electrolysis is fundamental for the production of pure hydrogen, and this must be taken into account in the hybrid system model, by implementing the laws of Faraday electrolysis.

Faraday's first law of electrolysis. The mass of the substance altered at the electrode during the electrolysis is directly proportional to the amount of electricity transferred to that electrode. The quantity of electricity indicates the amount of electrical charge, typically measured in coulombs [19].

Faraday's second law of electrolysis. When the same quantity of electricity is passed through several electrolytes, the mass of the substances deposited is proportional to their respective chemical equivalent or equivalent weight [19].

The first law can be used to obtain the amount of hydrogen generated according to a DC current in a certain amount of time, being relevant to the operation of the fuel cell. It can be expressed in mathematical form as follows

$$V_g = \frac{R_g \cdot I \cdot T \cdot t}{F \cdot p \cdot z} \tag{12}$$

The gas volume in liters is represented by V_g, R_g is the ideal gas constant equal to 0.0820577 (L·atm/mol·K), I means the current in amperes, T is the temperature in °K, t is the time in seconds, z is the number of excess electrons and takes the value of 2 for H_2 and 4 for O_2, p represents the ambient pressure in atmospheres, and F represents the Faraday constant equal to 96485.33 in C/mol.

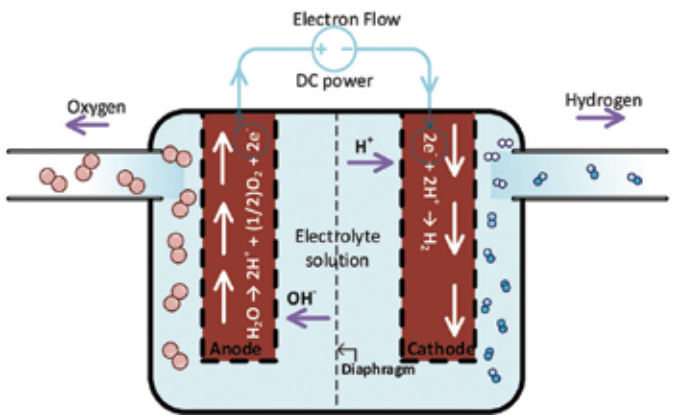

Figure 1. Water electrolysis experiment.

Electrolysis has the advantages of being static, simple, and able to operate for long periods without attention while generating hydrogen to be used in a fuel cell.

Considering Faraday's law of electrolysis (Eq. (12)) and the fact that the power required by the electrolyzer can be computed by means of the power equation $P_{el} = V_c \cdot I$, where I is the current, V_c represents the cell voltage, and P_{el} is the power required for the electrolyzer, the volume of hydrogen generated from a certain amount of power can be expressed as

$$V_{H_2} = \frac{P_{el} \cdot R \cdot T \cdot t}{2 \cdot F \cdot p \cdot V_c} \tag{13}$$

VH_2 is the volume of hydrogen produced by the cell. Implementing Eq. (13) the volume of hydrogen produced by the electrolyzer with P_{el} input power is deduced. Considering that the model applied to the HS will calculate the power required for the electrolyzer in the function of the wind power forecast, Eq. (13) is reorganized as

$$V_{H_2} = P_{el} \cdot l_{el} \tag{14}$$

where $l_{el} = \frac{R \cdot T \cdot t}{2 \cdot F \cdot p \cdot V_c}$.

2.1.4. Fuel cell model

The PEMFC is the type of cell that was used to develop the model and is characterized by an efficient production of energy with high power density represented in **Figure 2**. Since the cell separator is a polymer tape, the cell operates at a relatively low temperature, which potentially allows quick start-up, and issues such as sealing, assembly, and operation are less complex than in other cell types. The need for handling corrosive acids or bases in this system is removed [20].

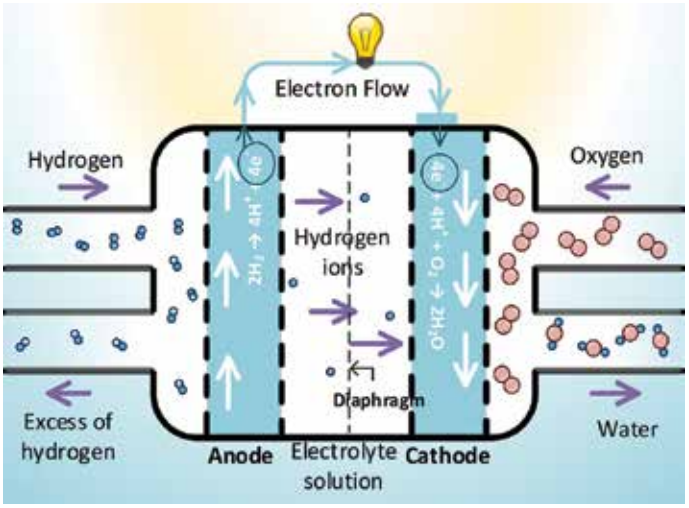

Figure 2. Schematic of representative PEMFC.

The cell has internal electrical losses such as ohmic, activation, and mass transport [20, 21]. The ohmic losses are caused by ionic resistance in the electrolyte and electrodes; electronic resistance in the electrodes, current collectors, and interconnects; and contact resistances. Ohmic losses are proportional to the current density, depending on materials selection and stack geometry and on temperature.

The activation-related losses stems from the activation energy of the electrochemical reactions at the electrodes. These losses depend on the reactions at hand, the electro-catalyst material and microstructure, reactant activities (and hence utilization), and weakly current density.

Mass transport-related losses are a result of finite mass transport limitation rates of the reactants and depend strongly on the current density, reactant activity, and electrode structure.

The cell voltage is calculated based on the reversible open-circuit voltage E and the voltage losses, as follows

$$V_c = E - \Delta V_{ohm} - \Delta V_{act} - \Delta V_{trans} \tag{15}$$

The internal losses in the fuel cell are neglected in this model, because their values tend to be very small and therefore do not significantly alter the result, as demonstrated in [22]. For the cell voltage, a value between 0.6 and 0.7 V can be assumed [23]. A value of 0.68 is assumed in accordance with the efficiency of the FC.

The operation of the fuel cell can be understood to be essentially the reverse process of electrolysis of water, as this technology recombines the hydrogen with oxygen to generate electrical power and water.

Individual fuel cell units are combined as modules in series or parallel configurations to provide desired voltage and output power. The mechanical arrangement must ensure not only electrical contact among units but also adequate circulation of gases, allowing catalyst reactions to take place at the correct temperatures and humidity levels [21]. The electric power generated by a FC is defined as

$$P_e = V_c \cdot I \cdot n \tag{16}$$

in which V_c is the voltage cell, I represents the current cell, and n is the number of fuel cells integrating the stack.

To know the amount of hydrogen needed by the fuel cell, one must know the number of fuel cells that make up the stack of the final FC array. By means of Eq. (12) and Eq. (16), the hydrogen used by the stack, in mol/s [21, 24], is deduced as

$$H_{2used} = \frac{P_{fc} \cdot n}{2 \cdot V_c \cdot F} \tag{17}$$

Another way to calculate the hydrogen used is in kg/s, while considering the molar mass of the hydrogen and the Faraday constant (F), deduced as

$$H_{2used} = l_{fc} \cdot P_{fc} \tag{18}$$

l_{fc} is determined by $1.05 \times 10^{-8} \frac{n}{V_c}$.

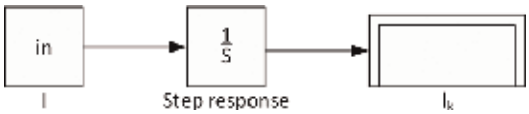

Figure 3. Step response function.

In order to design the MPC, the impulse response function for the fuel cell is needed. Taking into account that the FC is an electrochemistry element, its dynamic is very fast as demonstrated in [25, 26]. To compute the impulse response of the FC, the function in **Figure 3** is implemented to obtain $l_{fc,k}$ for future use in the MPC. The same function is required to obtain the impulse response for the electrolyzer and storage, $l_{el,k}$, and $l_{st,k}$, respectively.

3. Hybrid system setup and EMS strategy

The proposed HS, according to the historic wind measurements from meteorological stations in Mexico City, is composed by a 5 kW Iskra small wind turbine [27], a 2 kW KC200GT photovoltaic (PV) array [28], a 2.4 kW PEMFC [29], an electrolyzer from the brand Proton OnSite with a net production rate of 18.8 standard liter per minute [30], and a 16,500 l hydrogen storage [31]; the device modeling is subsequently illustrated. In order to achieve the desired output power from the HS, the use of a forecasting method as explained in this section is proposed.

The control is recreated in a computational form, in which the HS output is reflected in the activation, the power regulation, and the interaction between the HS elements as seen in **Figure 4**, where the continuous, dashed, and pointed arrows represent the electric, control data, and hydrogen flow, respectively. The HS is supposed to connect to the distribution network, taking into account the power level used by normal households in Mexico City at different times of the year [32]. The HS can be adjusted to work as a constant power generator or to meet a signal reference output power, based on the daily historic load of the household(s). This can make the user change the consumption habits in order to have a better response to the system and to decrease the total cost of their electric consumption [33, 34].

Figure 4 shows the flow of the main energies that sustain the HS where the left side is the hydrogen flow and the right side is the electric power flow with the inputs and outputs of the systems. This figure also shows the electric conversion AC/DC and DC/AC taking into account that the FC has a DC output. The power will be controlled, regulated, and distributed to the network and electrolyzer with the purpose of storing energy in the form of hydrogen.

In order to implement a controller, one must understand and describe the models used in the system. Therefore, in the following section, the basic operation of the HS components will be introduced.

Depending on the objective function, various MPC strategies can be implemented. Model predictive control has the inherent advantages like the use for controlling a great variety of processes, including systems with long delay times or of non-minimum phases or unstable

http://dx.doi.org/10.5772/intechopen.76760

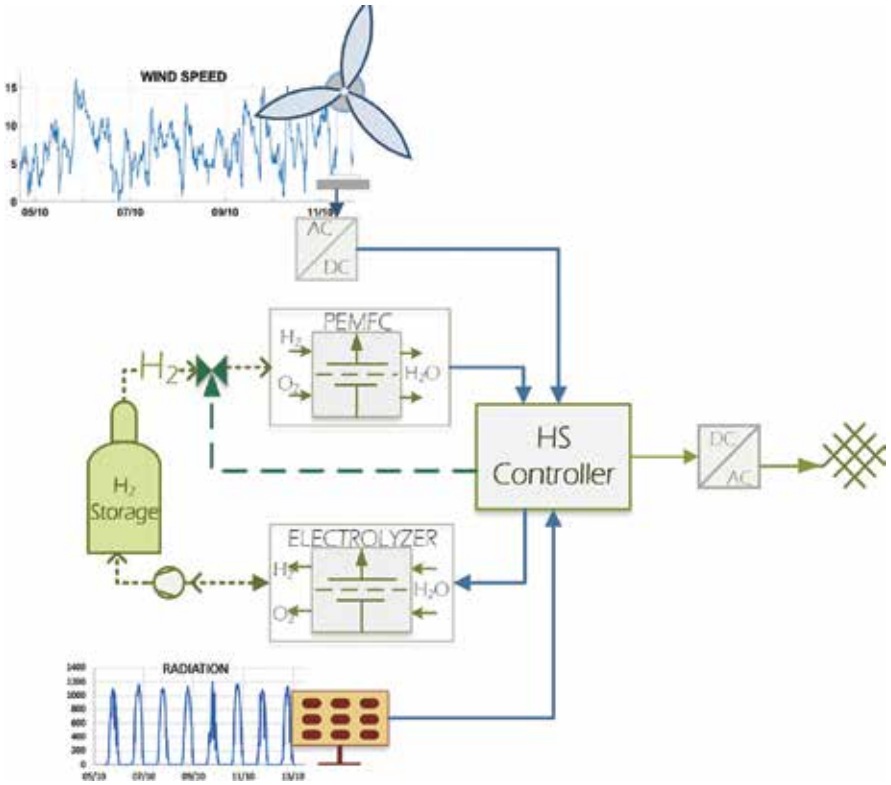

Figure 4. Wind-solar-FC hybrid system.

ones [35, 36]. In addition, the MPC introduces feedforward control to compensate measurable disturbances, allowing its application to this work to be more satisfactory [37].

Figure 5 shows the basic MPC structure; the future outputs for a horizon N are predicted at each instant t. The predicted outputs for $k = 1, \ldots, N$ depend on the known values up to instant t and on the future control signals, $k = 0, \ldots, N-1$, which are to be sent to the system. The future control signals are calculated by optimizing a criterion in order to keep the process close to the reference trajectory $P^{ref}_{t+k|t}$, which is computed as the result of

$$P_{t+k|t} = \widehat{P}^{w}_{t+k|t} + \widehat{P}^{pv}_{t+k|t} + P_{fcmax,k} - P_{elmax,k} \tag{19}$$

$\widehat{P}^{w}_{t+k|t}$ represents the forecasted wind power, $\widehat{P}^{pv}_{t+k|t}$ is the forecasted PV power, P_{fcmax} is the activation vector of the FC, and P_{elmax} is the activation vector of the electrolyzer, where the last two are computed according to the priority given in the different scenarios. Eq. (19) is then filtered through a moving average filter, which operates by averaging a number of points from the input signal to produce each point in the output signal [38]. In equation form it is written as

$$P^{ref}_{t+k|t}[k] = \frac{1}{M}\sum_{j=0}^{M-1} P_{t+k|t}[k+j] \tag{20}$$

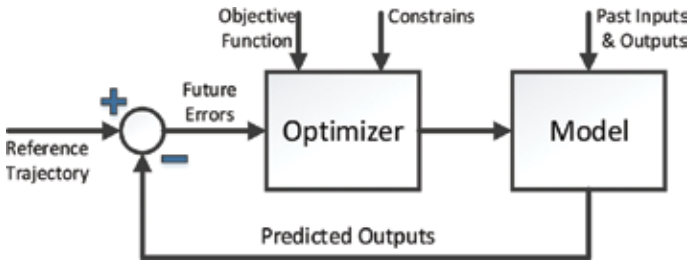

Figure 5. MPC structure.

where M is the number of points in the average. Afterward, $P^{ref}_{t+6|t}$ is reported, and $P^{ref}_{t+k|t}$ for $k = 1, \ldots, N$ is used in the MPC.

$P_{t+k|t}$ is computed considering that the activation vector of the FC and electrolyzer depend on the priority given by the behavior of the HS. Afterward, the forecast signal is filtered as to remove the high-frequency changes and leave a smooth signal to be used as the reference trajectory.

The MPC manages the electric power of the HS and takes into account the output power, the filtered forecast, and the actual wind power, so that the control decides how much power the FC is going to produce and how much power will be directed to the electrolyzer for saving energy for future fluctuations; thus, the output power will be almost without frequency changes and minimizing in a great extent the intermittence and variability of the wind power.

4. Forecast and MPC implementation in the hybrid system management

The purpose is to report to the system operator how much power will be delivered to the grid in the next hour. Along the scenarios a priority is given, and a constraint or condition will be added to compute $P_{t+k|t}$, changing the characteristics from Eq. (19) and recreating $P^{ref}_{t+k|t}$.

The reported data will be the trajectory followed by the HS by means of the MPC and will have the principal characteristic of being smooth in time as to avoid any operational instability like voltage or frequency in the grid because of the influence of the wind power. Furthermore, when a trajectory is applied to the control of the HS and successfully reached, it can be demonstrated that wind power as non-dispatchable energy, when implemented in a HS, can be converted to a semi-dispatchable electric source, making the management and distribution of energy more flexible.

Initially, an algorithm to find the optimal forgetting factor (λ), by simply fitting a sequence of λ values from 0.96 to 1 was implemented, and the λ value which minimized the root mean square error (RMSE) was found for each horizon and forecast, as seen in **Figure 6**.

The aforementioned optimal λ is implemented to compute the forecast for the different horizons applying RLS with the forgetting factor, which results in the forecast for the different

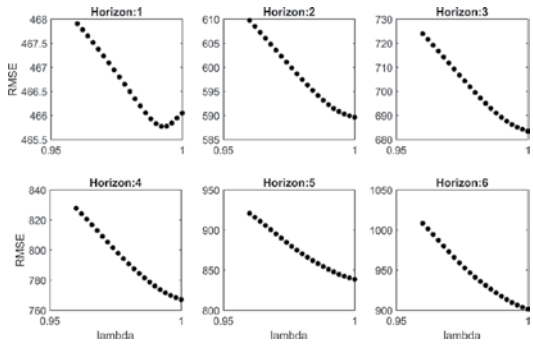

Figure 6. Optimal forgetting factor.

horizons k as shown in **Figure 7**. The algorithm implemented to forecast 1 h ahead, with a resolution of 10 min, is called a six-steps-ahead forecast.

The time series models are updated in each iteration of the process as described later in this section, taking into account the new data measured every 10 min. The expressions obtained for each horizon of wind forecast ($k = 1, \ldots, 6$) are

$$Y_t = 161.2 + 0.8324Y_{t-1} + 0.0461Y_{t-2} \tag{21}$$

$$Y_{t+1} = 248.3 + 0.8275Y_t - 0.00922Y_{t-1} \tag{22}$$

$$Y_{t+2} = 342.65 + 0.8228Y_{t+1} - 0.0698Y_t \tag{23}$$

$$Y_{t+3} = 439.93 + 0.7703Y_{t+2} - 0.0835Y_{t+1} \tag{24}$$

$$Y_{t+4} = 525.09 + 0.6905Y_{t+3} - 0.0641Y_{t+2} \tag{25}$$

$$Y_{t+5} = 634.7 + 0.7555Y_{t+4} - 0.1978Y_{t+3}. \tag{26}$$

The autocorrelation function (ACF) analysis result of the short-term forecast is shown in **Figure 8**, indicating that the used model is suitable for this study purpose.

Figure 9 shows the RMSE as a function of the horizon k (10-min steps). The black curve is the RMSE for persistence, and the red curve is for RLS. Some improvement of the RLS over the persistence is observed, but it is beyond the scope of the study to investigate the impact of using the forecasts compared to persistence.

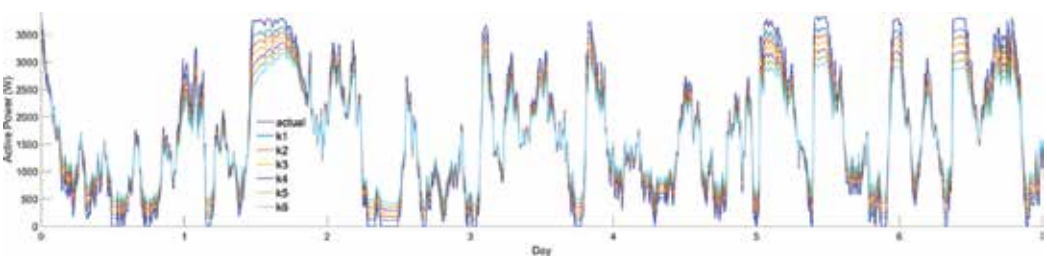

Figure 7. Actual and k-step ahead forecast.

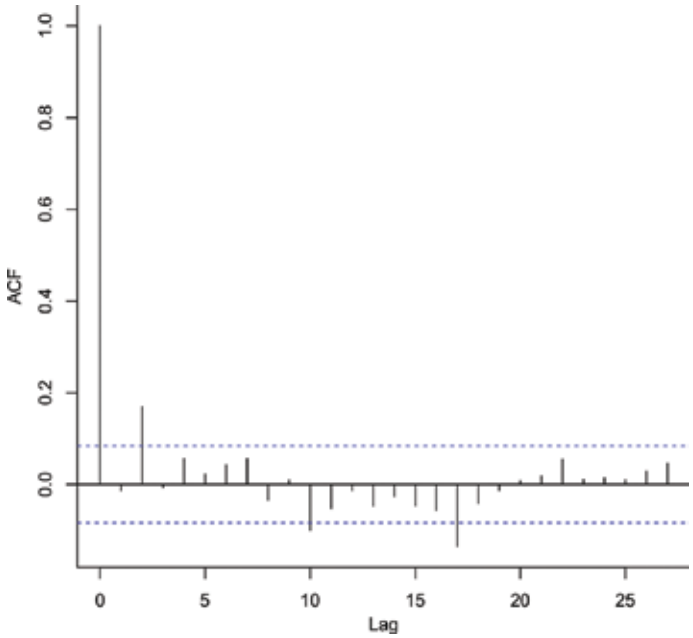

Figure 8. ACF of the residuals.

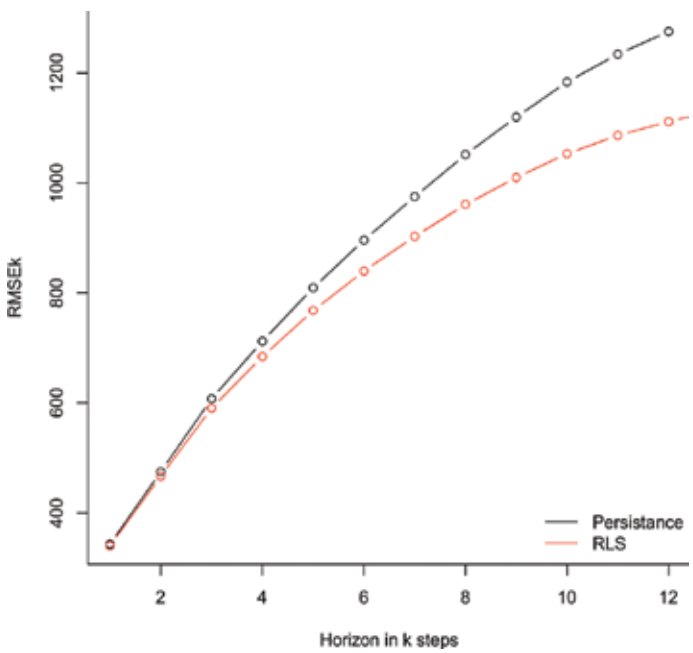

Figure 9. RMSE as function of the horizon.

The forecast is done using the following steps which are repeated every 10 min:

- Update historic data.
- Run 1-h-ahead forecast.
- Compute the "new trajectory."
- Update the "last trajectory," adding the last 10 min of the "new trajectory" at the end of the last one, as to always have a 1-h-ahead forecast generation.
- Report the new 1-h-ahead updated trajectory to the system operator.

Different EMS scenarios were tested to be applied in the interaction of the inner elements of the hybrid system, with a variety of priorities for the output power, using the proposed developed MPC method.

This section presents and explains the different scenarios of control with the more significant outputs within the ones implemented, and based on these scenarios, a decision about which one is more convenient to implement can be taken, depending on the purpose of the HS, the priorities, and output power needed.

The computational process for all scenarios is shown in **Figure 10** in a generalized way, in which constraints change in their decision-making depending on the priority for the HS of the case. The flowchart presents a never-ending iterative process, updating the historical wind measurements and managing the round-the-clock HS energy.

With the computed forecast and the application of the models for the different elements that integrate the HS, the objective function can be deduced and implemented to be minimized in the MPC:

$$\begin{aligned} \min_{P_{\theta,k}} \quad & \left\| P_{w,k} + P_{pv,k} - P^{ref}_{t+k|t,\,k} + P_{\phi,k} \right\| \\ \textit{subject to} \quad & \phi = \sum_{k=0}^{N} - l_{fc} P_{fc,k} + l_{el} P_{el,k} + l_{st,k} \phi_0 \\ & \phi_{min} \le \phi \le \phi_{max} \\ & -P^{nom}_{ele} \le P_{\phi,k} \le P^{nom}_{fc} \\ & P_{\phi,k} = P_{fc,k} - P_{el,k} \\ & 0 \le P_{el,k} \\ & 0 \le P_{fc,k} \end{aligned} \tag{27}$$

The MPC minimizes an objective function subjected to constraints and manages the power flow of the HS, where $\|\|$ is the vector norm or ℓ^2-norm; P_ϕ is the power flow from/to the elements connected to the storage calculated by the MPC; $P^{ref}_{t+k|t}$ is the reference trajectory based on the forecasted wind power computed with Eq. (20); P_{fc} is the power to be generated by the FC; P_{el} is the power destined to the electrolyzer; ϕ represents the level of storage; ϕ_0 represents

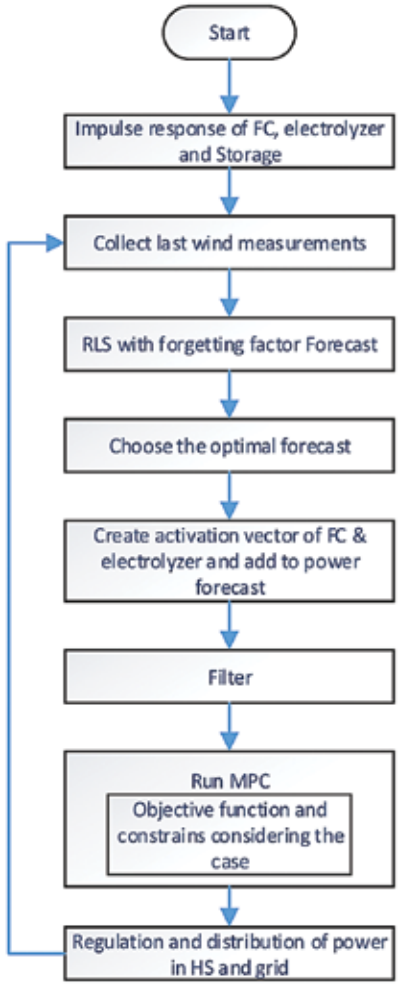

Figure 10. HS operation flowchart.

the last measure of H_2 stored; ϕ_{max} and ϕ_{min} are the physical limits of the storage; l_{el}, l_{fc}, and l_{st} represent the impulse response of the electrolyzer; and FC and storage, respectively, based on the aforementioned models.

The constraints for the FC and electrolyzer are vectors with the physical nominal values of the elements represented by P_{fc}^{nom} and P_{ele}^{nom}, respectively, and implemented in the MPC. $P_{w,k}$ represents the vector with the actual power ($k = 0$) and forecasted wind power ($k = 1, \ldots, N$) meaning $P_w = \left[P_{k=0}^{w}, \widehat{P}_{t+k|t}^{w}\right]$. $P_{pv,k}$ is the vector of actual and forecasted solar radiation, being a vector of the same form as P_w. **Figure 11** is explained for a better understanding of P_w, where $t = 27h30\text{min}$ represents the actual instant, being the $k = 0$ point. The continuous line before the actual point is the historic data incorporated in the time series analysis, and the dashed line after it is the 1-h-ahead forecast representing the six-steps-ahead, mentioned in Sections 2 and 3.

http://dx.doi.org/10.5772/intechopen.76760

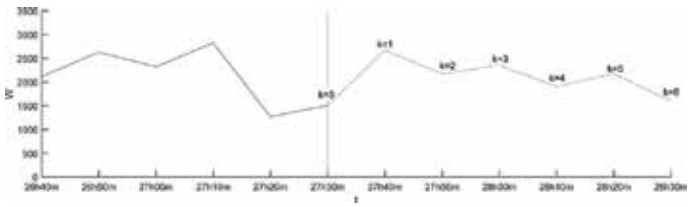

Figure 11. P_w forecast at t = 27h30min.

5. Energy management system scenarios

Two scenarios are implemented to validate the algorithm proposed in this work. The scenarios establish priorities and have the main purpose of zero network frequency disturbance and as a second purpose possession of a more stable and semi-dispatchable power generation.

The purpose of the first scenario MPC as an EMS is smoothing the wind power, employing the power generated by the FC in a prioritized way as an electric generation source. The second scenario focuses on having an as much as possible constant output power, from the HS and the probable "sacrifices" to accomplish it, regarding the wind power surplus.

Figure 12 displays the actual active wind and PV power available, in which the intermittence with abrupt ramps is noticeable, i.e., sudden changes from 20 to 3200 W in the wind power.

5.1. Smoothing the wind power

In this scenario, the priority is to smooth the wind power generated by the turbine, managing the output power of the whole HS at every moment. To compute $P^{ref}_{t+k|t}$ from Eq. (19), first one must calculate P_{elmax} and P_{fcmax} considering the restrictions of the electrolyzer and the FC.

To calculate the vector P_{elmax}, both physical and characteristic constraints for the scenario are considered. In this scenario, the hydrogen level in the tank will be at least lower than an upper threshold level (Γ_{elup}) when charging or until the maximum of the tank is reached because of surplus of wind power, and above a lower threshold (Γ_{eldown}) of the tank, described mathematically as

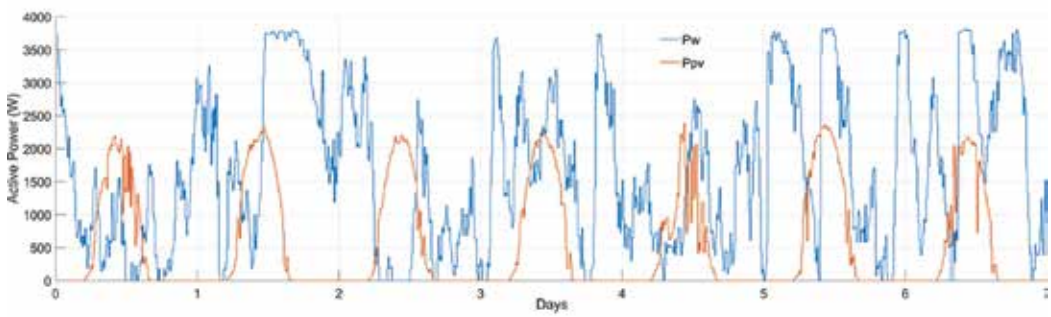

Figure 12. Actual wind and PV power.

$$P_{elmax} = \begin{cases} \widehat{P}^{w}_{t+k|t} + \widehat{P}^{pv}_{t+k|t} & \phi \le \phi_{max}\Gamma_{elup} \\ 0 & \phi > \phi_{max}\Gamma_{elup} \end{cases} \quad |\phi \le \phi_{max}\Gamma_{eldown}. \tag{28}$$

The hydrogen storage will be charged when the tank presents a specified level of hydrogen, represented by the lower threshold (Γ_{eldown}), bearing in mind a base amount of hydrogen in case of contingency because of the uncertainty of the wind speed. The base amount will be assumed as the hydrogen required to generate maximum power from the FC in the next 2 h, ensuring a smooth change in the output power without affecting the frequency of the network. In the charging period, the electrolyzer will use the wind power to produce hydrogen until the storage level reaches a specified upper threshold (Γ_{elup}) in which it stops charging. In this work, Γ_{elup} represents the hydrogen required for the FC to work 8 h ahead at maximum power.

Storage plays a great role when it comes to maintaining a stable output power of the HS for long periods of time. The activation and deactivation of the electrolyzer are the principal factors for maintaining a desired storage level. As seen in **Figure 13**, a global flowchart explains how it was applied in the model, giving an idea of how it can be modified depending on the priority of the storage required from the HS.

To ensure constant smooth output power from the HS, constraints were applied on the activation of the FC. As a result the FC generates more frequently and compensates the variability in the wind power, according to the amount of hydrogen stored. When there is no wind, the output power is determined by the nominal FC value. Given the uncertainty in the wind speed, this constraint was necessary to attain the designated power value without having to ask for backup from the grid. Therefore, the nominal value of the FC must be implemented in the MPC and in the activation of the FC. To compute $P^{ref}_{t+k|t}$ from Eq. (20), the activation vector of the FC is then calculated by

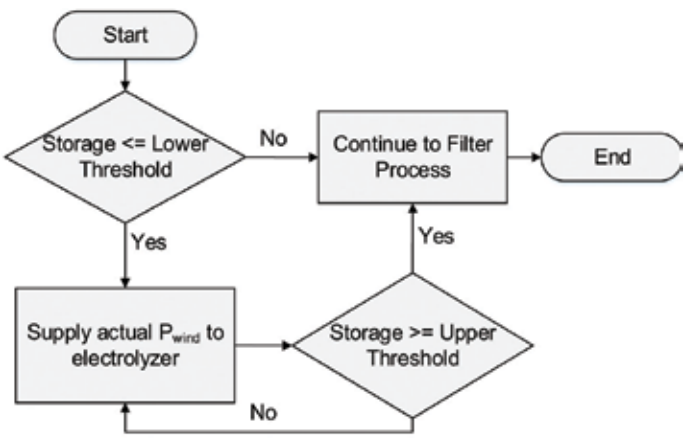

Figure 13. Activation of electrolyzer.

$$P_{fcmax} = \begin{cases} P_{fc}^{nom} - \left(\widehat{P}_{t+k|t}^{w} + \widehat{P}_{t+k|t}^{pv}\right) & P_{fcmax,k} > 0 \\ 0 & P_{fcmax,k} \leq 0 \end{cases} \quad |\phi_{max}\Gamma_{fc} \leq \phi \tag{29}$$

where the nominal power of the FC is represented by P_{fc}^{nom} and Γ_{fc} is the threshold of minimum percent of hydrogen stored for the FC to generate power; in case that the threshold cannot be met, the value of P_{fcmax} will be zero. Furthermore, P_{fcmax} is computed taking into account P_{fc}^{nom} to ensure that the max value asked from the FC will not be greater than the nominal power of the FC and to help linearize the output power of the HS.

The maximum power of the HS in this scenario will be determined as the sum of the wind power and the power from the FC given by $P_{fc,k} = P_{fc}^{nom} - \widehat{P}_{t+k|t}^{w}$.

The sum of the power generated by the FC and forecast for the wind turbine will be filtered using Eq. (20) which will smooth the flickers, resulting in the reference for the MPC (Eq. (27)); simultaneously, this reference will be the output power of the HS.

5.2. Prioritizing the constant output power level of the hybrid system

When the priority is to have an as much as possible constant output power from the HS, the resulting analysis of the previous scenario is of great importance. Because of the intermittence of wind speed, the appearance of many sags in the power forecast and actual power is common. To maintain a linear output power means the need to "sacrifice" other characteristics as, in this case, the magnitude of power supplied from the HS to the distribution network given by

$$P_{t+k|t}^{ref}[k] = \frac{a}{M}\sum_{j=0}^{M-1} P_{t+k|t}[k+j] \tag{30}$$

where a will take values between 0 and 1.

In this scenario, the filter at the control part of the model was modified from Eq. (20) as to have more energy stored and to decrease the output magnitude to 60% ($a = 0.6$) of the original power value. Thus, the residual 40% will be supplied to the electrolyzer and consequently will generate hydrogen to store. The updated filtered signal will be the output power of the HS for the next hour.

6. Results and discussions

Each subsection from Section 5 focuses on the required characteristics needed to smooth and flatten the output power of the HS in order to overcome the intermittence of wind power.

When the HS is connected to the network, it will not destabilize the frequency as demonstrated in this section. The obtained results show the first week behavior of the HS, for the reader to notice in a clear way the dispatchability and reduction of intermittence in comparison to a system without the application of the proposed model as the actual wind power.

6.1. Active power delivered from the HS

The designed HS system is to be connected to the distribution network as mentioned before. From results, it can be seen how the unpredictability from the wind power (**Figure 12**) is solved as shown in the HS active output power obtained with the proposed AEMS model (**Figure 14**). The network frequency will not be affected considering that the HS output power can be dispatched according to the final user needs and the information can be sent to the system operator with 1 hour prior.

Figure 14 presents the HS output power for both scenarios. Results from the first scenario show that because of the periods of charge, the HS output power has periods of no power delivered to the network and the implementation of the constraints required to activate the electrolyzer is also the moment of no power generated by the HS resulting from the electrolyzer consuming all the power generated by the wind turbine with the purpose of storing energy as hydrogen. Note in **Figure 14** that the response obtained from the second scenario, when compared to the first scenario, is flatter, more stable, and more constant as it was expected.

Observing the results of the different scenarios, the HS output power can be adjusted to meet a specific load which modifies the trajectory followed by the MPC and the constraints applied. In addition, because of the flexibility of the MPC, the constraints that rule the charge and discharge of the hydrogen storage can be modified considering the purpose of the HS.

The reduction of volatility of the power delivered to the distribution network is noticeable, comparing the wind power from **Figure 12** and the output power of the HS from **Figure 14**.

6.2. Hydrogen storage behavior

The behavior of the hydrogen generated by the electrolyzer and consumed by the FC in the different scenarios can be seen in **Figure 15**, where it can be noticed that when the electrolyzer works the hydrogen tank is charged and when the FC works the storage level of hydrogen will decrease.

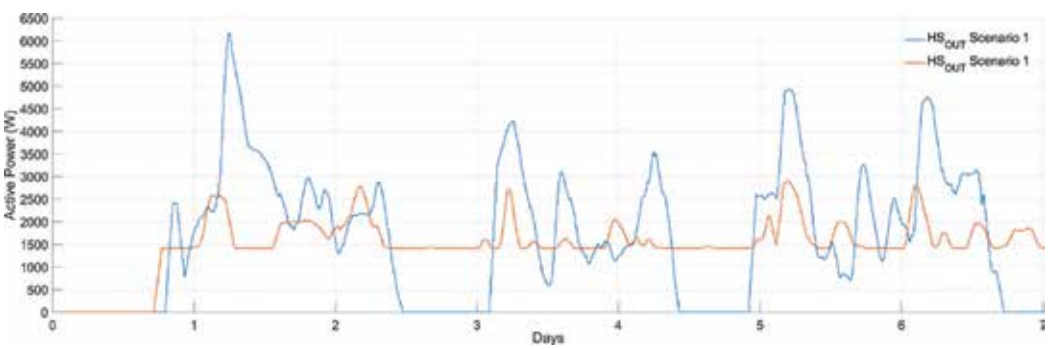

Figure 14. Total power generated by the HS in both scenarios.

http://dx.doi.org/10.5772/intechopen.76760

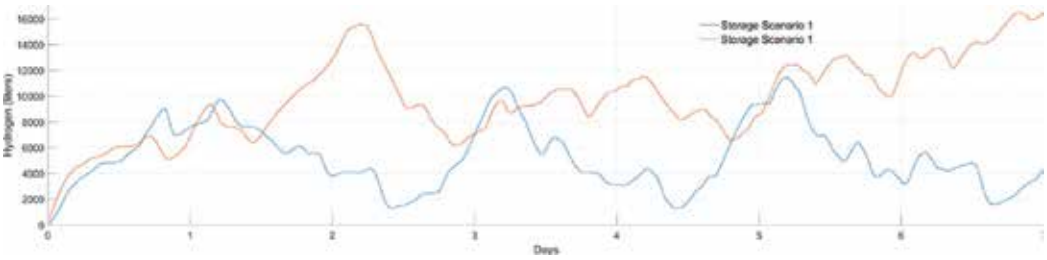

Figure 15. Behavior of hydrogen storage in the different scenarios.

The storage constantly maintains a minimum level of hydrogen as shown in **Figure 15**; thanks to this, the FC can work longer permitting a smooth or flat output from the HS.

Comparing the production and consumption of hydrogen from both scenarios, results show that there is 16% less production of H_2 and 5.6% less consumption of it in the second scenario at the end of the week. However, the storage of the second scenario presents 45% more hydrogen in comparison with the first scenario where it is almost empty as seen in **Figure 15**. These results are a consequence of the level of power required in each scenario. The second delivers a lower level of active power to possess a more constant output at all time, in contrast to the first scenario, which due to the level of power delivered needs periods of zero output power as to generate H_2 to storage.

The storage from the first scenario always has a good level of hydrogen ready to be used by the FC in a more efficient way as in **Figure 15**, but clearly because of the charging periods of hydrogen, the output power drops to zero at the output of the HS.

The hydrogen consumption is constant, and, therefore, the tank will not reach a high level of storage, tending instead to maintain a lower mean of hydrogen, as shown in **Figure 15**.

6.3. Findings of the method

Taking into account the importance of charging periods for the storage of hydrogen and of keeping an output power level as linear as possible, decreasing the output power level to generate hydrogen was required for longer periods of time and for the FC to work as backup power to have an almost linearized power level at the output of the HS.

The FC can act as a means of contingency to smooth the output power thanks to the hydrogen stored in the tank, and because of the decision-making based on the forecast that gives information about future possible fast changes in wind power, it is possible the use the FC as a measure for preventing disturbance of the frequency of the network.

The surplus of energy from the high peaks of wind power is saved as hydrogen for future implementation, making smooth wind power and semi-dispatchable HS-generated power possible.

7. Conclusions

One of the most important conclusions is the fact that wind power as a non-dispatchable kind of energy, when employed in a hybrid system with implementation of forecast, can be managed as a semi-dispatchable energy. The generation can be modeled based on the needs of the end user or as a base energy for long periods of time, depending on the capacity of the storage and output power required for the system. Consequently, the frequency of the system will not be compromised because of sudden changes in wind power. The proposed HS is meant to work in the distribution level for housing sectors and small stores.

In real life application, this HS model will help to keep the net frequency in the tolerance rate, given the fact that it will not be disturbed by the HS when connected as DG into the network, thanks to the no uncertainty and no intermittence in the HS output power.

When the priority is completely given to the FC generation, there is a high risk of running out of hydrogen and not meeting the full capacity of the HS.

Another finding is the fact that to generate a completely linear power output, there is a need to "sacrifice" other features such as magnitude power, storage limits, and even the times to recharge the hydrogen tank according to the needs of the end user; hence, it is recommended to compromise the involved parties regarding the HS.

The implementation of forecast is demonstrated to be of great importance in planning the dispatch of power, improving and taking contingency measurements as to avoid disturbing the network or even improving the network in the connection point if necessary.

Forecast applied to wind power and used for the MPC allows the manipulation of the elements that make the HS obtain the desired output power while avoiding penalties.

Acknowledgements

M.F.A.M gratefully acknowledges the support of DTU Compute and appreciates the financial support of the Cities project, supplementary to energy sustainability fund SENER-CONACYT through the CEMIE-OCÉANO project.

Author details

Maria Fernanda Alvarez Mendoza[1]*, César Angeles-Camacho[1], Peder Bacher[2] and Henrik Madsen[2]

*Address all correspondence to: malvarezm@iingen.unam.mx

1 Instituto de Ingeniería UNAM, Mexico City, Mexico

2 DTU Compute, Technical University of Denmark, Denmark

References

[1] Zhang H, Xing F, Cui H-Z, Chen D-Z, Ouyang X, Xu S-Z, et al. A novel phase-change cement composite for thermal energy storage: Fabrication, thermal and mechanical properties. Applied Energy. 2016;**170**:130-139. DOI: 10.1016/j.apenergy.2016.02.091

[2] Bagen BR. Evaluation of different operating strategies in small stand-alone power systems. IEEE Transactions on Energy Conversion. 2005;**20**:654-660. DOI: 10.1109/TEC.2005.847996

[3] Ma T, Yang H, Lu L. Performance evaluation of a stand-alone photovoltaic system on an isolated island in Hong Kong. Applied Energy. 2013;**112**:663-672. DOI: 10.1016/j.apenergy.2012.12.004

[4] Bouffard F, Galiana FD. Stochastic security for operations planning with significant wind power generation. 2008. pp. 1-11. doi:10.1109/PES.2008.4596307

[5] Zhao Y, Ye L, Li Z, Song X, Lang Y, Su J. A novel bidirectional mechanism based on time series model for wind power forecasting. Applied Energy. 2016;**177**:793-803. DOI: 10.1016/j.apenergy.2016.03.096

[6] Wang J, Botterud A, Bessa R, Keko H, Carvalho L, Issicaba D, et al. Wind power forecasting uncertainty and unit commitment. Applied Energy. 2011;**88**:4014-4023. DOI: 10.1016/j.apenergy.2011.04.011

[7] Bathurst GN, Strbac G. Value of combining energy storage and wind in short-term energy and balancing markets. Electric Power Systems Research. 2003;**67**:1-8. DOI: 10.1016/S0378-7796(03)00050-6

[8] Exizidis L, Kazempour SJ, Pinson P, de Greve Z, Vallée F. Sharing wind power forecasts in electricity markets: A numerical analysis. Applied Energy 2016;**176**:65-73. DOI: 10.1016/j.apenergy.2016.05.052

[9] Fathima AH, Palanisamy K. Optimization in microgrids with hybrid energy systems–A review. Renewable and Sustainable Energy Reviews. 2015;**45**:431-446. DOI: 10.1016/j.rser.2015.01.059

[10] McKenna R, Hollnaicher S, Fichtner W. Cost-potential curves for onshore wind energy: A high-resolution analysis for Germany. Applied Energy. 2014;**115**:103-115. DOI: 10.1016/j.apenergy.2013.10.030

[11] Santamaría-Bonfil G, Reyes-Ballesteros A, Gershenson C. Wind speed forecasting for wind farms: A method based on support vector regression. Renewable Energy. 2016;**85**:790-809. DOI: 10.1016/j.renene.2015.07.004

[12] Kavasseri RG, Seetharaman K. Day-ahead wind speed forecasting using f-ARIMA models. Renewable Energy. 2009;**34**:1388-1393. DOI: 10.1016/j.renene.2008.09.006

[13] Box GEP, Jenkins GM, Reinsel GC, Ljung GM. Time Series Analysis : Forecasting and Control. 5th ed. New Jersey, USA: John Wiley & Sons, Inc.; 2015

[14] Hastie T, Tibshirani R, Friedman J. The Elements of Statistical Learning. New York, NY: Springer New York; 2009. DOI: 10.1007/978-0-387-84858-7

[15] Madsen H. Time Series Analysis. Technical. Copenhagen: Chapman & Hall/CRC; 2008

[16] Rasmussen LB, Bacher P, Madsen H, Nielsen HA, Heerup C, Green T. Load forecasting of supermarket refrigeration. Applied Energy. 2016;**163**:32-40. DOI: 10.1016/j.apenergy.2015.10.046

[17] Twidell J, Weir AD. Renewable Energy Resources. 2nd ed. London: Taylor & Francis; 2006

[18] Santos DMF, Sequeira CAC, Figueiredo JL. Hydrogen production by alkaline water electrolysis. Química Nova. 2013;**36**:1176-1193. DOI: 10.1590/S0100-40422013000800017

[19] Ehl RG, Ihde AJ. Faraday's electrochemical laws and the determination of equivalent weights. Journal of Chemical Education. 1954;**31**:226. DOI: 10.1021/ed031p226

[20] EG&G Technical Services Inc. Fuel Cell Handbook. 7th ed. Virginia: U.S. Department of Energy; 2004

[21] Kunusch C, Puleston P, Mayosky M. Sliding-Mode Control of PEM Fuel Cells. London: Springer London; 2012. DOI: 10.1007/978-1-4471-2431-3

[22] Kunusch C, Puleston PF, Mayosky MA, Moré JJ. Characterization and experimental results in PEM fuel cell electrical behaviour. International Journal of Hydrogen Energy. 2010;**35**:5876-5881. DOI: 10.1016/j.ijhydene.2009.12.123

[23] Larminie J, Dicks A. Fuel cell systems explained. 2nd ed. UK: John Wiley & Sons, Inc.; 2003

[24] Sammes N, editor. Fuel Cell Technology. London: Springer London; 2006. DOI: 10.1007/1-84628-207-1

[25] Yan Q, Toghiani H, Causey H. Steady state and dynamic performance of proton exchange membrane fuel cells (PEMFCs) under various operating conditions and load changes. Journal of Power Sources. 2006;**161**:492-502. DOI: 10.1016/j.jpowsour.2006.03.077

[26] Kannan A, Kabza A, Scholta J. Long term testing of start–stop cycles on high temperature PEM fuel cell stack. Journal of Power Sources. 2015;**277**:312-316. DOI: 10.1016/j.jpowsour.2014.11.115

[27] Intelligent Energy-Europe. Catalogue of European urban wind turbine manufacturers potx 2011. p. 61. http://123doc.org/document/1227748-catalogue-of-european-urban--wind-turbine-manufacturers-potx.htm [Accessed: September 25, 2017]

[28] Kyocera. Model KC200GT high efficiency multicrystal photovoltaic module n.d.:2. http://www.kyocera.com.sg/products/solar/pdf/kc200gt.pdf [Accessed: September 25, 2017]

[29] Ballard. Datasheet: FCgen-1300 - Ballard - PDF Catalogue | Technical Documentation | Brochure n.d. http://pdf.directindustry.com/pdf/ballard/fcgen-1300/22779-383681.html [Accessed: September 25, 2017]

[30] FuelCellStore. Datasheet: Electrolyzer specifications S20, S40 n.d. http://www.fuelcellstore.com/hydrogen-generator-s40 [Accessed: September 25, 2017]

[31] Technologies Hb. Datasheet: HBank Technologies - Fuel Cell Application n.d. http://www.hbank.com.tw/fc/16500.html [Accessed September 25, 2017]

[32] Ramos Niembro G, Fiscal Escalante R, Maqueda Zamora M, Sada Gámiz J, Buitrón SH. Variables que influyen en el consumo de energía eléctrica. Boletín Iie. 1999;**23**:11-18

[33] Jiang L, Luo S, Li J. Intelligent electrical event recognition on general household power appliances. 2014 IEEE 15th Workshop on Control and Modeling for Power Electronics (COMPEL) 2014:1-3. DOI:10.1109/COMPEL.2014.6877183

[34] Mohsenian-Rad AH, Wong VWS, Jatskevich J, Schober R, Leon-Garcia A. Autonomous demand-side management based on game-theoretic energy consumption scheduling for the future smart grid. IEEE Transactions on Smart Grid. 2010;**1**:320-331. DOI: 10.1109/TSG.2010.2089069

[35] Camacho EF, Bordons C, Grimble MJ, Johnson MA. Model Predictive Control. London: Springer London; 2007

[36] Halvgaard R, Poulsen NK, Madsen H, Jorgensen JB, Marra F, Bondy DEM. Electric vehicle charge planning using economic model predictive control. 2012 IEEE International Electric Vehicle Conference, Greenville, USA: IEEE; 2012. pp. 1-6. DOI: 10.1109/IEVC.2012.6183173

[37] Maciejowski J. Predictive Control with Constraints. Harlow, England, New York: Prentice Hall; 2002

[38] Smith SW. The Scientist and Engineer's Guide to Digital Signal Processing. 2nd ed. California Technical Pub: San Diego, USA; 1999

Chapter 3

Energy Management System Designed for the Interconnected or Islanded Operation of a Microgrid Using LabVIEW Software

Lucia-Andreea El-Leathey

Additional information is available at the end of the chapter

http://dx.doi.org/10.5772/intechopen.74856

Abstract

Integration of distributed generation units and other users within the low and medium voltage distribution grid induces a variety of problems related to the management and control of microgrids. These aspects can be solved by using significantly different Energy Management Systems for the operation of microgrids, comparing to those applied to conventional power systems. The main objective of the Energy Management System is to ensure the rational use of energy, while minimizing its costs. The secondary objectives relate to increasing energy efficiency and reducing energy consumption, but especially to assuring the power facilities security. Moreover, the management of power systems to which renewable sources are connected is one of the main concerns of Distribution System Operators in order to ensure the safe operation, security of power supply, and the operation optimization from the economic side. The chapter regards the LabVIEW design and testing of an Energy Management System for the interconnected or islanded operation of a microgrid to the electric public grid. Furthermore, the chapter leads to the microgrids development in terms of operation and efficiency by achieving an Energy Management System designed for a small mixed microgrid with separate AC and DC rings bidirectionally interconnected by static converters.

Keywords: microgrid, power system, Energy Management System, LabVIEW, operating scenarios

1. Introduction

For the last couple of years, a new solution suitable to local energy distribution within existing power systems has been proposed and developed: microgrids [1].

The two microgrid definitions, which are currently in use, are provided by the US Department of Energy Microgrid Exchange Group and by CIGRÉ C6.22 Working Group, Microgrid Evolution Roadmap, respectively:

> *"A microgrid is a group of interconnected loads and distributed energy resources within clearly defined electrical boundaries that acts as a single controllable entity with respect to the grid. A microgrid can connect and disconnect from the grid to enable it to operate in both grid-connected or island-mode"* [2, 3].

> *"Microgrids are electricity distribution systems containing loads and distributed energy resources, (such as distributed generators, storage devices, or controllable loads) that can be operated in a controlled, coordinated way either while connected to the main power network or while islanded"* [2, 3].

The microgrid concept supports an alternative approach to the integration of distributed energy resources characterized by low installed capacity to distribution grids [4]. When compared to conventional power systems, the main advantage of microgrids consists of the controllable unit feature. Microgrids can be operated as a single load, ensuring easy control and compliance to rules and regulations without impacting the reliability and safety of the user's power supply.

Microgrids are designed to operate semi-independently, usually in grid-connected mode, providing options for isolated or islanded operation, either for economic, reliability, or

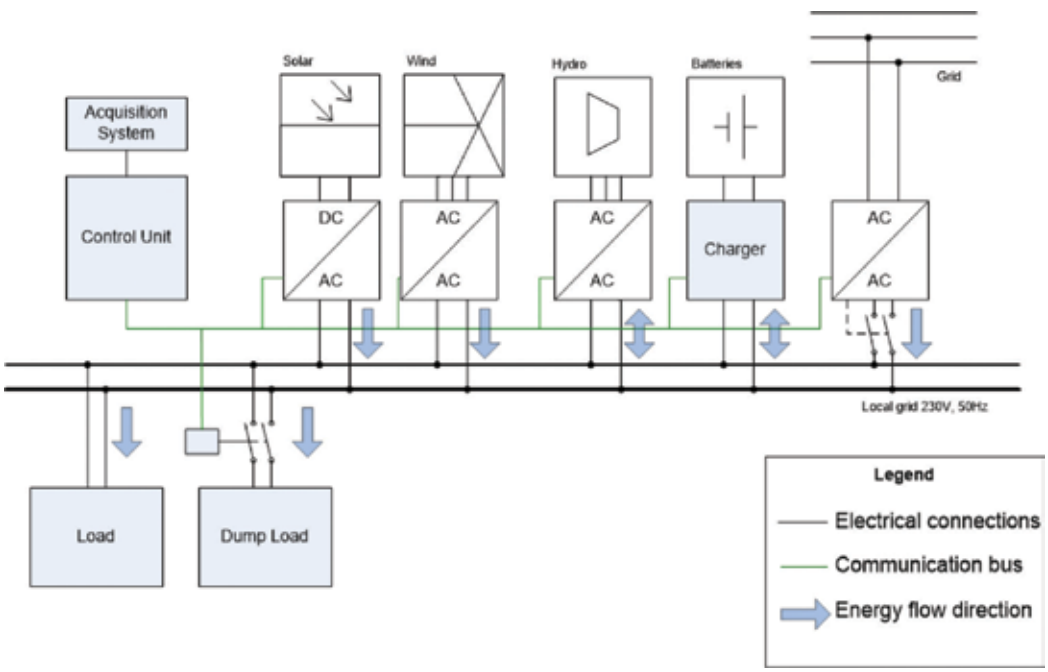

Figure 1. The conceptual model of a typical microgrid configuration [6].

security reasons. Also, the development of new energy sources as well as their integration within microgrids allows the supply of some isolated locations, such as islands or mountain areas, which are not connected to conventional power systems.

Currently, a typical microgrid configuration, **Figure 1**, consists of an open architecture, including electrical, communication, command, and control components, which allow the users and energy sources interconnection. Thanks to the capability of offering higher levels for power quality and reliability, a large number of users will adopt power supply solutions based on advanced technology and power electronics in order to minimize voltage sags, interruptions and other voltage fluctuations, or other power-quality disturbances.

Generic microgrids consist of a number of electric generators with static converters as interface modules, electric loads (to be connected either at DC or AC by inverter modules) as well as a connection (by transformer and conversion modules) to the electric distribution grid.

For an optimal microgrid operation, energy management strategies are necessary, proving their utility by adjusting the generated power for each distributed source [5] and by considering the energy storage which currently represents a main component of the energy sector.

2. Microgrid and Energy Management System configuration

2.1. Architecture of the AC/DC microgrid

The special operating conditions of the power systems require new solutions in order to ensure the continuity of the power supply. Therefore, the chapter proposes and analyzes the integration of renewable energy sources (RESs) (photovoltaic panels and wind turbines) into a mixed microgrid by using the LabVIEW software. Also, the MATLAB environment was used by introducing MATLAB scripts within the developed visual instruments (VI) diagrams.

The designed microgrid takes into account the following requirements:

- mixed microgrid, including various energy sources, which ensures the end user's power supply, by providing a high level of security;
- option to extend the grid infrastructure without achieving any changes in the existing equipment;
- option to connect to the electric public grid and to operate interconnected;
- option to store the generated power in order to establish the energy security and autonomy of the end user [6].

The developed microgrid model, **Figure 2**, includes the following components: distributed energy sources, distributed storage, backup sources for the generated power, critical or priority energy users (which do not allow any interruptions in the power supply) as well as standard users (which allow power supply interruptions) and one control unit that communicates to all the other components. The standard energy consumers, which can be considered by the

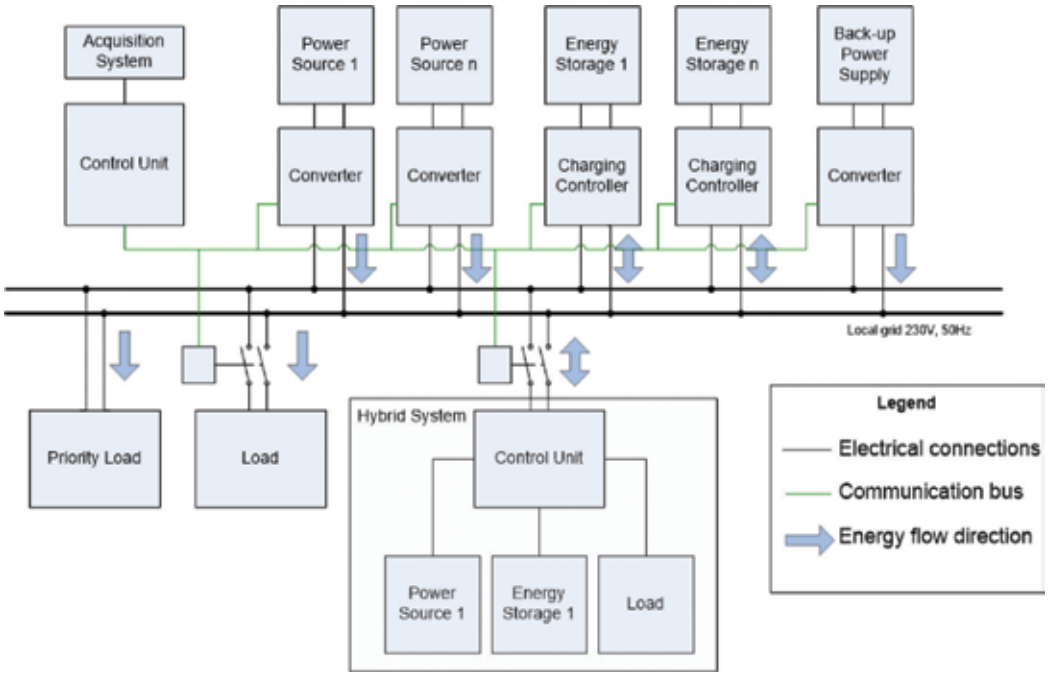

Figure 2. The developed model of mixed microgrid [6].

conceptual microgrid model, include, but are not limited to general lighting, local electrical heating and general electrical outlets. The critical consumers include the following essential services and equipment: technological processes that induce unacceptable interruption costs, safety lighting, or alarm and safety systems [7].

The microgrid model has been implemented by developing LabVIEW models for each component: photovoltaic panels, wind turbine, lead-acid batteries, and end users, all based on load curves and characteristics derived from the client's database.

2.1.1. Mathematical modeling of photovoltaic panels

The description and modeling of the PV panels was achieved by considering the simplified mathematical model based on the single-diode photovoltaic cell which gives the output power P as in Eq. (1):

$$P = U \cdot I = U_T \cdot I \cdot \ln\left(\frac{I_{ph} - I + I_0}{I_0}\right) - I^2 \cdot R_s \quad (1)$$

where

- U—voltage output (V);
- I—electric current generated by the solar cell (A);

- U_T—thermal voltage of the semiconductor (for a 300 K voltage, resulting as $U_T = 0.026$ V) (V);
- I_{ph}—electric current generated according to the values of irradiance and temperature (the theoretical cell current) (A);
- I_0—saturation current (A);
- R_S—series resistor which models the equipment power losses (Ω).

The model related to the external characteristic *I(V)* for a photovoltaic panel has been implemented by using the LabVIEW environment based on Eq. (1). Thus, **Figure 3** shows the diagram developed for a Kyocera photovoltaic panel. The diagram uses the electrical parameters from the technical specification supplied by the producer as well as the parameters suggested by the scientific literature [1, 8].

The photovoltaic panel model was then completed by modeling and implementing a maximum power point tracking (MPPT) controller circuit designed for solar power applications. This additional simulation was necessary given that photovoltaic panels are characterized by an optimization point which provides maximum power. This point generally varies according to the ambient environmental conditions. When adjusting the output voltage of the solar cells in a variable environment, permanent maximum power generation becomes a problem. Under these conditions, tracking the maximum power point for existing photovoltaic systems increases the efficiency in power generation [9].

The MPPT algorithm was implemented by measuring the electrical current for several voltage values at the required time interval. This method removes any possibility for the system to enter an unstable oscillation mode (sometimes affecting other types of algorithms). Also, the algorithm involves the constant pitch scanning of the foreseen operating range. The mentioned MPPT controller model represents a component of the AC/DC microgrid, suitable for the evaluation of the components interconnection mode.

In order to simulate the operation of the photovoltaic cell, the single-diode model with ideal *p-n* junction was used, as suggested by Eq. (1), which avoids complex calculations and leads to increasing the simulator running speed without introducing significant errors to the overall purpose of the microgrid simulator.

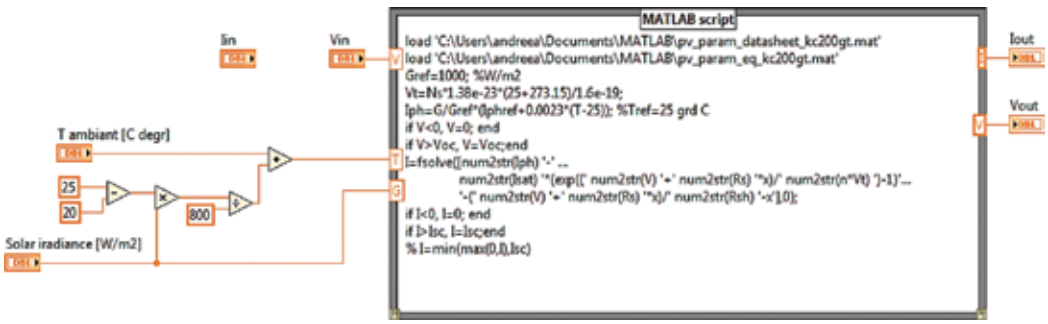

Figure 3. The diagram developed for the photovoltaic panel [1].

The MPPT simulator, initialized with the photocell parameters provided by the PV manufacturer, estimates the parameters required for the calculation model, receives from the rest of the microgrid simulator the irradiation and temperature values according to the climatic scenario, and performs a constant coverage scanning in order to determine the maximum power point. For further reducing the scaled range, the simulator starts from the maximum possible value of solar irradiation and reaches the null value of the electric current, calculating the value of generated power for each iteration. In a memory cell, only the maximum instantaneous current - power set of values is registered (which at the start of the determination is initialized and starts from 0), respectively, the power and intensity of the electric current. For each new measurement, the value of the regulated current is decremented, and the resulting power is compared to the maximum registered value. The pair of values represented by the electric current—power, which meets the condition of the highest power value, becomes the current stored value. When the instant measured power drops below 70% of the last determined maximum point, the scanning stops and the control value becomes the maximum power value.

The simulation shown in **Figure 4** is provided with a memory for the solar irradiance and temperature indicated by the last iteration climatic scenario. If the new values are different, the determination is resumed.

2.1.2. Mathematical modeling of wind turbines

Figure 5 shows the diagram developed for the evaluation of voltage and current outputs characteristic to a wind turbine. The determination of the wind turbine's output power was achieved by linear interpolation of the power characteristic in relation to the wind velocity.

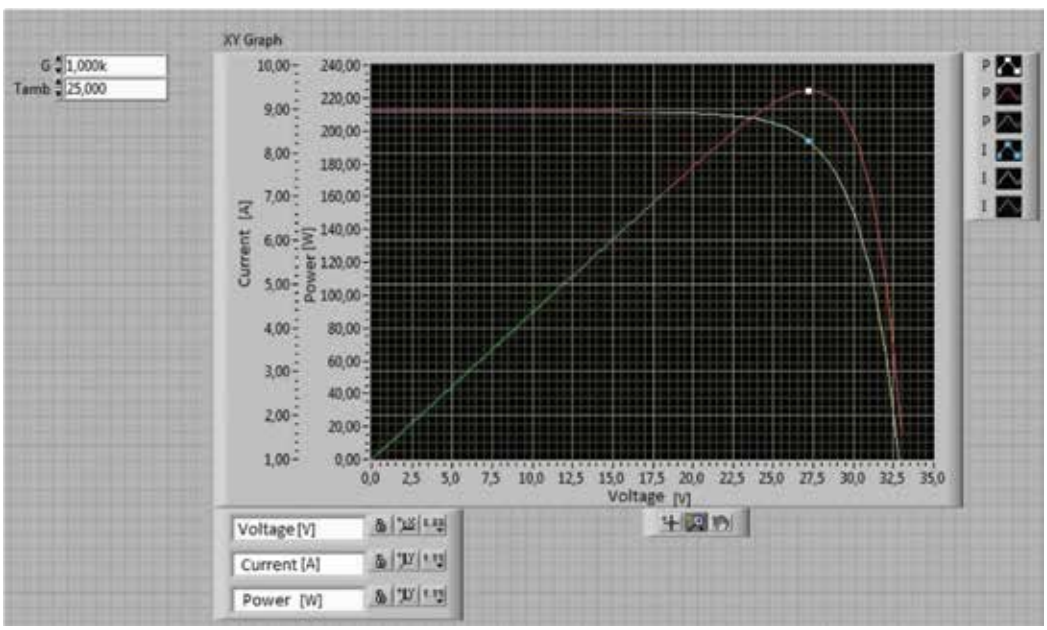

Figure 4. Simulation and modeling of the maximum power point for variable environmental conditions (G, T_{amb}).

http://dx.doi.org/10.5772/intechopen.74856

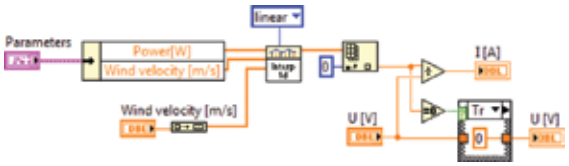

Figure 5. The wind turbine diagram implemented in LabVIEW [1].

The output current was computed by considering the wind turbine's operating voltage equal to the microgrid's voltage U_n = 24 V. Also, the theoretical power of the wind turbine, P (W), was taken into account, expressed in Eq. (2):

$$P = \frac{1}{2}\rho A C_p v^3 \tag{2}$$

where

- ρ—air density (kg/m^3);
- A—area of the surface described by the turbine rotor, which is perpendicular to the wind direction (m^2);
- C_p—power coefficient;
- v—wind velocity at the turbine entrance (m/s) [1].

2.1.3. Mathematical modeling of battery storage systems

Most power systems with insulated operation, which are designed for consumers' continuous supply, require battery storage systems in order to equalize the irregular nature of meteorological parameters. Currently, the most used batteries for renewable energy sources applications consist of lead-acid (PbA), lithium-ion (Li-ion) or nickel-cadmium batteries [10].

The mathematical models related to battery storage systems are targeting the simulation of real operation characteristics and are used for the behavior estimation related to variable charging and discharging conditions. The mentioned models are also suitable for storage batteries design due to the fact that they allow the analysis of charging and discharging modes independently of the supplied system.

The developed AC/DC microgrid is based on the Shepherd model which describes the electrochemical processes depending on the voltage and electric current values. The Shepherd model also considers the Peukert law, Eq. (3), in order to determine the battery voltage and state of charge.

$$E_b = E_0 - R_i I - K_i\left(\frac{1}{1-f}\right)I \tag{3}$$

where

- E_b—battery terminals voltage (V);
- E_0—open-circuit voltage at the battery terminals when the battery is completely discharged (V);

- R_i—internal resistance of the battery (Ω);
- K_i—polarization resistance of the battery (Ω);
- Q—capacity of the battery (Ah);
- I—electric current (A);
- f—fraction extracted from the battery (the capacity extracted from the battery rated to the fully charged battery's capacity Q_0) as suggested by Eq. (4)

$$f = \int_0^t \frac{I \cdot dt}{Q_0} \tag{4}$$

Figures 6 and **7** show an example simulation model of a PbA battery storage system operation when considering a discharging and afterwards a charging current rate of 0.8 A.

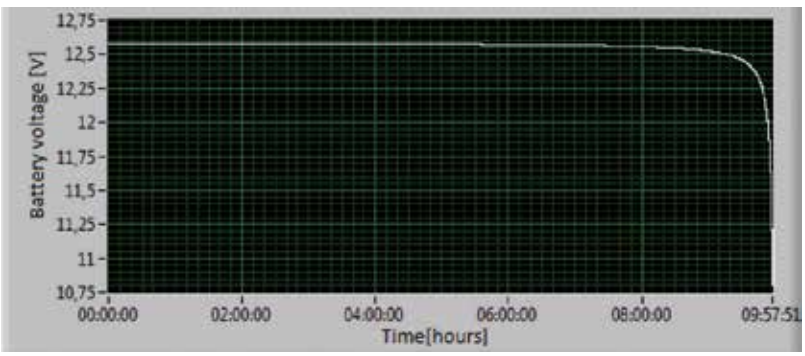

Figure 6. Voltage variation at the battery terminals during a discharging cycle for a discharge current rate of 0.8 A.

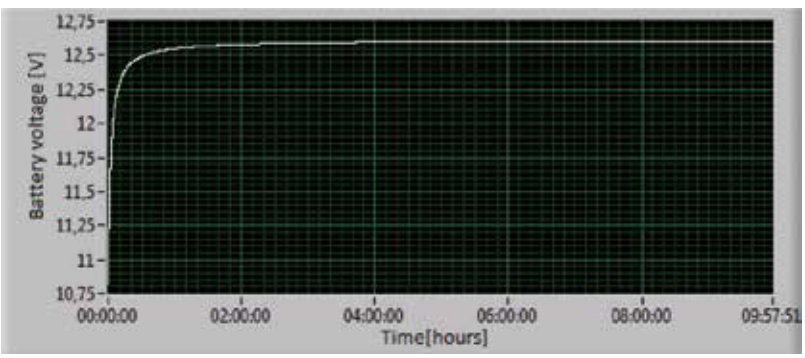

Figure 7. Voltage variation at the battery terminals during a charging cycle for a charge current rate of 0.8 A.

2.2. Configuration and structure of the Energy Management System

The main characteristics of the designed Energy Management System (EMS) consist of the following:

- The option of computing for any practical configuration of the microgrid, providing the possibility of adapting to the needs of each beneficiary.
- The option of implementing energy storage during low-cost periods and injecting it into the electric public grid during high-cost periods; even though this strategy is commonly used, EMS can still not be economically efficient due to limitations imposed by the storage equipment. Also, this involves risks in critical users power supplying.
- Ensuring and maintaining energy backup.
- The option of connecting or disconnecting backup sources that are not generally represented by RES and therefore dispose of limited available power and/or at an inconvenient price cost. In this case, EMS disconnects users according to their associated priority.
- The option of estimating the available power, which, in the absence of storage equipment, is achieved by monitoring and registering the primary energy sources like wind and sun.
- The option of implementing the electric public grid within the developed model of AC/DC microgrid as follows: either backup energy source, dump-load consumer or both [6, 11].

The algorithm covers the energy management functions and is based on the developed microgrid model which includes the control unit. Thus, for initializing it, the information about the components must be inserted as follows:

The *energy generation sources* require the following information:

- port—parameter assigned to communication/monitoring/control;
- installed power;
- dependent size and conversion factor—for the estimation of energy generation;
- available power;
- the production cost/kWh.

The *end users* require the following information:

- port—parameter assigned to communication/monitoring/control;
- installed power;
- priority—parameter which allows the end users selection for different operating scenarios;

- operation mode (without any interruptions, permanent or continuous, dump load—connection for injecting the production excess of electric power);
- sale price—electricity pricing for the energy which is sold to the end user (if applicable).

The *battery storage systems* require the following information:

- port—parameter assigned to communication/monitoring/control;
- storage capacity;
- storage cost—estimated cost/kWh depending on the limitations of the storage equipment.

The *Energy Management System* parameters consist of the following:

- LIM_SOC_SOURCES—the limit of storage devices for which the backup sources are connected;
- LIM_SOC_SAFETY—the limit of storage devices for which standard end users are disconnected;
- LIM_COST_SOURCES— the high-priced sources are connected only if necessary;
- INCOME_THRESHOLD—the price threshold for which the energy injection into the public grid begins;
- ALLOW_EMPTY_BAT—it allows the use of the stored energy for a maximum profit;
- T_AVERAGING—the averaging time of the measurements. This parameter influences the values of the reaction time [6, 11].

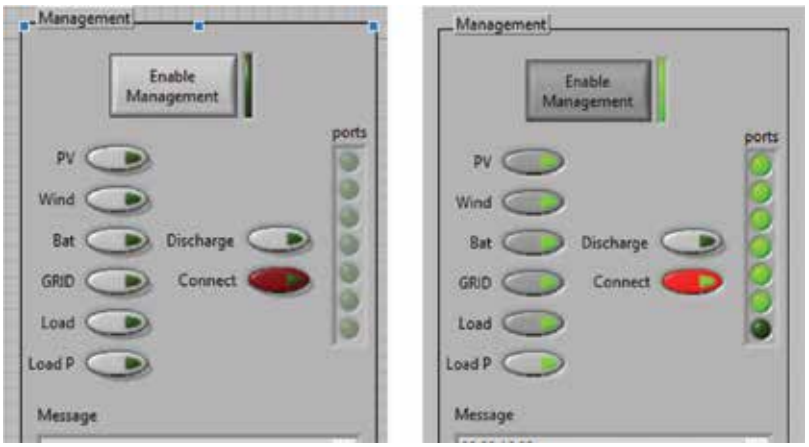

Figure 8. The graphical interface of the developed Energy Management System. The ON/OFF state for the microgrid components and activation/deactivation of the Energy Management System.

Figure 8 shows the graphical interface of the developed Energy Management System. This highlights the connection state (connected or disconnected) related to the considered distributed energy generation sources, battery storage systems, end users as well as the islanded or interconnected operation of the microgrid to the national power system. Also, the connection state regarding the "ports" vector has been envisaged, which has resulted in using the BUILD ARRAY function and thus connecting the communication/command parameters of each element in series [12]. The dependence between the connection state of each component (Boolean and "ports" elements) is shown.

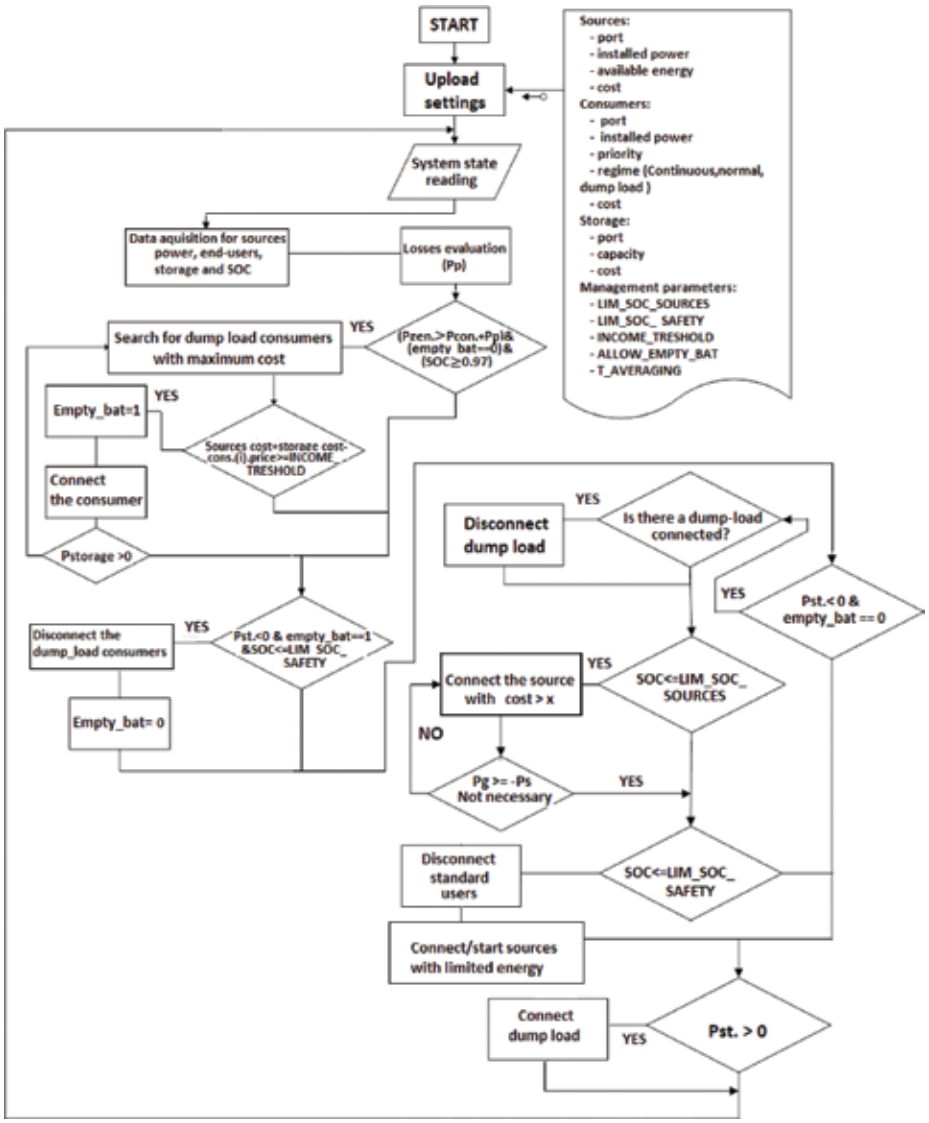

Figure 9. The block diagram of the Energy Management System concept [6, 11].

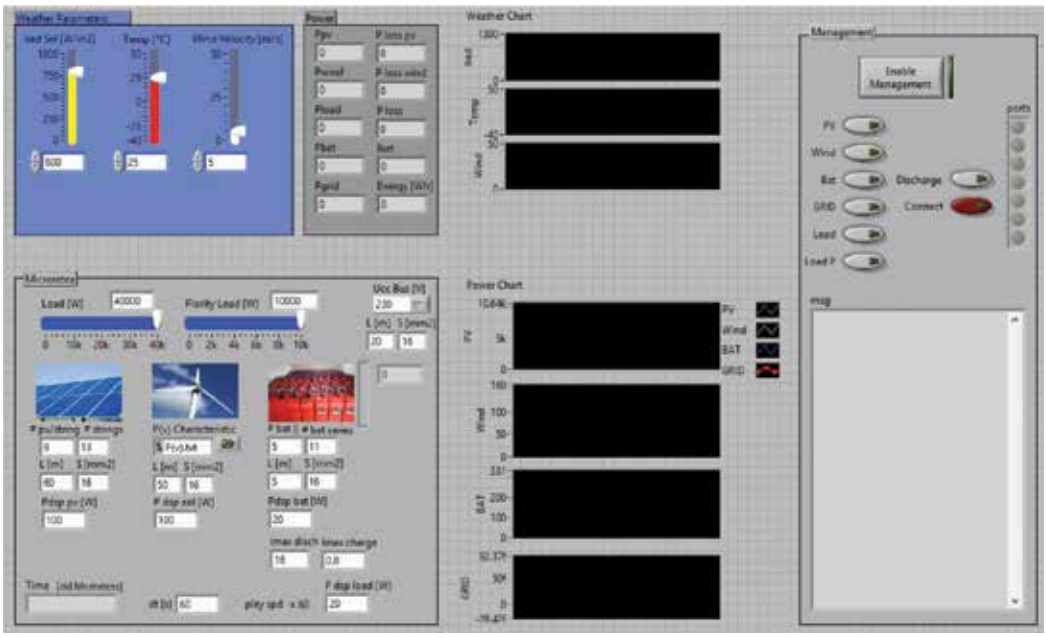

Figure 10. The graphical interface of the developed application for the modeling and simulation of a small-scale microgrid and the related Energy Management System.

Figure 9 contains the block diagram of the Energy Management System concept designed for the islanded or interconnected operation of the microgrid with the national power system while **Figure 10** shows the graphical interface of the developed application related to the microgrid design and simulation.

In addition to the LabVIEW environment, MATLAB was used as well by introducing a MATLAB script within the developed VI related to the Energy Management System. **Figure 11** shows a section of the main loop management, presenting a MATLAB residue code which was then implemented in the general LabVIEW diagram.

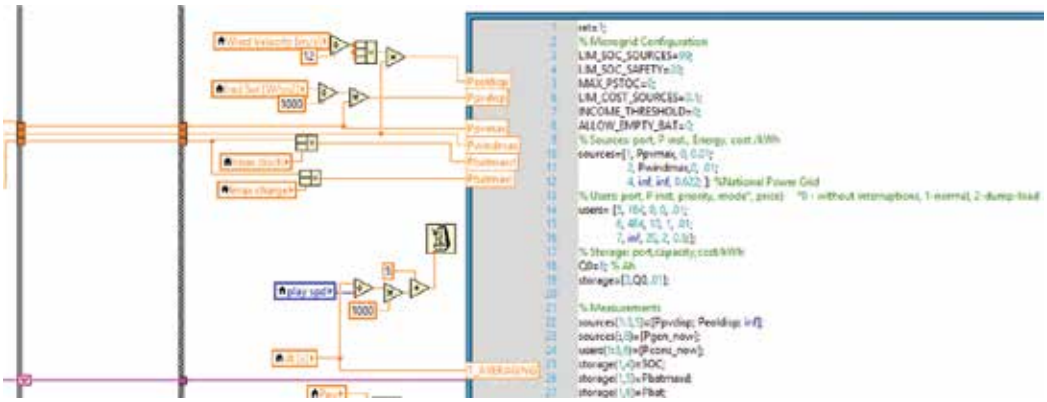

Figure 11. Section of the MATLAB script related to the LabVIEW Energy Management System.

3. Experiments and simulation results of the Energy Management System: operation scenarios

The Energy Management System implies independent automatic decisions from a potential user's decisions. The developed microgrid is operational even without an Energy Management System, but it is not provided with automatic decisions which aim the control of the energy flows or connection/disconnection actions of the component elements. Consequently, it results in the energy management for the optimization of both the microgrid operation and beneficiary's income/benefit. Moreover, in order to demonstrate the functionality of this system, the following operating scenarios, available for the "Enable management—ON" state, are suggested.

Operating scenario number I. The distributed energy generation sources (wind energy conversion system, photovoltaic system), the battery storage systems as well as the connection to the low-voltage distribution grid are available. This operating scenario involves the variation of the meteorological parameters during the microgrid functioning. Also, a calculation step $\Delta t = 40$ s is used, during which all the parameter values are maintained constant.

The first operating scenario, represented in **Figure 12**, considers two time moments when the meteorological parameters vary, respectively, t_1—the moment when the solar irradiation drops and t_2—the moment when the solar irradiation increases. These two time moments are established randomly by the user of the LabVIEW application.

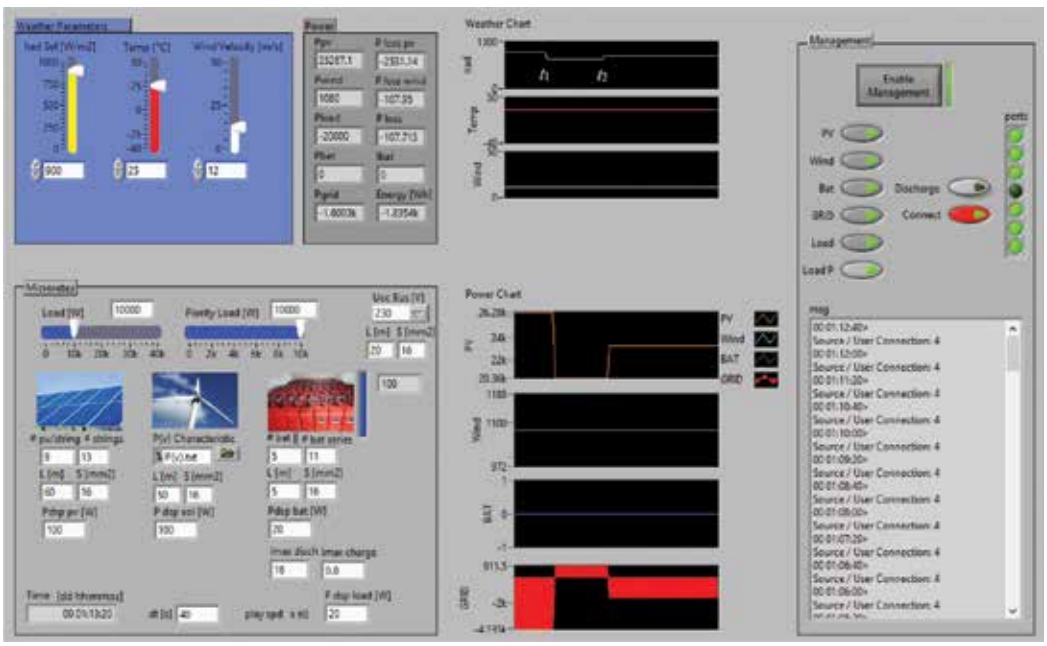

Figure 12. The graphical interface of the developed application for the modeling and simulation of a small-scale microgrid and the related EMS. Operating scenario number I.

It is to be noted that at the first moment t_1, the photovoltaic power plant lowers the power output from 26.28 to 20.36 kW due to a decrease of the solar radiation from 1000 to 800 W/m^2. Until then, there is no need to transfer any energy from the public electric grid. From this moment on, the generated power within the microgrid decreases, and a necessary input from the National Power System is needed (P_{grid} = 911.5 W). At the second considered moment t_2, the solar irradiance increases from 800 to 900 W/m^2. Therefore, the generated solar power increases from 20.36 to 23.28 kW, and the power input from the National Power System is no longer needed. Contrary to the situation before, after the moment t_2, the excess energy production will be injected into the public grid.

As suggested by **Figure 12**, it is possible to fully ensure the load supply (20 kW) from the production of energy from renewable energy sources during the intervals (0; t_1) and (t_2, end of the simulation), while maintaining the batteries fully charged. Following the supply of the battery storage systems and of the end users, the excess available energy will be injected into the public grid (P_{grid} = 1.6003 kW; *energy* = 1.8354 kWh). The power losses are also considered (related to lines and conductors and to the electronic power devices, respectively). It is noted that the Energy Management System decides to use the National Power System as an energy dump load while the excess energy production is injected into the public grid.

Operating scenario number II. The distributed energy generation sources (wind energy conversion system, photovoltaic system), the battery storage systems as well as the connection to the low-voltage distribution grid are available. In this case, the end users necessary energy is higher than the one considered in the first scenario ($P_{load} + P_{load\ p}$ = 50 kW) and higher than the energy produced from renewable sources. This operating scenario involves the variation of the meteorological parameters during the microgrid functioning. Also, a calculation step Δt = 20 s is used, during which all the parameter values are maintained constant.

The second operating scenario, represented in **Figure 13**, considers two time moments when the meteorological parameters vary, respectively: t_1—the moment when the solar irradiation drops and t_2—the moment when the location wind velocity increases. These two time moments are established randomly by the user of the LabVIEW application.

It is to be noted that at the first moment t_1, the photovoltaic power plant lowers the power output from 26.28 to 20.36 kW due to a decrease of the solar radiation from 1000 to 800 W/m^2. Until then, the necessary power from the public electric grid for the end users supply was equal to P_{grid} = 26.82 kW. From this moment on, the generated power within the microgrid decreases, and a larger necessary input from the National Power System is needed (P_{grid} = 31.87 kW). At the second considered moment t_2, the location wind velocity increases from 8 to 12 m/s. Therefore, the generated wind power increases from 450 W to 1.08 kW. The microgrid-generated power increases as well and consequently the power input from the National Power System decreases (P_{grid} = 31.242 kW).

As suggested in **Figure 13**, it is possible to fully ensure the load supply (50 kW) from the production of energy from renewable sources and the electric public grid. The power losses are also considered (related to lines and conductors and to the electronic power devices, respectively). It is noted that the Energy Management System decides to use the National Power System as an energy generation source, while the microgrid energy production is completed by the public grid.

http://dx.doi.org/10.5772/intechopen.74856

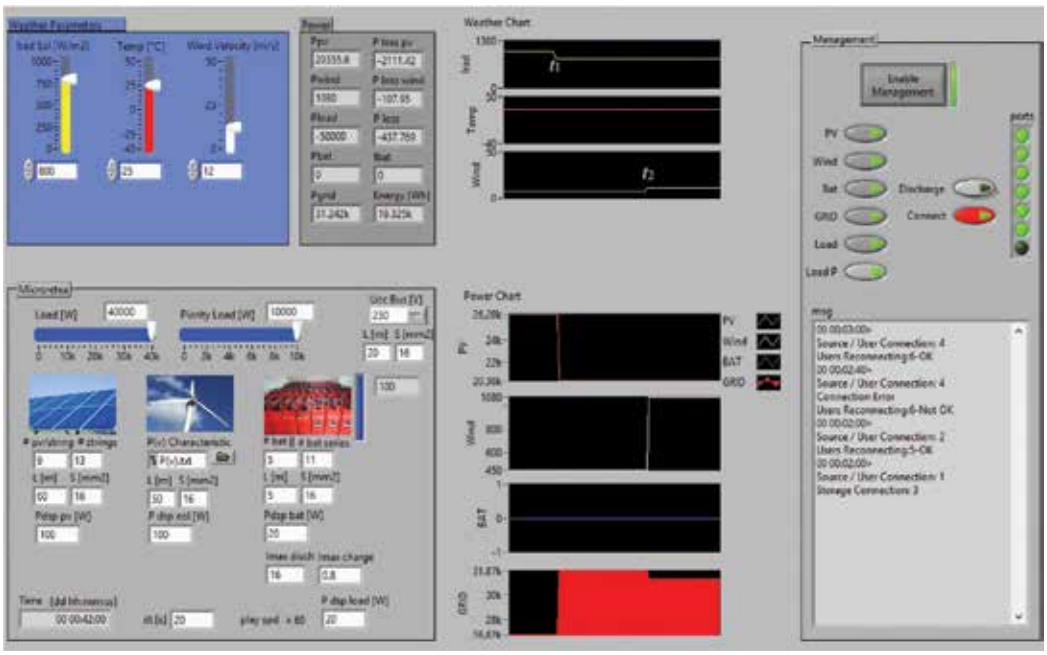

Figure 13. The graphical interface of the developed application for the modeling and simulation of a small-scale microgrid and the related Energy Management System. Operating scenario number II.

Operating scenario number III. The distributed energy generation sources (wind energy conversion system, photovoltaic system), the battery storage systems as well as the connection to the low-voltage distribution grid are available. This operating scenario does not involve the variation of meteorological parameters during the microgrid functioning. A calculation step $\Delta t = 30$ s is used, during which all the parameter values are maintained constant.

As shown in **Figure 14**, at the first moment t_1, the unwanted discharge of the battery storage system takes place in order to supply the end users. The battery discharges up to a safety limit of 15%, established by the Energy Management System. Until the moment t_1, the necessary power from the public electric grid for the end users supply was equal to $P_{grid} = 27.11$ kW. From this moment on, when the battery discharges, the power input from the National Power System decreases to $P_{grid} = 16.557$ kW due to the energy transfer from the storage systems ($P_{bat} = 10.71$ kW).

The Energy Management System detects the unwanted discharge of the battery storage system and stops its discharging at the moment t_2, when the 15% limit is reached. Thus, **Figure 15** shows a new charging cycle of the considered storage systems and the complete load supply from renewable energy sources as well as from the electric public grid ($P_{grid} = 27.657$ kW, $P_{pv} = 26.284$ kW, $P_{wind} = 160$ W).

These two time moments t_1 and t_2 are established randomly by the user of the LabVIEW application.

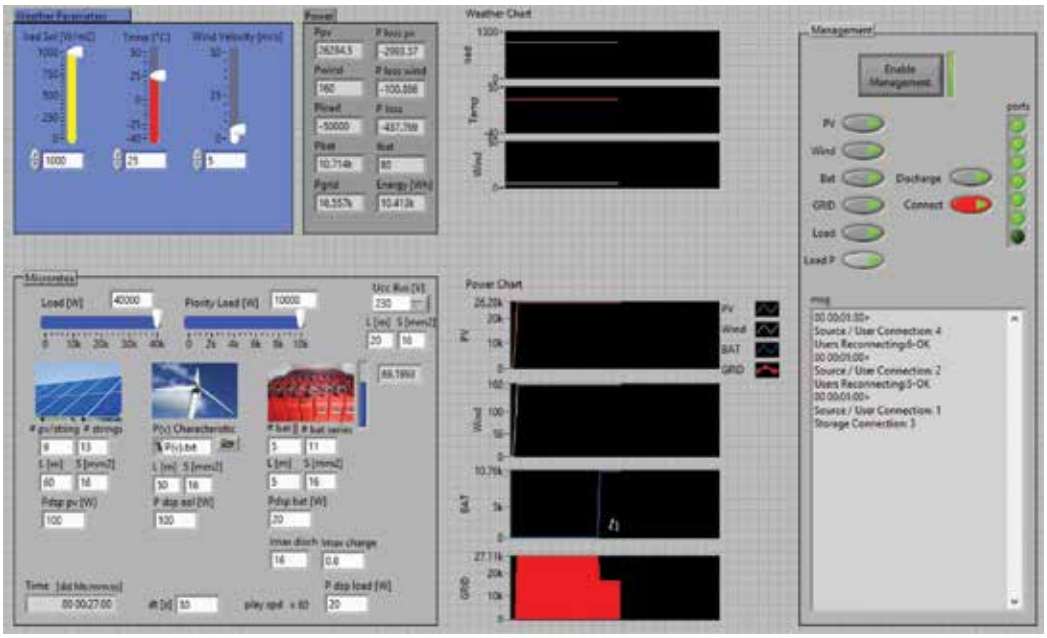

Figure 14. The graphical interface of the developed application for the modeling and simulation of a small-scale microgrid and the related Energy Management System. Operating scenario number III—Section 1.

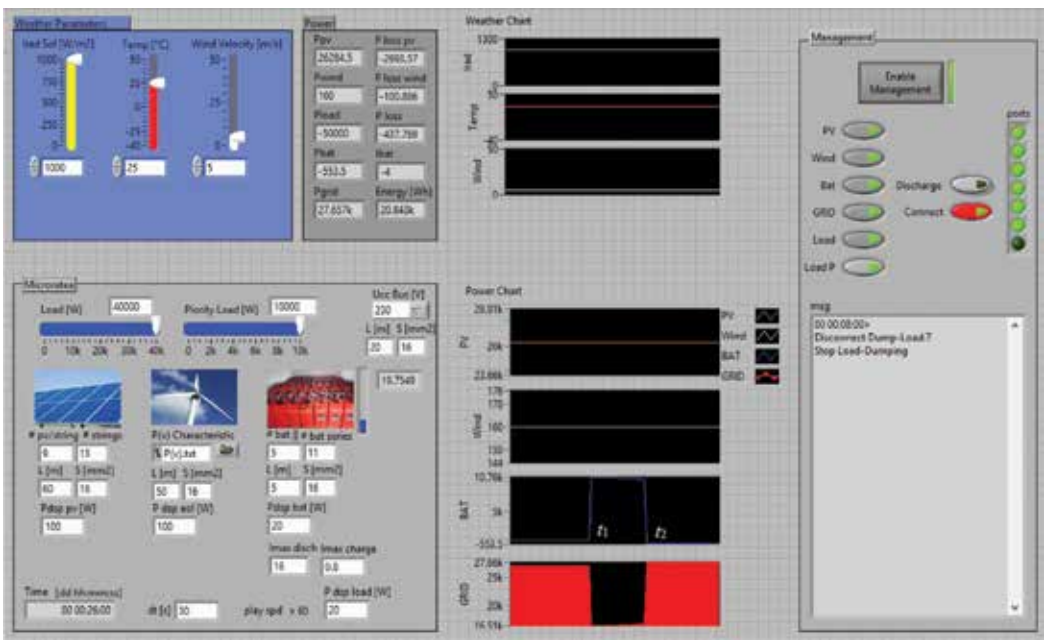

Figure 15. The graphical interface of the developed application for the modeling and simulation of a small-scale microgrid and the related Energy Management System. Operating scenario number III—Section 2.

http://dx.doi.org/10.5772/intechopen.74856

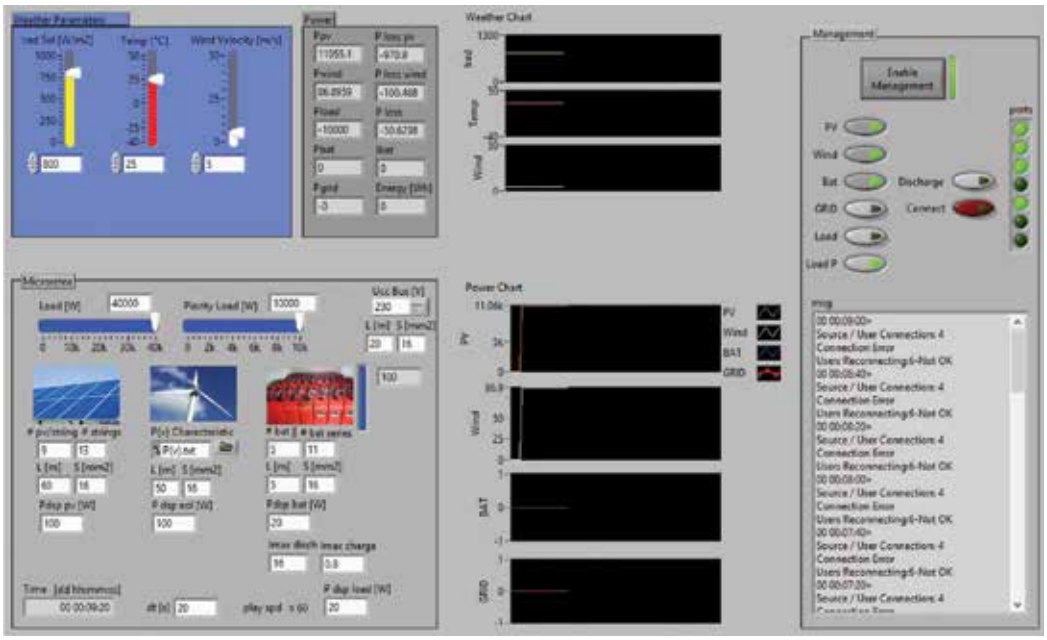

Figure 16. The graphical interface of the developed application for the modeling and simulation of a small-scale microgrid and the related Energy Management System. Operating scenario number IV—Section 1.

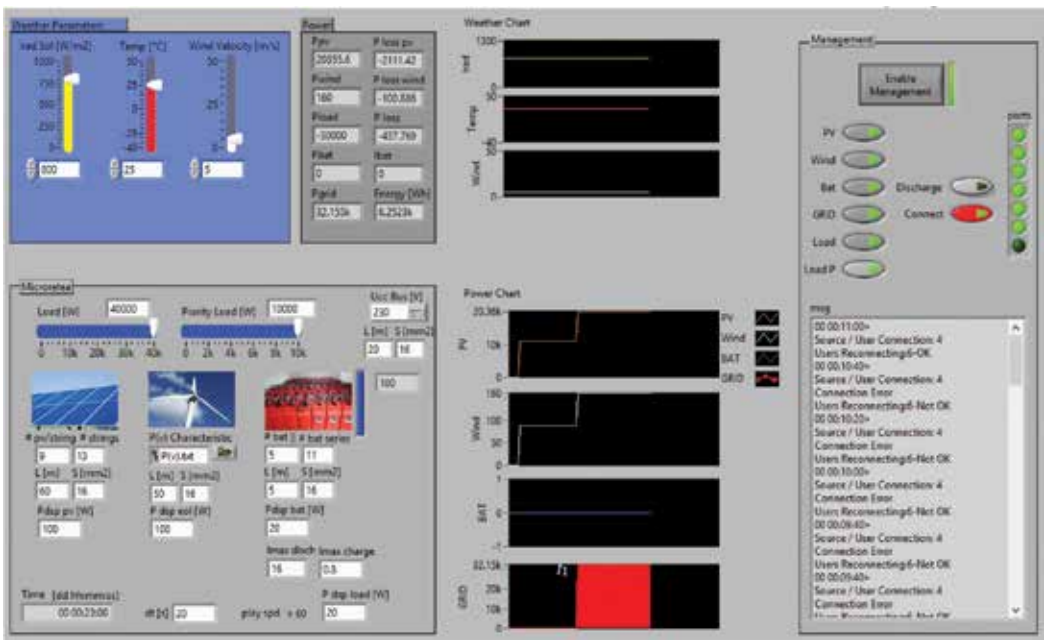

Figure 17. The graphical interface of the developed application for the modeling and simulation of a small-scale microgrid and the related Energy Management System. Operating scenario number IV—Section 2.

Operating scenario number IV. The distributed energy generation sources (wind energy conversion system, photovoltaic system) as well as the battery storage systems are available. This operating scenario does not involve the variation of meteorological parameters during the microgrid functioning. A calculation step $\Delta t = 20$ s is used, during which all the parameter values are maintained constant. **Figure 16** shows the absence of the connection to the low-voltage distribution grid.

The Energy Management System evaluates initially the necessary of the end users' power supply ($P_{load} + P_{load\,p} = 50$ kW), establishes that there is not enough energy for the complete supply and then connects only the priority or critical load (*Load P*) and not the standard one (*Load*). As seen from **Figure 16**, EMS attempts the reconnection, but it fails and supplies only the priority load.

At the moment t_1, when the connection to the low-voltage distribution grid becomes available, EMS decides to use the National Power System as an energy generation source, while the microgrid energy production is completed by the public grid ($P_{grid} = 32.155$ kW). Thus, the other consumers are also reconnected ($P_{load\,p} = 40$ kW) as indicated in **Figure 17**.

The time moment t1 is established randomly by the user of the LabVIEW application.

4. Conclusion

The proposed LabVIEW solution regarded a small mixed microgrid with two separate AC and DC rings bidirectionally interconnected by static converters. In this respect, the mathematical modeling of PV panels, wind turbine, and battery storage systems was achieved, followed by their implementation within the mentioned microgrid by using the LabVIEW environment.

Furthermore, an Energy Management System related to the microgrid model was developed. Thus, the chapter intends to develop an intelligent Energy Management System suitable to the microgrid components (wind energy conversion system, photovoltaic systems, and battery storage systems). The LabVIEW application is provided with a graphical interface, which allows to identify and establish the initial conditions (meteorological parameters, component elements) as well as the microgrid's characteristic parameters.

The diagram corresponding to microgrid LabVIEW modeling and simulation is equipped with Boolean buttons representing the connection status (disconnected or connected) of the distributed generation sources, storage elements, and end users and highlighting the islanded or interconnected operation with the low-voltage distribution grid. To that end, various operating scenarios were proposed, for which the results and operability of the Energy Management System were analyzed. It is to be noted that the developed EMS is suitable to any practical configuration of the microgrid, microgrid that can be adapted to the requirements of each beneficiary.

Acknowledgements

This work was supported by the following grants of the Romanian Ministry of Research and Innovation, CCCDI–UEFISCDI: project number PN-III-P1-1.2-PCCDI-2017-0391 /

CIA_CLIM - Smart buildings adaptable to the climate change effects, and project number PN-III-P1-1.2-PCCDI-2017-0254/ SMARTIRRIG - Innovative technologies for irrigation of agricultural crops in arid, semiarid and subhumid-dry climate, within PNCDIIII. The work was also financially supported by ANCSI, Romania, under the scientific Programme NUCLEU 2009-2015, Contract PN 09350201.

Moreover, I would like to thank Professor Nicolae Golovanov for his expert advice and also my colleague from the National Institute for Research and Development in Electrical Engineering ICPE-CA, Bucharest, Romania, Dr. Adrian Nedelcu, who provided the simulation insight and expertise that greatly assisted the research.

Conflict of interest

The author declares that there is no conflict of interest. Thus, there are no conflicts of interest to disclose.

Appendices and nomenclature

EMS	Energy Management System
MPPT	maximum power point tracking
P_{con}	power consumption
P_{gen}	generated power
P_{p}	power losses
$P_{storage}$ (P_{st})	stored power
PV	photovoltaic
RES	renewable energy sources
SOC	state of charge

Author details

Lucia-Andreea El-Leathey

Address all correspondence to: andreea.elleathey@icpe-ca.ro

National Institute for Research and Development in Electrical Engineering ICPE-CA, Bucharest, Romania

References

[1] Mituleț LA, Nedelcu A, Nicolaie S, Chihaia RA. LabVIEW design and simulation of a small scale microgrid. UPB Scientific Bulletin, Series C, Electrical Engineering and Computer Science. 2016;**78**(1):235-246. ISSN: 2286-3540

[2] Microgrids at Berkeley Lab [Internet]. Available from: https://building-microgrid.lbl.gov/microgrid-definitions [Accessed: January 10, 2018]

[3] El-Leathey LA, Nicolaie S, Chihaia RA, Oprina G. technical economic analysis of a small-scale microgrid for a specific location. Electrotehnica, Electronica, Automatica (EEA). 2016;**63**(3):134-140. ISSN 1582-5175

[4] Albu M. Advanced Electrical Systems – Smart Grids for Electric Power Distribution. Student Curriculum, 2012-2013

[5] Yunwei L, Nejabatkhah F. Overview of control, integration and energy management of microgrids. Journal of Modern Power Systems and Clean Energy. 2014;**2**(3):212-222

[6] Research Project Financed by ANCS Romania. Increasing the Efficiency of Technological Equipment and Processes for Energy Conversion from Renewable Sources, Objective 5: 1.5 kW Experimental Model of Autonomous Power Supply System Consisting of Integrated Renewable Energy Sources Grid. Contract no. 09350201. Coordinator: INCDIE ICPE-CA (Team Member)

[7] Albert H, Gheorghe S, Golovanov N, Elefterescu L, Porumb R. Electric Power Quality, Contributions, Results, Perspectives. Bucharest: AGIR; 2013. Available from: http://www.agir.ro/carte/calitatea-energiei-electrice-contributii-rezultate-perspective-121705.html

[8] Chouder A, Silvestre S, Taghezouit B, Karatepe E. Monitoring, modelling and simulation of PV systems using LabVIEW. Solar Energy. 2013;**91**:337-349

[9] Using NI CompactRIO to Design a Maximum Power Point Tracking Controller for Solar Energy Applications. Available from: http://sine.ni.com/cs/app/doc/p/id/cs-11738# [Accessed: January 10, 2018]

[10] Tiwari GN, Dubey S. Fundamentals of Photovoltaic Modules and their Applications. RCS Publishing, Cambridge; 2010

[11] El-Leathey LA. The Interconnected Operation of a Microgrid with the National Power System [Thesis]. University POLITEHNICA of Bucharest - Faculty of Power Engineering; 2016

[12] Marzband M, Sumper A, Chindriș M, Tomoiagă B. Energy Management System of Hybrid Microgrid with Energy Storage. Agir Bulletin. 2012;3(June–August): 635-642

Chapter 4

Transformation of Conventional Houses to Smart Homes by Adopting Demand Response Program in Smart Grid

Mohammad Shakeri and Nowshad Amin

Additional information is available at the end of the chapter

http://dx.doi.org/10.5772/intechopen.74780

Abstract

In an ever-growing state of electricity demand due to population growth as well as modernization of societies, it has compelled us to look for many options to cope with the situations. However, for a balanced electrical power demand and supply, it is necessary to respond requirement at any time without any interruption with the strategy of demand response programs (DRP) to the users. In order to promote smart usage of electrical power, smart grid networks are gradually transforming conventional grids in many places. As a part of smart grid, conventional houses may be transformed to smart house by simply implementing some intelligent controller with interfaces like smart plugs to the conventional electrical appliances. This chapter elaborates a new strategy of home energy management system (HEMS) in a smart grid environment to transform any ordinary premises to smart house to be energy efficient by simply rescheduling operation time.

Keywords: smart grid, demand response, home energy management systems (HEMS), smart appliance, smart plugs

1. Introduction

Until recent times, peak-hour electrical demand and supply were usually controlled by human-interface-based load control approach. The strategy required cooperation of the consumers to calculate and analyze their consumption in peak hours to reduce their consumption and eventually electricity costs. Although this strategy was simpler and cheaper for utility companies, the method was not effective in most of the cases as usually consumers lacked knowledge about the consumption of their electrical appliances. Therefore, changing the

perspective to smart usage of electrical power within the limitation, a new avenue called demand response programs (hereafter, DRPs) is considered as the most helpful to control the electricity consumption [1]. This may be realized by simply replacing the conventional electrical appliances to smarter appliances or even installing some smart interfaces like smart plugs to convert them to smarter ones.

DRPs enable us to reduce the greenhouse gas emission and improve grid efficiency as well as stability of the power plant by the smart usage of the electricity. In other words, more efficiency in the electricity market can be achieved by smartening the supply, consumption, distribution, and storage methods. Some of the advantages of using DRPs are listed as follows:

- The programs can reduce the overall power consumption at peak hours and consequently reduce the electricity price by shifting the loads to off-pick hours.
- The programs can help the utility companies to economically produce electricity.
- The programs can be useful in abnormal or emergency conditions.

According to some studies [2, 3], DRPs are defined as the modification in demand by shifting or shedding the loads when there is a shortage or excess of power in response to the condition of suppliers. Since 1970s, DRPs appeared in the United States to control peak hours. In those decades, incentive programs [4] and priced-based programs such as time of use price (TOU) [5] were utilized to analyze and control the demand [6]. In the following decades, gradually other strategies and techniques have been used as demand response programs such as critical pick price (CPP) [7], real time price [8], 1-day-ahead price [9], and incremental block rate (IBR) price [10, 11]. **Figure 1** shows the different types of demand response programs used till date in a chart.

However, DRPs could not individually reduce the electricity consumption or increase the rate of participants, as consumers do not have enough knowledge or cannot calculate and analyze their power consumption to control the electrical appliances according to commands from the utility companies [12]. Thus, intelligent equipment and technologies in grid infrastructure have appeared to control the dwellings' electricity consumption independently.

Nowadays, it is possible to develop small, cheap, and efficient smart controllers that can be used to gather different types of data, store, and analyze them by utilizing integrated technologies such as embedded systems, microcontrollers, and wireless communication technologies. Network sensors have a wide range of application in many aspects such as smart homes, military services, forecasting, industrial agriculture, and building energy management system.

Collected data can be sent in any communication ways, such as wireless network or to the host services to be shown on the web [13] in real time. Intelligent buildings are new concepts that refer to an electricity demand that use sophisticated technologies to provide better performance for energy management system. This could happen by using smart controllers besides the bidirection communication that enables the utility companies to monitor and control the power consumption of the group of residential units autonomously [14, 15].

Energy management systems can control the operation of appliances in response to electricity price or commands of utility companies to optimize the electricity consumption at peak hours. This can be done by smartening the electrical appliances in residential units to control their

http://dx.doi.org/10.5772/intechopen.74780

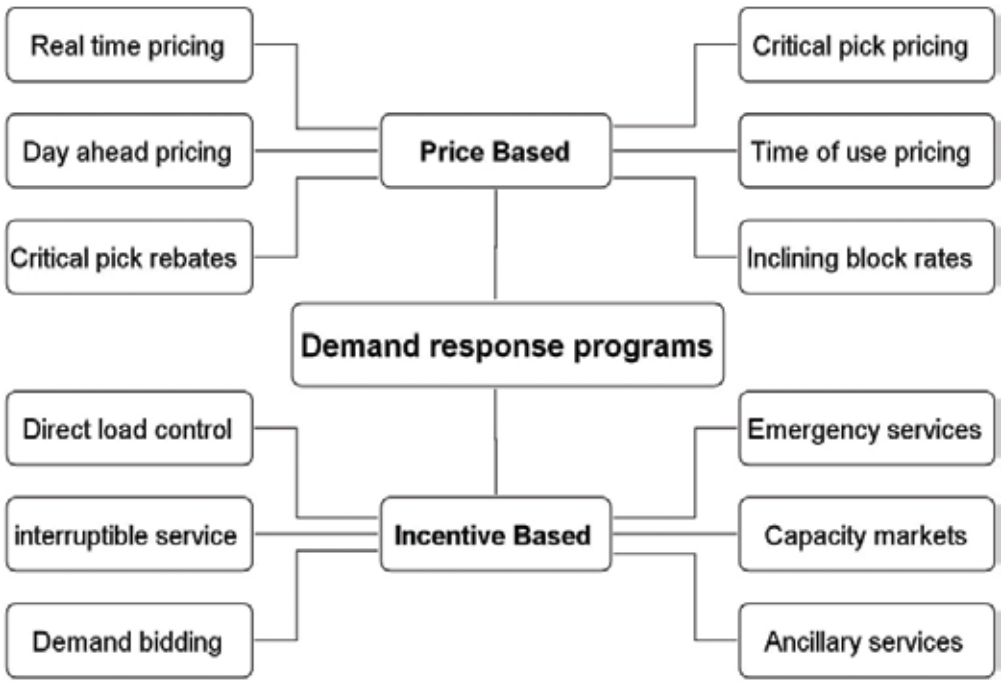

Figure 1. Demand response programs used till date.

power consumption. However, the majority of appliances that are used in demand are still uncontrollable and they cannot participate in demand response programs to optimize the overall power consumption. Therefore, the main objective in participating in smart grid is by converting the conventional electrical appliances into the smart appliances by utilizing smart plugs. These smart plugs are able to monitor and control the electrical appliances by running on scheduled operation of the appliances.

2. Development of electrical grids

2.1. Conventional grid

Over the last few decades, government bodies in many countries were responsible for controlling and monitoring of the electrical power plants while power systems were barely owned by the private sectors. The grid was designed to look like a tree, where generators were considered as the trunks, transmission paths represented as the branches, and loads considered as leaves [16] as shown in **Figure 2**. Therefore, this structure of the power plants was not efficient enough to ensure the benefits of the producers.

Privatization of the power system was the key solution for many governments to provide the competitive market at different levels of generation, distribution, and transmission. Therefore,

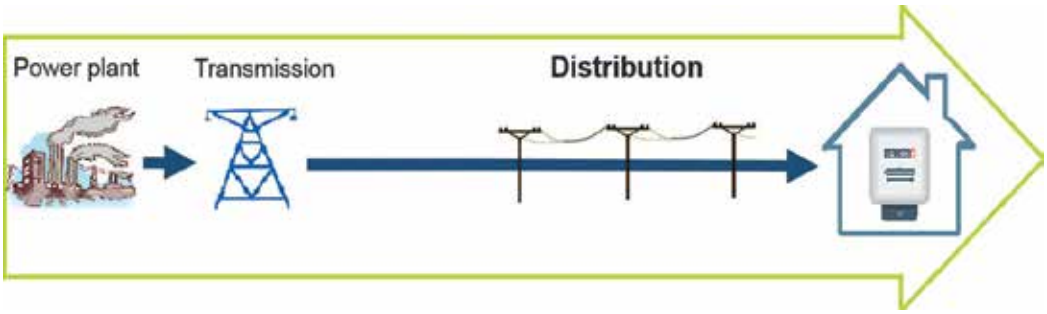

Figure 2. Structure of the traditional power plants.

electrical power industry was split into two categories such as the wholesale sector to be managed and controlled by government and the retailer sector to be controlled by private companies.

Until recently, the wholesale sector consisted of the generation side that produces electric power in bulk volume and transmits it to the demand sites and industries through transmission lines. Then, the retailer companies purchased the electricity on behalf of demand side. Therefore, in this deregulated electricity market, only the generation side competed with each other to sell their product to customers in order to increase their profit, while demand side had no power/activity in this respect.

In other words, demand side dealt with electrical power like a merchandise that was always available. Therefore, this issue showed the kind of rigidity of the power plants. Sooner, it was realized that demand side needed to participate in the energy market as a tool to control the power consumption and would yield any cost to be purchased for electrical power. The outage is the most important uncertainty in generation side, which may have occurred by the lack of generation or excess of demand. Moreover, the current grid is not built and designed for variable renewable energy generation and interactive demand response programs. Hence, the grid of the future should accommodate the changes [17].

2.2. Smart grid

The spread of renewable energy resources, demand response programs, and distributed generators put the traditional grids, which are commonly designed based on the centralized and fuel-based generators, to face challenges such as increasing the efficiency of the grid and reducing the greenhouse gas emission [6]. Furthermore, there are many important factors such as the consumer's participation in the electricity market, integrating the new technologies, and improving the reliability of the grid that have led to incorporate the smart grids in many countries.

The smart grid is the new conception of bidirectional flow of data as well as the electricity power. This can lead to the higher flexibility of the grid to be monitored, controlled, and communicate between the supply chain and demand side to improve the efficiency, reduce the consumption and electricity price, and thus maximize the reliability of the electricity supply chain. Continual development of electrical energy technologies such as distributed generators, storage devices, and demand management systems has been changing the ways

of production and consumption of the societies. These methods enable us to reduce the greenhouse emission and improve the grid efficiency and stability. Moreover, we can achieve more efficiency in electricity supply chain by providing a smart supply of the energy as well as smarter consumption.

Nowadays, a large number of renewable generators with the lower power production have joined the grid tree. The utmost problem of renewable energies is that their flexibility is lower than the fuel-based generators, in other words, the output power of renewable energies is uncontrollable and depends on the atmospheric conditions. Smartening the grid and transforming the consumers from static users to the active players are the key issues to overcome the lack of flexibility. In order to achieve this, some rules are made and operated through utility companies that are called demand response programs. The main goal of using DRP is to shift or shed the loads from peak to off-peak hours to shave the overconsumption at peak hours.

Utility companies are able to operate the DRPs through home energy management systems (HEMSs) over the smart grid infrastructure. HEMS is an important part of the smart grid that enables the residential customers to execute demand response programs autonomously. There are many autonomous control systems to help the utility companies to reduce the overconsumption at peak hours efficiently; however, it may limit or violate the residents' comfort in many cases.

The main objective of HEMS is to optimize the electricity consumption during peak hours and consequently optimize the electricity price at the minimum sacrifice in the residents' comfort. Smart electricity dispatching among users and an optimal electricity consumption pattern would be beneficial from HEMS. Energy pricing, CO_2 management, electricity consumption monitoring, and demand consumption detection are only some of the applications of house automation as HEMS.

The presence of distributed generation such as solar, wind, biomass, and storage devices will help to efficiently save the peak hours without sacrificing the resident's comfort by using HEMS. **Figure 3** represents the infrastructure of the smart grid with HEMS.

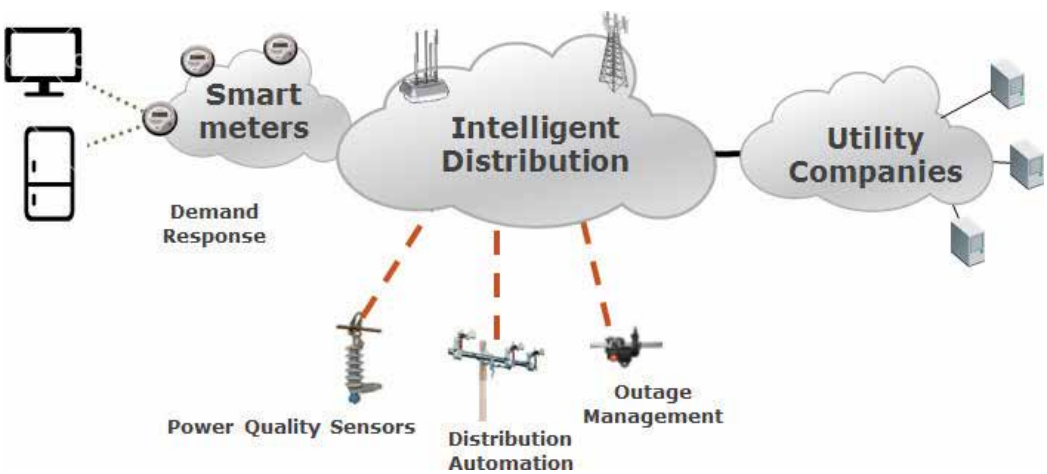

Figure 3. Infrastructure of the smart grid with HEMS.

HEMS consists of smart meter and smart appliances. Smart meters are devices to collect, monitor, and analyze the electricity consumption of the demand. These data are sent to the utility companies in real time to ensure more accurate electricity bills. Such devices provide many services such as electricity quality monitoring (voltage and frequency), demand control, dynamic service tariffs, and so on. In the smart home, electrical appliances are networked together and allow users to access and operate the appliances through a local controller or the Internet. Smart appliances are also able to respond to signals that are sent by utility companies to optimize the electricity usage during peak hours.

3. Proposed home energy management system

As mentioned earlier, HEMS is a demand response tool that helps utility companies to shift or interrupt the demand to optimize the power consumption and production. HEMS has the ability to make a communication between smart appliances and utility companies to improve the energy consumption of the premise. HEMS is utilizing the smart appliances and smart meter (local controller) to monitor and control the overall power consumption of the residential dwellings. Smart appliances are able to communicate with the smart meter, which is responsible for collecting the required data of the smart appliances for further analysis. **Figure 4** shows a simple structure of the smart home. Currently, the majority of the appliances in residential units are traditional and uncontrollable. Therefore, it is desired to convert the traditional electrical appliances to the smart appliances through smart plugs and smart meter. This is more complicated than a simple on and off switch. For instance, a smart air conditioner might extend its cycle time slightly to reduce its consumption on the grid.

In the following sections, smart meter, as well as smart plugs and transmission unit, will be introduced briefly.

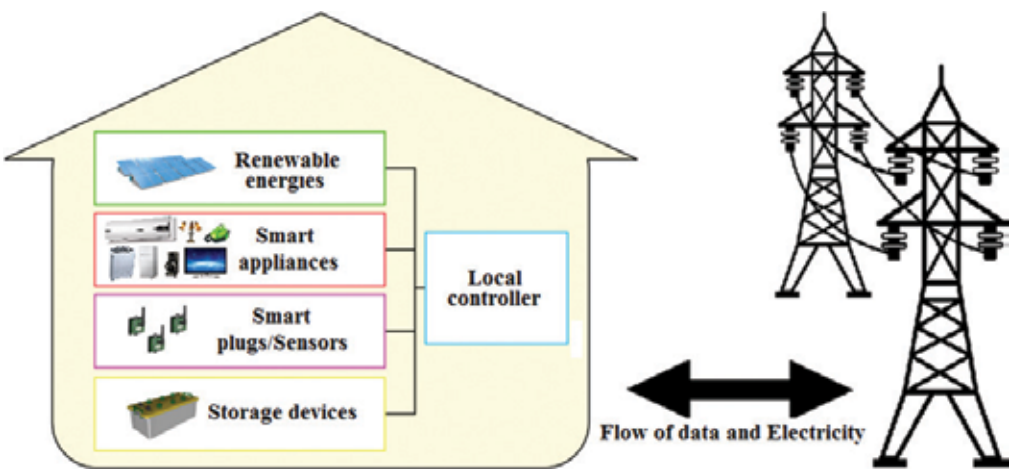

Figure 4. Simple structure of smart home (HEMS).

3.1. Smart meter/controller

Smart meters are devices to collect, monitor, and analyze the electricity consumption of the demand. These data are sent to the utility companies in real time to ensure more accurate electricity supplies. Such devices provide many services such as electrical power quality monitoring (voltage and frequency), demand control, dynamic service tariffs, and so on.

Integrating smart meters to premises involves complex communication technologies and may lead to relevant economics and environmental profits for power companies and consumers. As an example in demand side, consumers can be informed remotely on energy costs and related carbon emission data. These data can be recorded and displayed online for the consumers.

A smart meter consists of two main parts such as local controller and transmission unit. At each time interval, smart meter aggregates the data from smart plugs, analyzes the data, and communicates with utility companies for further decisions. The smart meter aims to control the operation of appliances on the grid to decrease the electricity cost taking price signal and occupant's comfort into account. **Figure 5** represents the simple structure of the smart meter. Eq. (1) demonstrates the cost of electricity function, while C_P is the cost of electricity at the time τ, and T_G indicates the consumed power from the grid at the time τ

$$\text{Electricityprice} = \sum_{\tau=1}^{24} C_P(\tau) * T_G(\tau) \tag{1}$$

3.2. Smart plugs for conventional electrical appliances

The smart plug consists of three main parts such as a sensing unit, a micro-controller unit (MCU), and a transmission unit as shown in **Figure 6**. The aim of using the smart plug is to convert the conventional appliances to smart appliances.

A. Sensing unit: This unit can collect the ambient data, convert the analog data to digital, and send them to MCU unit. Current, voltage, temperature, and light lumens are some of the parameters that could be measured through sensors. These data are aggregated through MCU and sent to the local smart meter via wireless communication for further analysis. As an example, ACS 712 current sensors with Hall Effect measurement besides the lm 35 temperature sensors are used here as an example.

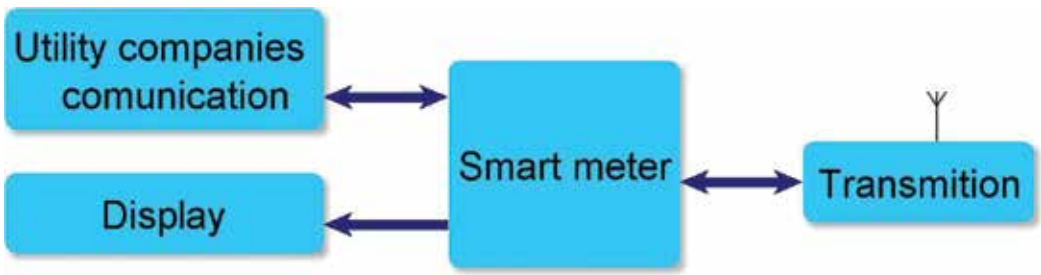

Figure 5. Simple structure of a smart meter.

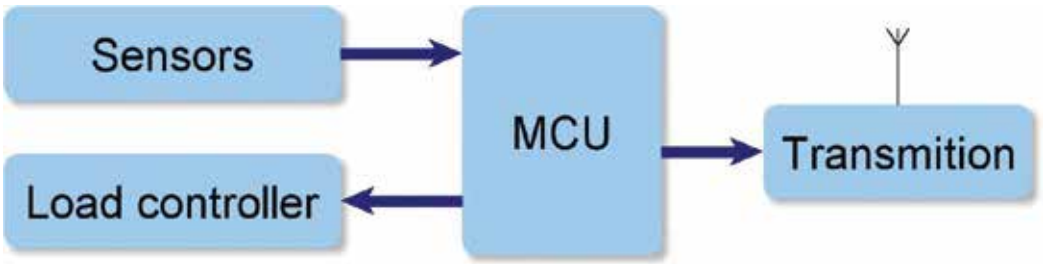

Figure 6. Simple structure of an intelligent wireless smart plug.

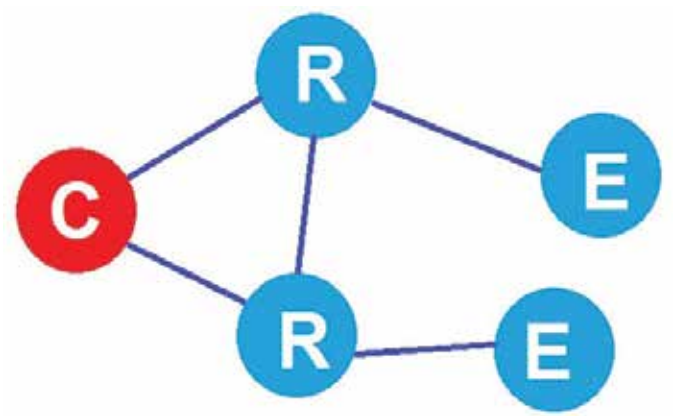

Figure 7. Layout of the communication among wireless modules.

B. MCU unit: This is the central unit or the microcontroller unit, which is interfaced to the sensor units and responsible for analyzing, storing, and sending the collected data to the local controller/smart meter through the transmission unit.

C. Transmission unit: This unit is responsible for sending the collected data by MCU as well as to the smart meter [18]. XBee 802.15.4 model XBIB-R-DEV enables us to send data via wireless communication with low power consumption and low cost. The operating frequency of this module is 2.4 GHz. It has serial USART interface connection, which makes it easier to interface with other devices. **Figure 7** represents the layout of the communication among smart plugs, whereby C is for coordinator, R represents router, and E represents end user.

The smart meter is connected to a coordinator wireless module and smart plugs are connected to the routers/end users. When a new device is connected to the network, it sends a predefended frame, which includes the type of module that could be a router or an end user and address of the module. The smart meter reads the data then about the module and stores the 64-bit address of the module in its EEPROM. Therefore, from then onwards, the smart meter can communicate with the smart plugs through the wireless network of XBee modules. **Figure 5** shows the implemented smart meter as well as the smart plug.

http://dx.doi.org/10.5772/intechopen.74780

Smart plugs that are proposed and implemented in the HEMS are categorized in two groups. The first category is the normal smart plugs. These plugs can control the electrical appliances by measuring the power consumption of them and send/receive the commands to/from a smart controller. The second category of the smart plugs is the thermal smart plugs. These plugs are connected to the thermal appliances such as air-conditioning system and refrigerator. They are able to measure the inside temperature of the thermal appliances beyond the ability of normal smart plugs.

3.3. Energy management strategy

There are many methods to reduce the power consumption during peak hours such as direct load control [19], dynamic electricity pricing to incentivize the costumers [20], load management based on game theory [21], and keeping the overall consumption of the building under the certain value [22], which are used as the optimization strategy for electricity price minimizing in this chapter. In order to reduce the electricity price according to Eq. (1), it is required to reduce the electricity consumption ($T_G(\tau)$) as much as possible. Therefore, the smart meter tries to keep the overall consumption of the building under the predefined value. Residents can turn on any appliance at any time. Each smart plug is interfaced with one appliance; therefore, when one of the residents tries to turn on an electrical appliance, the related smart plug sends a request to the smart meter. Then, the smart meter checks the electricity price, rated power, as well as the priority of the related appliance. If the electricity price is cheaper, related electrical appliance will be operating on the grid. Otherwise, the operation of the electrical appliance with the lower priority value is curtailed for some time, and a new appliance operates on the grid. However, if the priority of the new appliance is lower than the other appliances, the operation of the new appliance is delayed for some time to keep the overall consumption of the building under that predefined level.

4. Observation and analysis of the proposed HEMS

The aim of using the smart controller is to manage the appliances on the grid to optimize the electricity price. A case study has been observed in a studio-type apartment with ordinary electrical appliances for two persons as shown in **Table 1**. The priority of the appliances is adjusted by residents based on their comfort level. Here, it is assumed that the utility company sends signal to the smart meter to keep the overall consumption of the building ($T_G(\tau)$) under the 3000 W at any time interval. Otherwise, the electricity price will be increased as the penalty for the residents.

The apartment is then equipped with the proposed intelligent plugs to control the electricity consumption during daytime. In order to understand the performance of the intelligent plugs and smart meter, two scenarios are studied and compared, which will be discussed in this Section. It is assumed that electricity price is calculated and sent by the utility company at each time interval. As an example, **Table 2** shows the hourly changes of electricity price during 24-h

Electrical appliances	Rated power (W)	Quantity	Priority
Refrigerator	200	1	7
Air conditioner	1600	1	9
Coffee maker	1200	1	6
Toaster	1000	1	5
Iron	1000	1	8
Television	100	1	8
Fan	70	1	7
Hair dryer	1300	1	6
Lamps	90–110	4	8
Low wattage devices	80–110	2	7

Table 1. Rated power and priority of electrical appliances.

Time (h)	Electricity price ($)
00:01–05:00 AM	0.05
05:01–09:00 AM	0.12
09:01 AM to 03:00 PM	0.09
03:01–07:00 PM	0.12
07:01–09:00 PM	0.09
09:01–00:00 PM	0.05

Table 2. An example of electricity price during 24-h interval [23].

interval. The aim of the HEMS is to keep the overall consumption of the apartment under the predefined level.

Now, in order to understand the performance of the smart plugs, two different scenarios are opted. In the first scenario, residences are using electricity from the grid without any control algorithm and they are prioritizing their comfort at any cost. Therefore, the temperature of the apartment is set at 18°C, while the output temperature is varied between 24 and 30°C. The power consumption of the appliances without optimization algorithm from 5:00 to 22:00 h is shown in **Figure 8**, at the time the electricity price is more expensive.

As found in **Figure 8A**, there are some overconsumption times during 6:00 and 8:00 as well as 12:00 and 14:00 h. The room temperature is fluctuating around 18°C. Electricity consumption of the house without any control on the operation of the appliances during 24 h is 21 kWh and the total price is 2.04 USD/day.

By contrast, the overall power consumption of electrical appliances with optimization algorithm as scenario 2 is shown in **Figure 9** at the time when the electricity price is more expensive.

Results show that the total consumption of the building is 20 kWh by deploying the intelligent plugs during 24 h and the total price during 24 h is 1.85 USD/day. **Figure 8A** shows the

http://dx.doi.org/10.5772/intechopen.74780

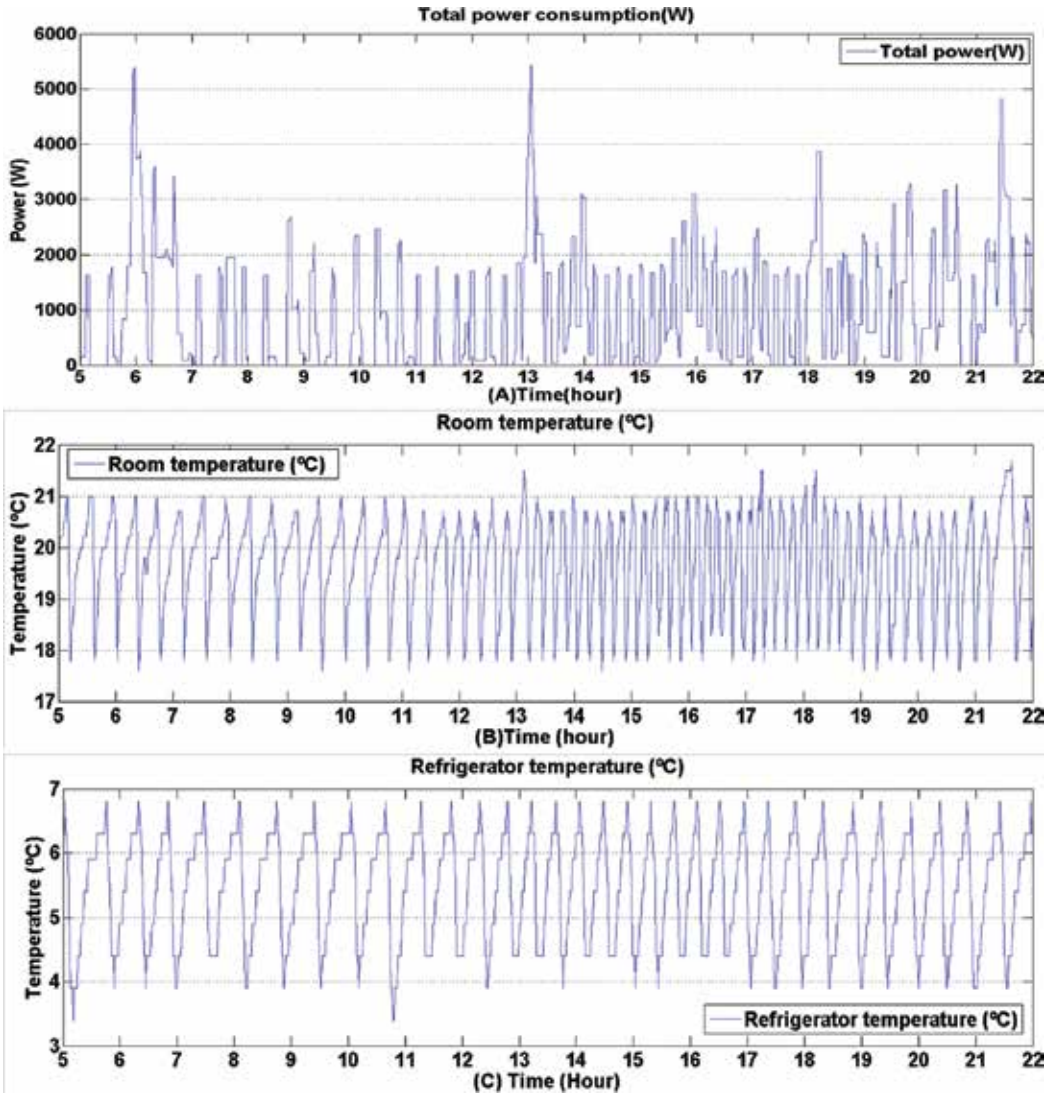

Figure 8. (A) Total power of electrical appliances without using smart plugs and controller, (B) Room temperature fluctuation during the period and (C) Refrigerator temperature.

success in controlling the temperature of the building as well as shifting the operation of the shiftable appliances during peak hours. As an example, the overconsumptions between 6:00 and 8:00 h as well as 12:00 and 16:00 h are decreased after the deployment of the smart plugs and smart controller.

Table 3 shows the comparison between two scenarios executed in terms of the total power consumption of the electrical appliances in a day.

As found here, deployment of the proposed smart plugs can reduce the electricity price by approximately 8% as demonstrated in scenario 2 as compared with the home without any

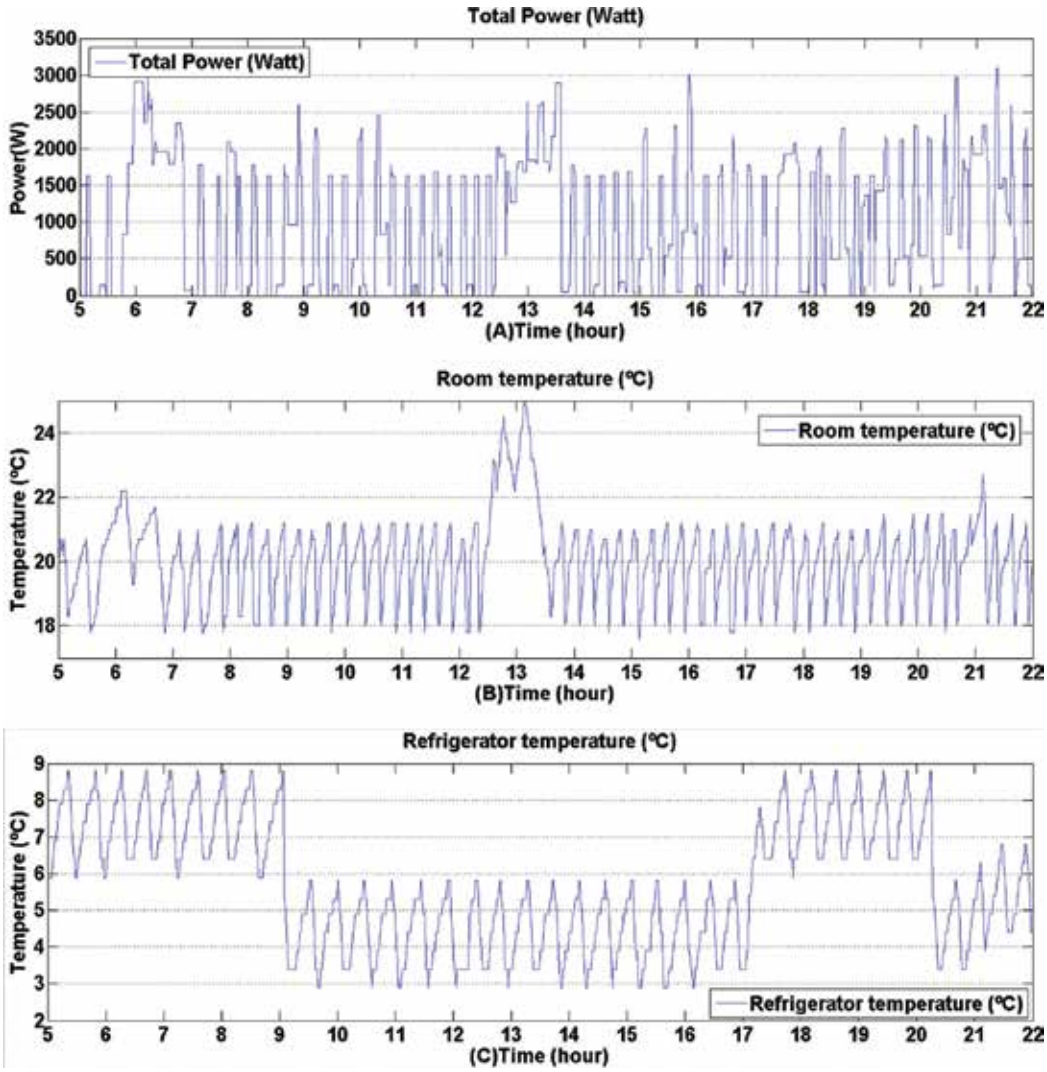

Figure 9. (A) Total power consumption trend of electrical appliances after deploying smart plugs, (B) room temperature fluctuation, and (C) refrigerator temperature fluctuation during the period.

Case studies/scenarios	Total consumption (kWh)
Without optimization strategy and smart plugs	21
Utilizing the optimization strategy through smart plugs	20.40

Table 3. Comparison among the scenarios.

control as shown in **Figure 10**. This saving comes from deferring the operation of the shiftable appliances as well as from controlling the temperature of the house. Comparing between the usual case and HEMS-adopted scenarios, it is obvious that the utilization of smart plugs in

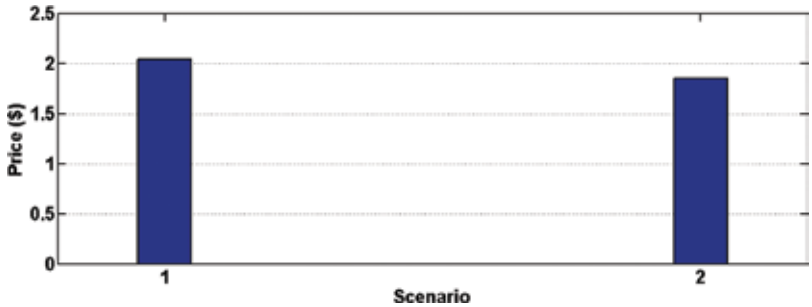

Figure 10. Comparison of the purchased electricity price between two different scenarios.

dwellings has a huge impact on the overall power consumption and consequently it cuts off the electricity price. Therefore, it is obvious that smart plugs and smart controller as HEMS play an important role in the future of the DRPs.

5. Conclusion

In this chapter, home energy management system (HEMS) as a part of smart grid is introduced, where smart plugs along with a controller are designed to optimize the overall power consumption of any ordinary house. These plugs can control the overall power consumption of the appliances, aligning with the electricity price in places where electricity price is calculated by utility companies in advance and sent a day ahead or in real time to the smart meter. The smart meter then controls the electrical appliances through smart plugs according to the priority of the appliances, electricity cost, and rated power of appliances to optimize the electricity consumption in case of certain limitations. The results show that the proposed wireless smart plugs together with the controller are able to reduce the electricity cost up to 8% per day by shifting the operation of the electrical appliances to optimized time slots. Hence, the implemented algorithm through smart controller and smart plugs has the potential to minimize the electricity price by simply optimizing the power consumption during peak hours on a distribution grid to be recognized as a part of smart grid.

Author details

Mohammad Shakeri[1] and Nowshad Amin[1,2]*

*Address all correspondence to: nowshad@uniten.edu.my

1 Department of Electrical, Electronic and Systems Engineering, Faculty of Engineering and Built Environment, Universiti Kebangsaan Malaysia, Bangi, Selangor, Malaysia

2 Institute of Sustainable Energy, Universiti Tenaga Nasional, Jalan Ikram-Uniten, Kajang, Selangor, Malaysia

References

[1] Stoll P, Brandt N, Nordström L. Including dynamic CO_2 intensity with demand response. Energy Policy. 2014;**65**:490-500

[2] Beaudin M, Zareipour H. Home energy management systems: A review of modelling and complexity. Renewable and Sustainable Energy Reviews. 2015;**45**:318-335

[3] Faruqui A, Sergici S. Household response to dynamic pricing of electricity: A survey of 15 experiments. Journal of Regulatory Economics. 2010;**38**:193-225

[4] Hurley D, Peterson P, Whited M. Demand Response as a Power System Resource. Synapse Energy Economics; 2013;1-76

[5] Vardakas JS, Zorba N, Verikoukis CV. A survey on demand response programs in smart grids: Pricing methods and optimization algorithms. IEEE Communications Surveys & Tutorials. 2015;**17**:152-178

[6] Costanzo GT. Demand Side Management in the Smart Grid. Polytechnique Montréal. 2011;1-94

[7] Shariatzadeh F, Mandal P, Srivastava AK. Demand response for sustainable energy systems: A review, application and implementation strategy. Renewable and Sustainable Energy Reviews. 2015;**45**:343-350

[8] Ahmed MS, Mohamed A, Khatib T, Shareef H, Homod RZ, Ali JA. Real time optimal schedule controller for home energy management system using new binary backtracking search algorithm. Energy and Buildings. 2017;**138**:215-227

[9] Wu X, Hu X, Moura S, Yin X, Pickert V. Stochastic control of smart home energy management with plug-in electric vehicle battery energy storage and photovoltaic array. Journal of Power Sources. 2016;**333**:203-212

[10] Shirazi E, Jadid S. Cost reduction and peak shaving through domestic load shifting and DERs. Energy. 2017;**124**:146-159

[11] Rastegar M, Fotuhi-Firuzabad M, Zareipour H. Home energy management incorporating operational priority of appliances. International Journal of Electrical Power & Energy Systems. 2016;**74**:286-292

[12] Muthamizh Selvam M, Gnanadass R, Padhy NP. Initiatives and technical challenges in smart distribution grid. Renewable and Sustainable Energy Reviews. 2016;**58**:911-917

[13] Wang W, Zou YX, Shi G, Zhu Y. A web service based gateway architecture for wireless sensor networks. ICACT 2009. 11th International Conference on IEEE; 2009. pp. 1160-1163

[14] Zhou B, Li W, Chan KW, Cao Y, Kuang Y, Liu X, Wang X. Smart home energy management systems: Concept, configurations, and scheduling strategies. Renewable and Sustainable Energy Reviews. 2016;**61**:30-40

[15] Sumathi S, Kumar LA, Surekha P. Solar PV and Wind Energy Conversion Systems: An Introduction to Theory, Modeling with MATLAB/SIMULINK, and the Role of Soft Computing Techniques. Springer International Publishing; 2015

[16] Xie L, Carvalho PM, Ferreira LA, Liu J, Krogh BH, Popli N, Ilic MD. Wind integration in power systems: Operational challenges and possible solutions. Proceedings of the IEEE. 2011;**99**:214-232

[17] Farhangi H. The path of the smart grid. IEEE Power and Energy Magazine. 2010;**8**:18-28

[18] Abu-Baker A, Huang H, Johnson E, Misra S, Asorey-Cacheda R, Balakrishnan M. Maximizing α-lifetime of wireless sensor networks with solar energy sources. In: IEEE Military Communication Conference—MILCOM. 2010. pp. 125-129

[19] Sharifi R, Fathi S, Vahidinasab V. A review on demand-side tools in electricity market. Renewable and Sustainable Energy Reviews. 2017;**72**:565-572

[20] Fernandes F, Morais H, Vale Z, Ramos C. Dynamic load management in a smart home to participate in demand response events. Energy and Buildings. 2014;**82**:592-606

[21] Mohsenian-Rad AH, Leon-Garcia A. Optimal residential load control with price prediction in real-time electricity pricing environments. IEEE Transactions on Smart Grid. 2010; **1**:120-133

[22] Shakeri M, Shayestegan M, Abunima H, Reza SS, Akhtaruzzaman M, Alamoud A, Sopian K, Amin N. An intelligent system architecture in home energy management systems (HEMS) for efficient demand response in smart grid. Energy and Buildings. 2017;**138**:154-164

[23] Zhu T, Mishra A, Irwin D, Sharma N, Shenoy P, Towsley D. The case for efficient renewable energy management in smart homes. In: Proceedings of the Third ACM Workshop on Embedded Sensing Systems for Energy-Efficiency in Buildings, ACM. 2011. pp. 67-72

Chapter 5

Unconventional Backup Structures Used in Smart Microgrids

Lucian Pîslaru-Dănescu and
Laurențiu Constantin Lipan

Additional information is available at the end of the chapter

http://dx.doi.org/10.5772/intechopen.75989

Abstract

The continuity of power supply to users is considered to be one of the main problems in the design and implementation of low-voltage smart microgrid configurations. Switching to the backup power supply, when using two frequency converters, one of which is alternately maintained in cold reserve, is presented. Switching to the backup power supply, in the case of low-voltage symmetrical smart microgrids, is another highlighted aspect. In the case of modern residential buildings, the automatic switching is necessary between two or more types of users, critical and noncritical ones to the available sources, like the public grid, photovoltaic panels, power generator, etc. Also, in this study, the implementation of smart power microgrids, featuring auto-reconfiguration, is proposed. It is considered the conversion of the public grids to active (distribution/using) smart power microgrids, which have the autoconfiguration option and use high-tech smart devices, like recloser type. Thus, the faults and contingencies will be limited or even removed, creating the frame for the supplied equipment (in a continuously increasing number due to the local and regional expansion) to operate until the removal of the fault.

Keywords: low-voltage smart microgrid, active grid, recloser device, circuit breaker, backup power supply

1. Introduction

Among the automation systems used for the continuity of power supply to users, the most important one is represented by the automatic transfer switch (ATS) [1]. The scope of the ATS is to start the automatic operation of the backup power supply when the normal power supply

can no longer satisfy the requirements of the consumers. The following will illustrate, in terms of the reserve supply, some possible topologies related to low-voltage electrical grids. First of all, it is considered the switching to the backup power supply, in the case of a low-voltage symmetrical grid when using two frequency converters, one of which is alternately maintained in cold reserve. Both frequency converters are of the FR-A540-22 K Mitsubishi electric [2] type. The only user is represented by an asynchronous motor with the short-circuited rotor, having the rated active power equal to P = 22 kW. The problem of ensuring continuity in power supply is all the more important if we refer to asynchronous motors powered by frequency converters that are used in applications such as gondolas and cable cars, the action of the water pumps within the drinking water abstraction and treatment plants, and the operation of large power compressors. The use of the methods described in the case of switching to the backup power supply, in the case of a low-voltage symmetrical grid when using two frequency converters, one of which is alternately maintained in cold reserve, could be a fair solution. In the second case, it is considered the switching to the backup power supply, in the case of low-voltage symmetrical smart microgrids, using in the modern residential buildings. This symmetrical low-voltage grid uses two transformers, one of them being alternatively in hot reserve. The users are divided into two categories, normal and safety ones. And for this case, one study on the ATS operation will be achieved. Also for the case of modern residential buildings, the ATS operation will be considered, in the event that they use both electric generator and photovoltaic panels. Finally a study about the implementation of recloser devices for autoconfiguration and automatic connecting/disconnecting decisions, in order to switch to the backup power supply, was initiated. Also, taking into account a series of scientific, technological, or socioeconomic aspects in terms of importance, the implementation of smart power grids is proposed [3]. This smart grids show auto-reconfiguration characteristics, by using recloser devices [4]. A very important aspect of the electrical systems is related to the safety in operation [5], lack of accidents, and extended damages. Starting from the necessity of a safe power supply system, more and more countries choose to use computerized and special telecommunications systems [6]. Moreover, in the field of electricity transmission, a high degree of operation safety is required. The characteristics of each considered microgrid determine a series of specific technical problems [7]. When considering the grid operation criteria and the specific needs of the users, the settings of the smart recloser equipment must be properly configured. Thus, the indication of the short circuits between phases, the indication of the faults between phases and earth, the signaling of defects, the signaling reset, the storage and the effective operation temperature, or the referral mode are of particular importance and may raise important shares of difficulty, in particular regarding the operation algorithm.

2. Switching to the backup power supply, in the case of a low-voltage symmetrical grid when using two frequency converters, one of which is alternately maintained in cold reserve

In practice, the situations where electrical power systems need to be fed redundant can be solved through a backup of power supplies. Ensuring backup in this case must follow

a logic sequence of power so that the consumer can be powered at any time from a single power source. Also, providing short circuits and overload protection is an important aspect. If an asynchronous motor with nominal active power P = 22 kW is powered by a single frequency converter, FR-A540-22 K Mitsubishi electric type, a low-voltage grid configuration can be used as in **Figure 1**. Switching to the backup power supply, in the case of a low-voltage symmetrical grid when using two frequency converters, one of which is alternately maintained in cold reserve, can only be done by microprogramming the two frequency converters. It is considered a low-voltage grid configuration using two frequency converters, **Figure 2**, FR-A540-22 K Mitsubishi electric type, in which one of the converters is alternatively cold reserve depending on the need. The only consumer is an asynchronous

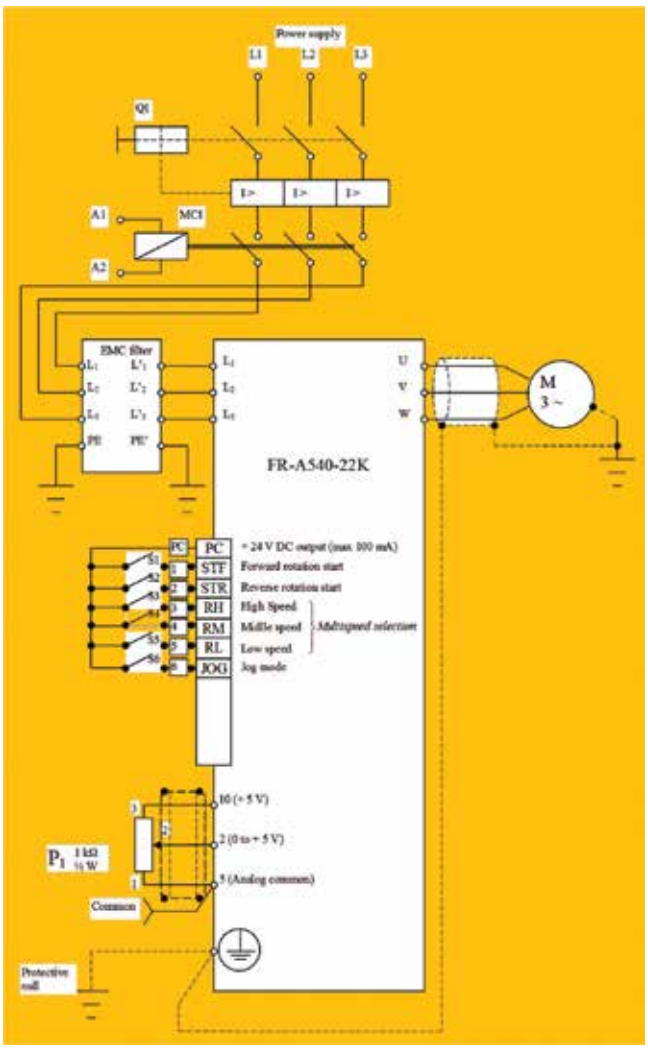

Figure 1. Mitsubishi electric frequency converter FR-A540-22 K type, used to power an asynchronous motor with a short-circuit rotor with nominal active power P = 22 kW.

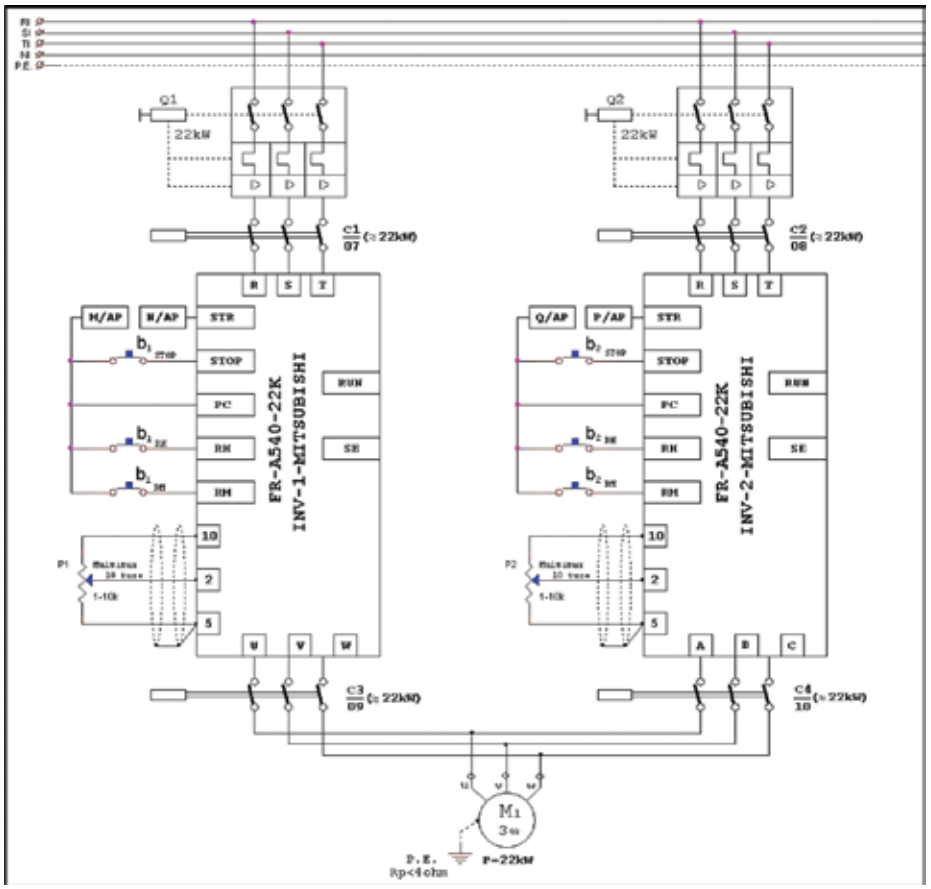

Figure 2. Switching to the backup power supply, in the case of a low-voltage symmetrical grid using two frequency converters managed by a programmable microautomaton [1].

motor with a short-circuit rotor with nominal active power P = 22 kW. When considering redundant backup drives, using two frequency converters in order to ensure the power supply continuity, it is desirable that the interlocking management as well as the activation/deactivation commands be achieved by means of a programmable micro-automat, with software-established logic. The digital inputs of the two frequency converters, such as the frequency converter activation/deactivation commands, are performed via OUT 1 and OUT 2 outputs, **Table 1**, and are managed by a microprogrammable automaton, [8, 9] Alpha Mitsubishi, AL 2–24 MR-D type, **Figure 3**. When using two frequency converters, one of which is alternately maintained in cold reserve, the output interlock management of the frequency converters is very important. The interlock aspect is achieved by C3 and C4 switches, **Figure 2**, activated by the OUT 8 and OUT 9 output of the microprogrammable automaton Alpha Mitsubishi, AL 2–24 MR-D type, **Table 1**.

By a key selection, b_5 and b_6, respectively, **Figure 4** [1], it is decided which of the converters will supply the load, represented by the M1 asynchronous motor with the short-circuited rotor.

Inputs	Outputs	Allocated inputs	Allocated outputs	Input/output account
—	OUT 1	—	START/STOP MSB1	Enable/disable the Mitsubishi 1 inverter
—	OUT 2	—	START/STOP MSB2	Enable/disable the Mitsubishi 2 inverter
—	OUT 3	—	h1	The signaling lamp 220 V~—Mitsubishi 1 inverter fault
—	OUT 4	—	h2	The signaling lamp 220 V~—Mitsubishi 2 inverter fault
—	OUT 5	—	C5	Activates the C5 switch coil which controls the brake
—	OUT 6	—	C1	Activates the C1 switch coil of the force circuit
—	OUT 7	—	C2	Activates the C2 switch coil of the force circuit
—	OUT 8	—	C3	Activates the C3 switch coil of the force circuit
—	OUT 9	—	C4	Activates the C4 switch coil of the force circuit
IN 1	—	b_1, b_2, b_3, b_4	—	4 × HUPA, mushroom-type buttons NI, operated when faults are produced
IN 2	—	b_5	—	The ND contact—left selector key on the left Zero—right
IN 3	—	b_6	—	The ND contact—right from the key selector is left Zero—right
IN 4	—	b_7	—	Commands the state START/STOP of Mitsubishi 1 inverter
IN 5	—	b_8	—	Commands the state START/STOP of Mitsubishi 2 inverter
IN 6	—	b_9	—	Auxiliary ND of the C5 switch which controls the brake
IN 7	—	b_{10}	—	The pin NI of the heat block from the break circuit
IN 8	—	b_{11}	—	Auxiliary ND of the C3 switch
IN 9	—	b_{12}	—	Auxiliary ND of the C4 switch
IN 10	—	b_{13}	—	Auxiliary ND of the C1 switch
IN 11	—	b_{14}	—	Auxiliary ND of the C2 switch
IN 12	—	b_{15}	—	Pin for the S1proximity sensor
IN 13	—	b_{16}	—	Fault removal

Table 1. The assignment of the inputs and outputs for microprogrammable automaton.

Figure 3. Microprogrammable automaton Alpha Mitsubishi, AL 2–24 MR-D type.

Also, the enabling/disabling command management for the frequency converters is achieved by the OUT 1 and OUT 2 programmable micro-automaton outputs, **Table 1**.

In **Figure 5**, it is presented the flowchart where the logic of switching as well as electrifications can be seen (it is preferable to study together with **Figures 2**, **4**, and **Table 1**).

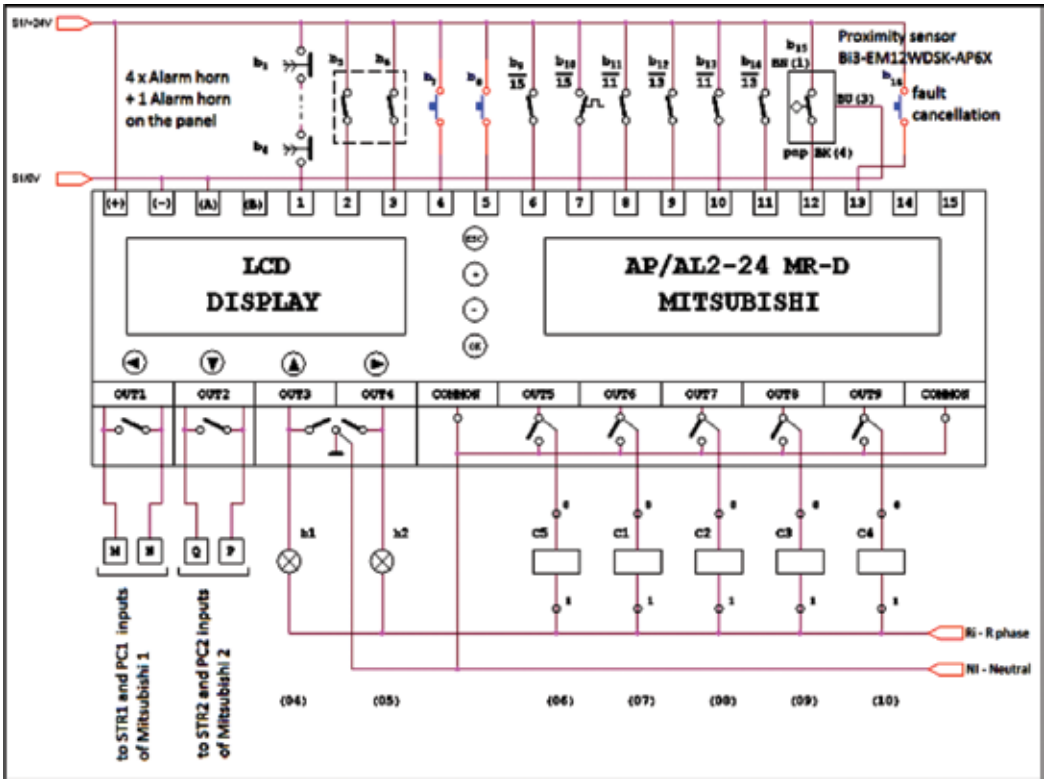

Figure 4. Connecting the inputs/outputs of the microprogrammable automaton alpha Mitsubishi, AL 2–24 MR-D type [1].

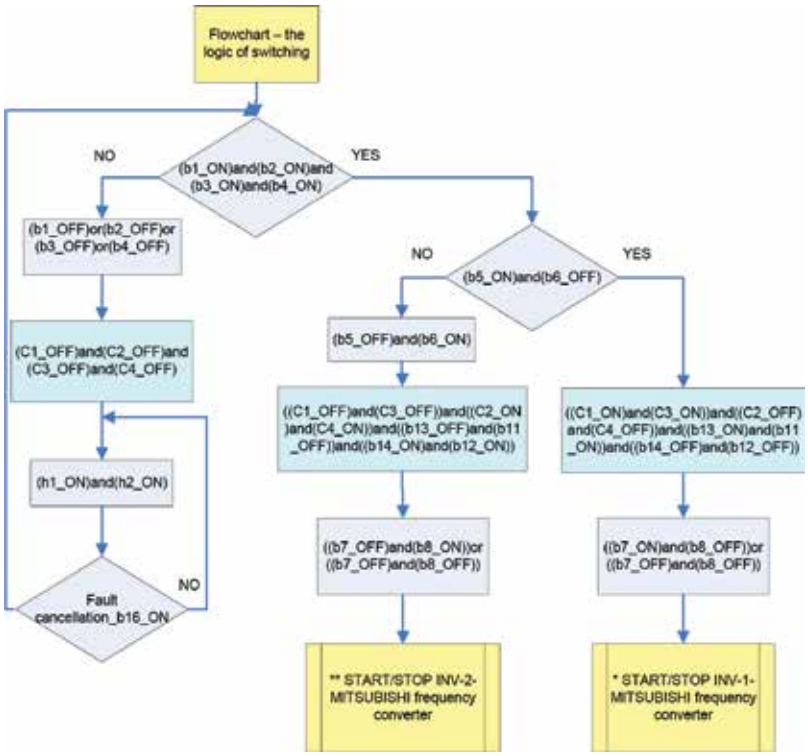

Figure 5. Flowchart, the logic of switching and electrifications. *There is the possibility to obtain a variable frequency by actuating the P1 potentiometer, **Figure 2**. **There is the possibility to obtain a variable frequency by actuating the P2 potentiometer, **Figure 2**.

3. Switching to the backup power supply, in the case of low-voltage symmetrical smart microgrids in the modern residential buildings

In the case of modern residential buildings, the automatic switching between the three-phase public grid and an electric generator can be achieved by the automatic changeover source, with automatic transfer switch (ATS) function, located in the low-voltage electrical station, **Figure 6**. The microgrid is symmetrical and uses two identically transformers, T1 and T2, one of the transformers being alternately in hot reserve state [1]. The users are divided into two categories: critical (b) and noncritical ones (a), **Figure 6**. When the users are supplied from the public grid by using one of the transformers, T1 or T2, correspondingly, one of the circuit breakers MP1 or MP2 is closed, while the "C" couple is also closed. The two circuit breakers (TN) NS250 types are closed, and the other two circuit breakers (TS) NS250 types are open so that the backup power supply path is maintained disconnected. In this case, all users are supplied, both (a) and (b) categories, from the three-phase public grid as shown in **Figure 6**. In a low-voltage grid, two distinct situations can occur:

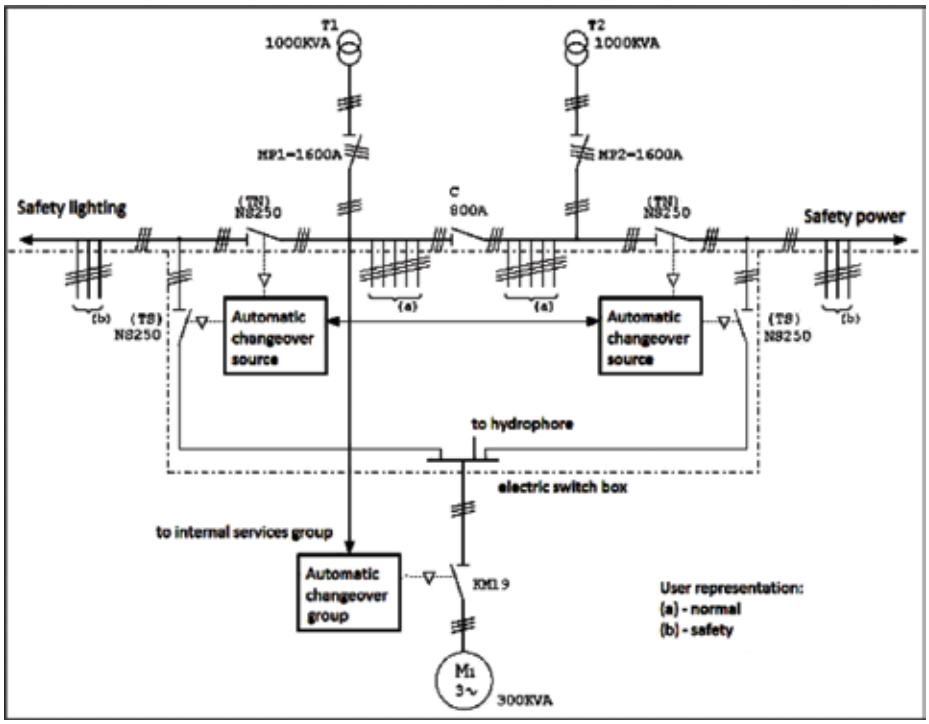

Figure 6. Single-line diagram of force for switching to the backup power supply in the case of a low-voltage symmetrical grid using two transformers and an electric generator [1].

1. The situation where ATS intervention is required.
2. The situation where ATS intervention is unnecessary.

For the ATS facility to distinguish between these two situations, it must meet the following conditions simultaneously:

a. To get into action when the voltage level on the consumers' bars drops below a certain minimum value.

b. The automatic action of the reserve should not be made immediately, but only after a certain time period, called ATS time delay (t_{ATS}).

c. Switching the backup path to achieve only after the disconnection of the normal power supply.

d. It operates once, so that if after the operation of the ATS a new activation command is given, the ATS should not work again.

When the condition of minimum voltage on the station's bars is not satisfied in accordance to the abovementioned conditions, (a)–(d), the power supply is ensured by the M1 electric generator, **Figure 6**.

The minimum voltage coils of the "MP1" or the "MP2" circuit breakers (as the case may be) and of the "C" couple, respectively, **Figure 6**, can determine their triggering, if the voltage drops well below the nominal limit. It achieves disconnecting the normal power supply path (the public grid), and for a time t_{ATS}, both consumers in group (a) as well as consumers of the group (b) will not be powered. Note that the ATS facility is composed in this case of two systems, "automatic changeover source" type, **Figure 6**. The ATS function of the automatic changeover source commands the two (TN) NS 250 circuit breakers, by opening them, and the other two (TS) NS 250, by closing them. Another important aspect is the existence of the "automatic changeover group" type, **Figure 6**, which is absolutely necessary for triggering a delay timing, t_{GROUP} in starting the M1 electric power generator and the automatic closing of the KM 19 switch, only after the transient phenomena has been removed and a permanent regime of the electric generator has been set. Obviously $t_{ATS} < t_{GROUP}$. The electric generator's services must be ensured at all times. If during timeout t_{ATS} the voltage on the bars is not found (allowing the ATS to operate), the electric power generator will be started. After the expiration of time t_{GROUP}, the automatic closing of the KM 19 switch is achieved, the M1 electric power generator injects electric power on the base station bars and supplies power only the (b) group users, referred in **Figure 6** as safety power and emergency lighting. When the tension on bars returns, after "delay timing" t_{STOP} has been passing, the following processes take place: firstly, the automatic changeover group command stops of the M1 electric power generator and then the automatic opening of the KM 19 switch is achieved. Obviously $t_{ATS} < t_{STOP}$. Next, the ATS function of the automatic changeover source commands the two (TN) NS 250 circuit breakers, by closing them, and the other two (TS) NS 250, by opening them. Finally, closing the breaker MP1 or MP2 (as the case may be) and of the "C" couple, respectively, it can also be done automatically or manually.

4. Switching to the backup power supply, in the case of a low-voltage smart microgrids using an electric generator set and the photovoltaic panels

In the case of modern residential buildings that use an electric generator set and the photovoltaic panels, the functions that are provided by the ATS regard the following:

a. When the three-phase public grid is available and connected, all the users are powered from this grid.

b. When the three-phase public grid is not available, the electric generator will be connected. Both critical and noncritical users will be powered by the electric generator.

c. When the three-phase public grid and the electric generator set are not available, the critical users are supplied by the photovoltaic panels' energy generation.

The automatic switching is necessary between the two types of users, critical and noncritical ones to the available sources, in this case the three-phase public grid, an electric generator set, and photovoltaic panels that are shown in **Figure 7**.

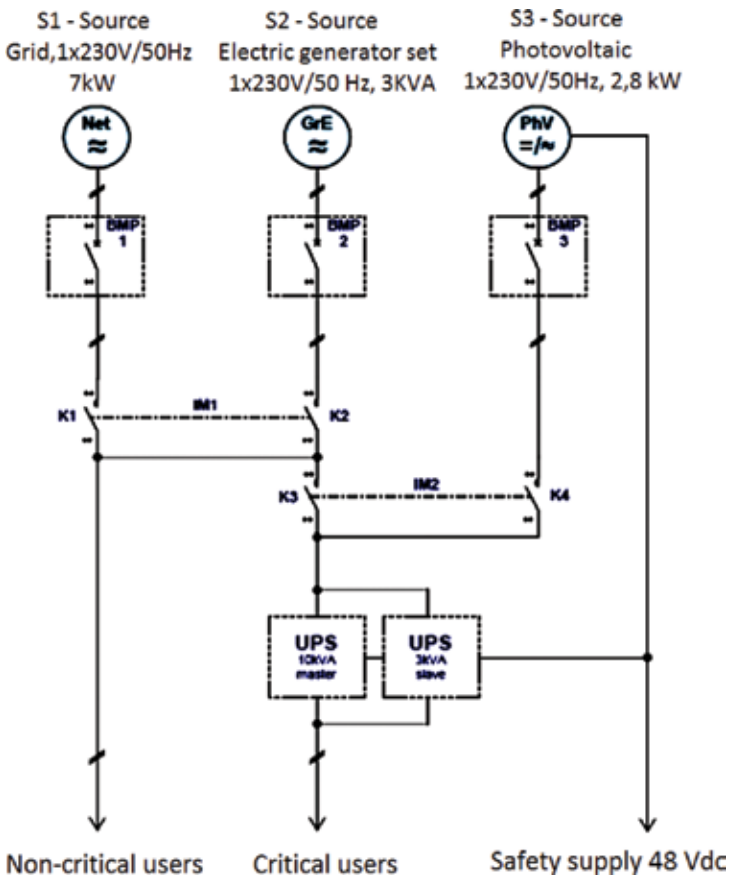

Figure 7. Electric power diagram for switching to backup power supply in the case of a low-voltage smart microgrid using an electric generator set and the photovoltaic panels (courtesy of Sirius Trading & Services srl, Romania).

To implement the above basic functions and the control algorithm, the system also integrates the following additional functions:

a. Monitoring the presence of voltage on the three sources (three-phase public grid, an electric generator set and photovoltaic panels).

b. Monitoring the state signals of the electric power generator set, such as the presence and level of fuel, the good operation of the filter, the command temperature of the shock, as well as the heating resistor's temperature of the fuel (command).

c. Connecting/disconnecting of the electric power generator set when the three-phase public grid is available/unavailable, respectively.

d. Checking confirmation commands from the circuit's commutation wires and providing alternatives if commands are unconfirmed.

e. Counting the number of three-phase public grid voltage drops, disconnection time of the public grid, the number of connections, and time of operation per electric generator set

and photovoltaic source time. These functions are performed through a software program [9] which is implemented on an AL 2–24 MR-D, Alpha Mitsubishi programmable micro-automat, **Figure 3**.

In this case, the ATS automation must work in the following way:

- When the public grid is not available, the triggering delay timing of the electric generator set is initiated; if the voltage grid does not reappear during this delay timing, the startup procedure of the electric generator set will be initiated.
- Several connecting attempts are possible, their number being set by the user. The duration of the connecting command and the related pause between the attempts can also be established by the user.
- When the electric generator set is connected and the output voltage is detected, the connecting command is maintained for another short period of time in order to avoid its disconnection.
- After switching on the electric generator set and expiring the timer entry (also set by the user), critical and noncritical users are switched to the electric generator set circuit.
- Upon reappearance of the voltage on the public grid and after the end of the public grid stabilization (user settable), the users are disconnected from the electric generator and reconnected to the public grid.
- Simultaneously for the electric generator set, the stopping procedure is initiated with the fuel shutdown and timed with the activation of the group shutdown command.
- In the case of public grid and group unavailability, vital consumers are supplied by the photovoltaic panels' energy generation.
- Fault and nonconfirmation conditions are stored and remain active even if the system is disconnected and then reconnected; resetting requires operator intervention to repair the causes that triggered them and press the reset button.

5. The implementation of recloser devices for autoconfiguration and automatic connecting/disconnecting decisions, in order to switch on the backup power supply

As smart grids are composed of sensitive equipment at voltage interruptions in increasing proportion, higher-power-quality issues have become increasingly important. In order to reduce the rate of long-term interruptions and thus improve the quality of energy, for medium voltage (MV) distribution networks, it is proposed to use the recloser devices. Thus, it can prevent long outages by eliminating temporary malfunctions, before the fuses are operating in the system. Reclosers also offer control, measurement, automation, and telecommunication capabilities. This makes it possible to control in real time the intelligent network that now allows maneuvers for various purposes. Reclosers also provide consecutive automatic

Figure 8. The Tavrida electric recloser concept, up to 40.5 kV (RMS) rated maximum voltage and up to 1250 A (RMS) rated continuous current [10] (courtesy of Tavrida electric).

closing cycles to eliminate transient faults and minimize network interruption. The reclosers, **Figures 8**, **9**, and **10**, incorporate some breakers with vacuum extinguishing chambers (vacuum breaker), inside a polycarbonate shell for each pole, **Figures 11** and **12**. Each breaker, corresponding to each pole, is embedded in a polymer bush. This bush includes both current and voltage sensors. The breaker with contacts in vacuum is considered a nonmaintenance electrical switching apparatus. The drive mechanism has a high reliability and requires a revision at about 10 years or after 10,000 maneuvers.

The implementation of the smart devices, as recloser type for automatic connecting/disconnecting decisions so that the branched or even looped operation could be possible by using the lines without any faults until the removal of the existing ones, allows auto-configuration of the smart microgrids.

Voltage sensing is carried out by conductive rubber screens that are capacitively coupled to the high-voltage (HV) terminals, and current sensing is performed by six Rogowski sensors,

Figure 9. The Thomas & Betts recloser concept, up to 38 kV (RMS) rated maximum voltage and up to 800 A (RMS) rated continuous current [11] (courtesy of Thomas & Betts).

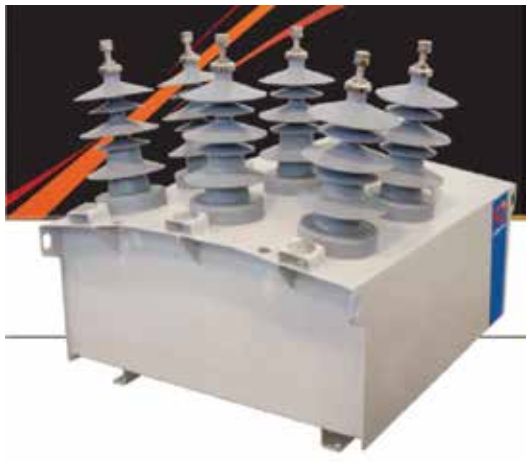

Figure 10. The REVAC recloser concept, up to 36 kV (RMS) rated maximum voltage and up to 630 A (RMS) rated continuous current [12] (courtesy of REVAC).

one sensor per HV terminal, **Figures 11** and **12 (**Tavrida Electric recloser). Rogowski sensors are current sensors that produce a safe, low-voltage output [10]. The mechanism is operated by three separate magnetic actuators, one per pole, **Figure 11**. These magnetic actuators are mechanically interlocked to guarantee correct a three-phase operation. The device is latched into the closed position by magnetic latching. Each magnetic actuator utilizes a single coil which is used for both opening and reclosing operations [10] (Tavrida Electric recloser).

These recloser's devices can be successfully applied to the electric grids without isolated neutral. The conversion of the public grids to active (distribution/using) grids that use the high-tech smart devices like reclosers is expected to make in the future. Moreover, there is also considered

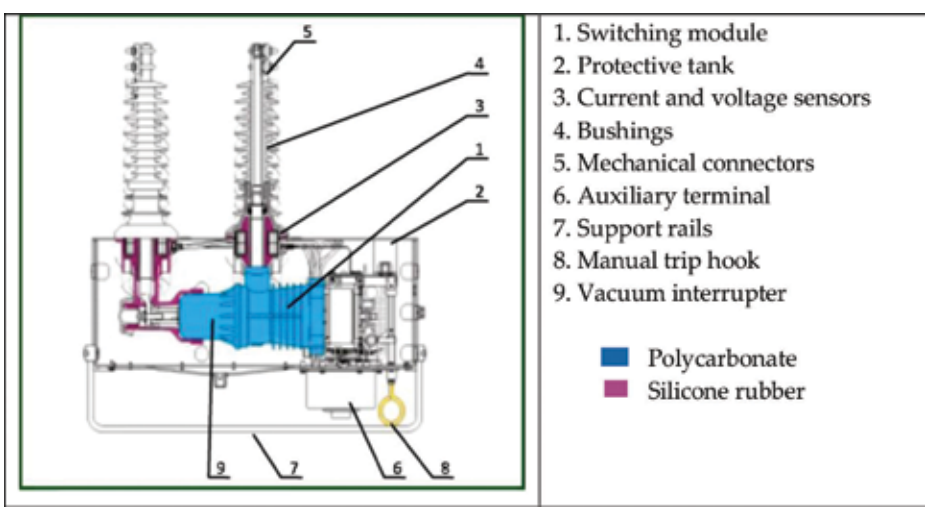

Figure 11. The Tavrida Electric recloser, the components of a pole (courtesy of Tavrida Electric) [10].

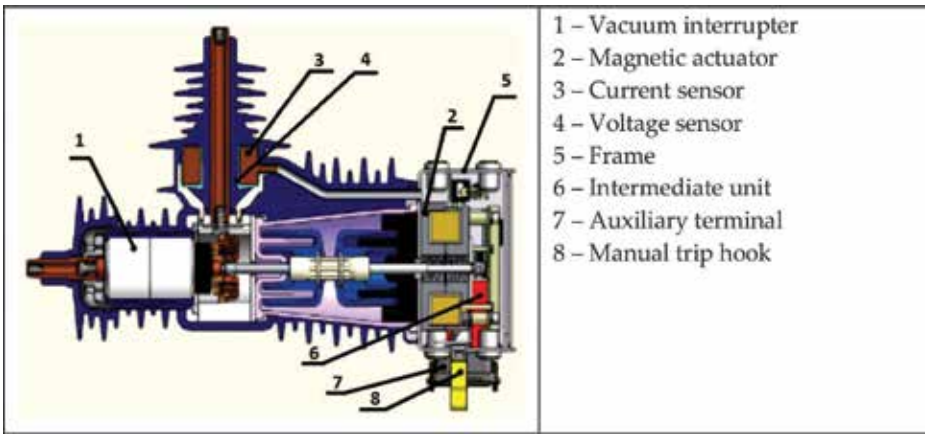

Figure 12. The Tavrida Electric recloser, actuating the vacuum interrupter (courtesy of Tavrida Electric) [10].

grouping these within smart microgrids which have the autoconfiguration option [13]. Thus, the faults and contingencies will be limited or even removed, creating the frame for the supplied equipment (in a continuously increasing number due to the local and regional expansion) to operate until the removal of the fault. The characteristics of the analyzed public grids with isolated neutral regard their operation in general with a radial structure, **Figure 13**. Thereby, when a fault is produced, all the equipment is disconnected until the removal of the fault.

In order to switch on the backup power supply, Substation 1 or Substation 2, respectively, **Figure 14**, is possible to the implementation of the recloser devices for autoconfiguration and automatic connecting/disconnecting decisions, in conjunction with a circuit breaker. And more important for this configuration is that this circuit breaker can also be assimilated with a smart recloser device, recloser 3, **Figure 14**.

These smart recloser devices can be used in order to monitor both the isolation resistance and other parameters of the considered microgrids. The actual implementation of the recloser devices for programming connecting/disconnecting process is also considered. Thus, the lines without any faults allow the continuity of power supply to consumers until the faults' removal. Furthermore, these electric grids, already active, are able to reconfigure based on the recloser devices to the initial operation mode, previous to the fault

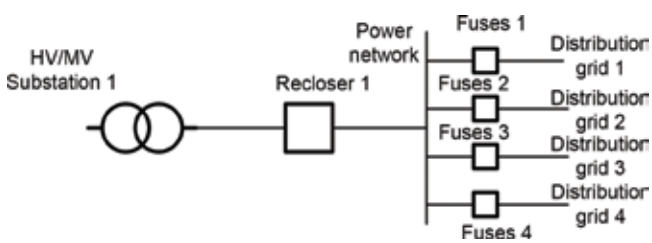

Figure 13. Radial structure of a public grid with isolated neutral.

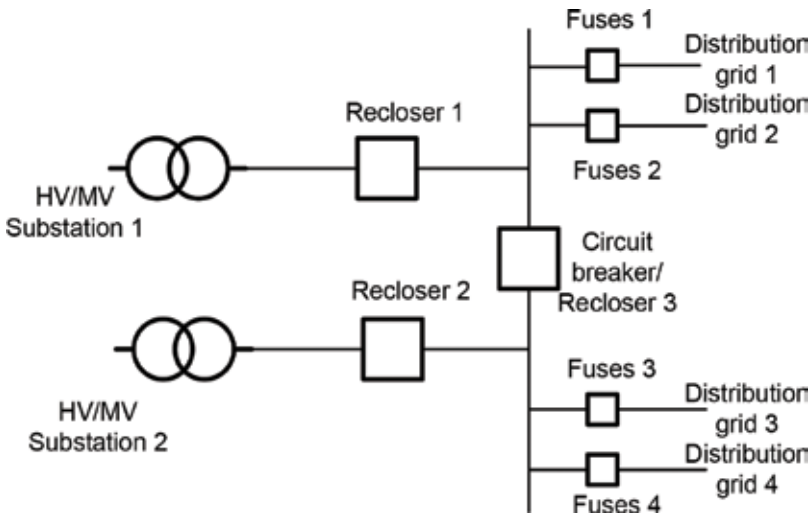

Figure 14. Implementation of the recloser type devices for switching on the backup power supply. The case of two radial structures of a public grid with isolated neutral.

propagation. This is done by programming an opening/closing sequence, depending on the characteristics of the microgrid. For example, **Figure 15** is showing a possible process of reclosing.

Reclosing interval can be defined: the open-circuit time between an automatic opening and the succeeding automatic reclosure [14]. Obviously, as reclosing interval increases, "risk of arc" reignition (RAR) will decrease.

Among the advantages of using these smart recloser devices, the following are mentioned:

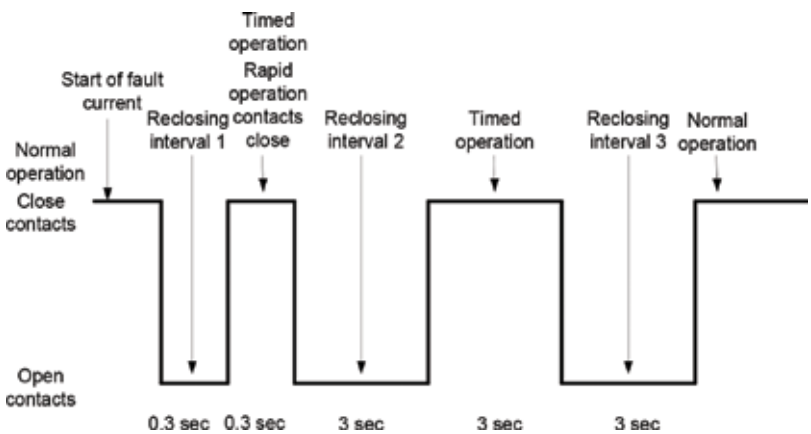

Figure 15. Recloser operation mode, a possible process of programing reclosing.

- Increased economic efficiency: the unpredictable blackouts of electrical grids are removed, the maintenance time and costs are reduced, the weak points of the installations are quickly observed, and better organization of investment is possible.
- Increased operation safety: accidental interruptions of electrical grids are not possible due to insulation faults, the exact location of the insulation faults can be established, the electrical installations are maintained at a high operation level, and the circuits are being monitored both online (under load) and offline (off).
- Optimal maintenance: The insulation faults are found and quickly indicated, automatic location of a system section (subcircuits) with isolation faults is possible, optimal personnel and repairing time planning, complete and centralized information regarding the electrical installation state, monitoring and remote diagnosis via the Internet/Ethernet.
- Enhanced protection against fire: the insulation faults are found in incipient phase. Thus, there are no major isolation faults, the isolation faults representing the main fire starters. The use of insulation transformers as well as monitoring and remote diagnosis via Internet/Ethernet allows the separation of certain sections (electrical subgrids) that can be exposed to fire from the rest of the power system.
- Enhanced protection against accidents: the removal of electroshocks by disconnecting the faulted systems or circuits and the prevention of disturbances in the control circuits of various equipment and electric machines.

6. Conclusions

This chapter proposes some solutions about the topics of unconventional backup structures used in smart microgrids. The issue is of interest particularly in connection with the problem of ensuring continuity in power supply. In this context, firstly the case of the switching to the backup power supply, in the case of a low-voltage symmetrical grid when using two frequency converters, one of which is alternately maintained in cold reserve, is presented. The only consumer is an asynchronous motor with a short-circuit rotor with nominal active power P = 22 kW. The logic of switching and electrifications is ensured by using an associated software of a microprogrammable automaton. Secondly, the switching to the backup power supply, in the case of low-voltage symmetrical smart microgrids using an electric generator set or using an electric generator set and the photovoltaic panels, in the case of modern residential buildings, is proposed. The microgrid is symmetrical and uses two identically transformers, T1 and T2, one of the transformers being alternately in hot reserve state. The users are divided into two categories: critical and noncritical ones. Finally, the implementation of recloser devices for autoconfiguration and automatic connecting/disconnecting decisions, in order to switch on the backup power supply, is presented. It is expected in the future realized the conversion of the public grids to active (distribution/using) grids that use high-tech smart devices like reclosers. The grouping together of these smart microgrids that have the auto-reconfiguration option through implementation of the recloser type devices is also considered in the development of smart grids. In this context the implementation of the recloser-type devices for switching on the backup power supply, for the case of a two radial structures of a public grid with isolated neutral, is presented.

Author details

Lucian Pîslaru-Dănescu[1]* and Laurențiu Constantin Lipan[2]

*Address all correspondence to: lucian.pislaru@icpe-ca.ro

1 National Institute for Research and Development in Electrical Engineering ICPE-CA, Bucharest, Romania

2 University Politehnica of Bucharest, Bucharest, Romania

References

[1] Pîslaru-Dănescu L, Lipan L-C, El-Leathey L-A. Microgrids smart structures used for back-up power supply. EEA—Electrotehnica, Electronica, Automatica. 2016;**64**(3):68-74. Print ISSN: 1582-5175

[2] ***Mitsubishi Electric. FR-A540-22K. Technical Catalogue. 2005

[3] Boaski MAF, dos Santos C, Sperandio M, Bernardon DP, Ramos MJ, Porto DS. Coordination and selectivity of protection devices with reliability assessment in distribution systems. In: Volosencu C, editor. System Reliability; December 20 2017. ISBN 978-953-51-3706-1. Print ISBN 978-953-51-3705-4. DOI: 10.5772/intechopen.69603. http://dx.doi.org/10.5772/intechopen.69603

[4] Oerter C, Neusel-Lange N. Smart control of low voltage grids. IEEE Power & Energy Society General Meeting 2014. Panel Session: Advanced Modelling and Control of Future Low Voltage Networks. July 31st 2014

[5] *** IEEE Guide for Safety in AC Substation Grounding, ANSI AEEC Std 80/86, New York

[6] Chousidis C, Nilavalan R, Lipan L. Expanding the use of CTS-to-self mechanism for reliable broadcasting on IEEE 802.11 networks. In: Proceedings of the IEEE International Conference on Wireless Communications and Mobile Computing Conference (IWCMC), 4-8 Aug, 2014. Nicosia, Cyprus: IEEE; 2014. pp. 1051-1056. DOI: 10.1109/IWCMC.2014.6906500

[7] Khan M, Ashton PM, Li M, Taylor GA, Pisica I, Liu J. Parallel detrended fluctuation analysis for fast event detection on massive PMU data. IEEE Transactions on Smart Grid. 2015;**6**(1):360-368. DOI: 10.1109/TSG.2014.2340446

[8] ***Mitsubishi Electric. Simple application controllers, Alpha & Alpha XL, Technical Catalogue. 2005

[9] ***Mitsubishi Electric. Simple application controllers, Alpha XL, Programming Manual α2 Simple Application Controllers. April 2005

[10] ***Tavrida Electric. Recloser based automation solutions for smart grid up to 40,5KV. Technical Catalogue Rev. 4. 1.2.2013, 2013

[11] ***Thomas&Betts. Introducing the new Elastimold® Recloser. Technical Catalogue. 2012

[12] ***Revac. Pole mounted vacuum Recloser. Technical Catalogue. 2007

[13] Azari RN, Chitsazan MA, Niazazari I. Optimal recloser setting, considering reliability and power quality in distribution networks. American Journal of Electrical Power and Energy Systems. 2017;**6**(2):1-6. DOI: 10.11648/j.epes.20170601.11

[14] Celli G, Ghiani E, Pilo F, Tedde S. Extending switching reclosing time to reduce interruptions in distribution networks. In: Proceedings of the 21st International Conference on Electricity Distribution (CIRED'21); 6-9 June 2011, Frankfurt Germany. 2011. pp. 1-4, Paper 700

Chapter 6

Assessment of Reliability of Composite Power System Including Smart Grids

Thotakura Bharath Kumar, M. Ramamoorty and
O. Chandra Sekhar

Additional information is available at the end of the chapter

http://dx.doi.org/10.5772/intechopen.75268

Abstract

The large service interruptions of power supply in the transmission system have significant impact on modern society. The aim of the power system engineers is to prevent and mitigate such events with optimal decisions in design, planning, operation and maintenance. Due to the rapid growth in the power demand and competitive power market scenario, the transmission and distribution systems are frequently being operated under heavily loaded conditions. This tends to make failure of components more frequent in the power system necessitating large downtime to repair or replace the equipment. A majority of the service interruptions are happening due to lack of proper planning and operation of power system. Therefore, complete reliability assessment in generation, transmission and distribution systems is needed at the planning stage. The reliability assessment in smart grids is very much beneficial to the power operator and reduces the risk of grid failure due to failure of major components in power systems. This chapter is confined to composite power system reliability assessment. The composite power system combines both the generation and transmission systems' adequacy. The generation system in the composite power system includes both conventional and renewable sources. The composite power system reliability assessment is quite difficult due to the large number of equipment, interconnected network topology and uncertainties in generation capacity. The reliability assessment concentrates mainly on the use of probabilistic states of components in generation and transmission systems to evaluate the overall reliability. This analysis will result in a cost-effective system configuration to provide continuous power supply to the consumers at reasonable cost. The reliability level of the system is measured by the defined indices. One of these indices is the probability of average power availability at load bus. This reliability assessment mainly focuses on development of methods to evaluate the probability of average power availability at load buses for a specified system configuration. This chapter discusses the two main techniques called node elimination method and modified minimal cut set method.

Keywords: composite power system reliability, failure rate, repair rate, minimal cut set, Monte Carlo simulation

1. Introduction

The modern power system has become a highly complex network, due to the integration of a large number of generating sources and large transmission and distribution networks. The above-stated reasons will affect the reliability of the smart grid. The main requirement of the power system is to provide electricity for a wide range of consumers with various requirements. It is not possible to serve the consumers continuously due to the random failures of equipment in the power system network. This causes the consumers' service interruptions frequently irrespective of the planned maintenance. It affects the reliability of power supply at the consumer bus and smart grid as well. Therefore the power engineers must consider the term "reliability" at the level of designing and planning of the power system network or smart grid. Reliability is the general quality of the system and defined as "It is an ability of the system to perform a desired function within a specified period of time under stated conditions" [1].

In view of above-mentioned reasons, there is a need for complete reliability assessment of the present power system. The evaluation of reliability plays an important role in power system analysis, design, upgrades and operations, especially in bulk power system. Power system reliability assessment methods have been developed over the years, and many publications are available on this subject [1–8].

2. Power system reliability assessment

The power system reliability is a measure of the ability of the system to meet the consumer requirements with quality electrical energy. In general "reliability" is usually divided into two aspects of system adequacy and system security [9, 10], as shown in **Figure 1**.

According to the North American Electric Reliability Corporation (NERC), adequacy and security are defined as [11]:

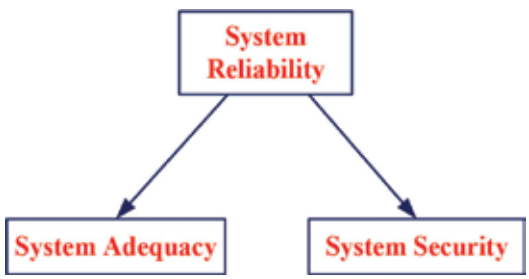

Figure 1. Power system reliability subdivision.

Adequacy—"The ability of the power system to supply the total electrical demand and power requirements of the end use customers at all times, by taking into the account of scheduled and reasonably expected unscheduled outages of system components."

Security—"The ability of the power system to withstand sudden disturbances such as electric short circuits or unexpected loss of system elements."

The work reported in this chapter is limited to adequacy assessment of the power system. The fundamental techniques used for the assessment of adequacy can be categorized in terms of their application to segments of a complete power system. These segments of the power system are shown in **Figure 2** and can be defined as the functional zones of generation, transmission and distribution [12]. Hierarchical levels are formed by combining the functional zones of the power system.

The assessment of reliability at hierarchical level I (HL-I) is only concerned with the generation facilities. In this level, the total power system generation including interconnected renewable generation is examined to decide its ability to serve the total system load demand considering the possible contingencies. The reliability assessment at HL-I is usually defined as generating capacity reliability assessment. The reliability assessment at hierarchical level II (HL-II) combines both the generation and transmission in evaluation of the integrated ability of the composite power system to deliver energy to the bulk supply points. This analysis is generally termed as composite power system reliability assessment or bulk power system reliability assessment. The reliability assessment by considering all the three functional segments is

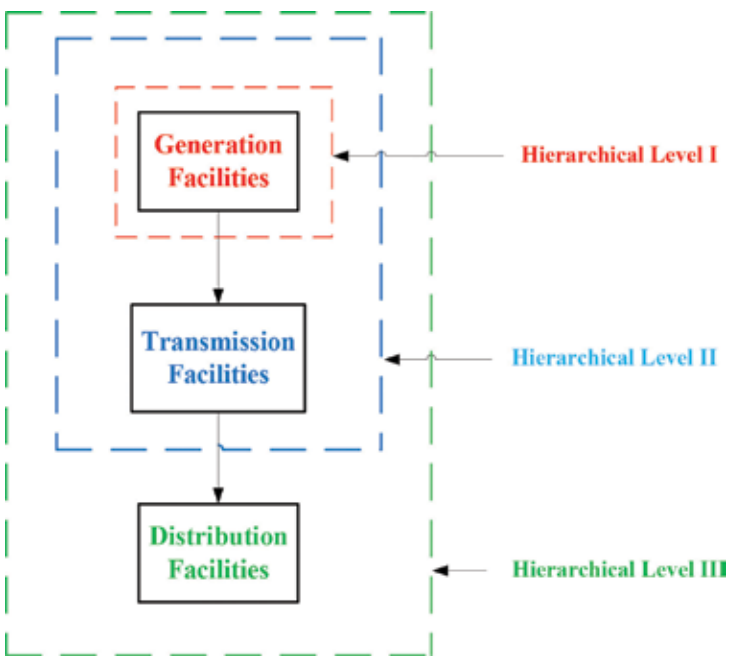

Figure 2. Structure of hierarchical level.

known as HL-III analysis. The work reported in this book is confined to the reliability assessment at HL-II level (composite power system) and is focused on adequacy analysis.

The basic role of an electric power system is to supply its customers with electrical energy as economically as possible and with a reasonable degree of continuity and quality. Power system reliability is generally expressed in terms of indices that reveal the system capability and the quality of service provided to its customers. The reliability concept and techniques first applied on practical power systems were mostly based on empirical experience and were all deterministically based. Many of methods are still in use today. These earlier concepts of reliability assessment, however, are inherently deterministic and do not account for the probabilistic or stochastic nature of system behavior, customer demands or component failures. The application of probabilistic methods for reliability assessment can consider the inherent stochastic nature of the power system and provide quantitative measures for power system reliability and thus complement the limitations of deterministic methods. Power system reliability assessment using probabilistic methods has been in practice since 1947. These are discussed in detail in the following sections. Research on reliability assessment over the last 60 years has been directed toward the evaluation of reliability indices applying probabilistic methods [13, 14]. Many reliability indices are defined over the years to judge reliability of the power system. The most commonly used reliability indices are discussed in [15]. The research work reported in this book is mainly focused on the average power availability for the bulk consumers connected to the power system network.

3. Literature review

The main function of the modern power system is to satisfy the energy needs of the consumer as economical as possible and with reasonable level of continuity and quality. The power system is made up of different components like circuit breakers, transformers, relays, etc. Failure of these components will result into customer supply interruption and cause loss of load. In order to assess the continuity of power supply to the consumers and improve it if possible, there is need of complete reliability assessment. By considering the failure (λ) and repair (μ) rates of all the components in the system, the average power availability is calculated with tracing of power flow paths. This is a basic method followed by power engineers earlier [1–14]. After tracing of paths, the equivalent failure and repair rates are calculated by series-parallel approach. But in the present complex power system, it is very difficult to identify those paths. Later star-delta and delta-star conversion methods developed, but again identification of those networks is a difficult task in complex systems [14]. The reliability of any system is determined using either deterministic or probabilistic methods. Deterministic methods present the reliability assessment with the information on how a system/component failure (called contingencies) can happen or how system/component success can be achieved. The traditional deterministic criterion used particularly in bulk electric systems (BES) is known as the N-1 security criterion [14] under which the loss of any bulk system component will not result in system failure. The main weakness of deterministic method is that they do not react to the stochastic nature of power system behavior, consumer demands or component failures. Power

system behavior is stochastic in nature, and therefore it is reasonable to believe that the probabilistic methods are able to react to the real factors that influence the reliability of the system. Probabilistic methods present quantitative indices (reliability indices), which can be used to make a decision on whether the power system performance is acceptable or if changes need to be made.

An analytical method will constantly give the same numerical result for the same system, same model and same set of input data. Hence these methods tend to provide a high degree of confidence in the reliability assessment. Analytical methods, however, usually need assumptions to simplify the solutions. This is particularly the case with complex network and generating system with integration of renewable generation. The resulting analysis can therefore lose some of the confidence on the results obtained. This difficulty can be reduced or eliminated by using a simulation approach. Monte Carlo simulation method is a well-known method and is used to estimate the reliability indices by simulating the actual process and random nature of the failure and repair of the system/components. This method, therefore, treats the problem as a series of experiments. There are advantages and disadvantages in both methods. Generally, Monte Carlo simulation method requires a large computation time compared to analytical methods. Monte Carlo simulation methods, however, can theoretically take into account virtually all aspects and contingencies inherent in the planning, design and operation of a power system [12, 14].

Considerable research has been done in the last two decades in the area of composite power system reliability assessment using analytical, Monte Carlo simulation and mixing of both methods [1–14]. There are two types of Monte Carlo methods, such sequential and nonsequential types. Nonsequential method is widely used in the evaluation of power system reliability. The research work presented in this book is mainly concentrating on the difficulties associated with the traditional methods and presented some simpler methods for reliability assessment.

4. Composite power system reliability assessment

The research work presented in this book concentrates on HL-II, i.e., composite power system reliability assessment. These reliability studies will assess the ability of the composite generation and transmission system (composite power system) to not only satisfy the consumer requirements but also tolerate the random failures and execute preventive maintenance of electrical components. The reliability performance of any system is generally evaluated by the reliability parameters or indices. The composite power system reliability is judged in this research work by considering "average power availability" and "loss of load expected" as reliability indices at the bulk consumer buses. There are many publications that are dealing with composite power system reliability assessment [1–14]. In the evaluation of reliability in composite power system, many technical issues are involved such as load uncertainty, generation adequacy, integration of nonconventional sources, multiple outages, etc. [4, 13]. By keeping these technical issues in view, this research work addresses some new and improved methods for the assessment of composite power system reliability.

The composite power system reliability assessment presented in this book considers all equipment in the system such as circuit breakers, transformers, generators, buses, lines, etc.

5. Reliability assessment techniques

The electric power systems are good examples for reliability assessment. In many power systems, the average duration of interruptions faced by a customer is just a few hours per year, which indicates that high availability of power supply to consumers is ensured considering scheduled and unscheduled outages (random failures). The high power availability can be achieved by proper maintenance and monitoring of the equipment. There are several methodologies developed over the years for the reliability measurement. The early methods used were all deterministic and are not convenient to apply for large interconnected power system. Also the deterministic methods cannot consider the stochastic nature of the system and load [14].

Later probabilistic methods are developed to obtain meaningful information regarding the system reliability. The probability of random failure and repair durations during the operating life of the component is assumed to be exponentially distributed. Based on this, the mean time to failure (MTTF = $1/\lambda$) and the mean time to repair (MTTR = $1/\mu$) can be evaluated [15]. These indices for each component are used to obtain the overall system reliability. In this chapter, the average power availability at the load bus is used as a measure for the reliability assessment of the system. The reliability study in the interconnected power system is complex due to the large number of components and network topology. So far the reliability assessment in interconnected power system is achieved through tracing of the power flow paths [10–14]. But tracing of power flow paths in a large power system network becomes difficult and takes time. Simple and more convenient method based on electrical circuit approach is presented here.

The probability of power availability and unavailability of a component having failure and repair rates (λ and μ) is given in Eqs. (1) and (2). The failure and repair rates of each component in the power system are assumed to be constant throughout the operation. The probabilities of failure and repair rates are exponentially distributed. The component failure and repair rates are independent of other components, and their future states are not dependent on their past history. So the probability of present state changes is governed by the exponential distribution and not dependent on past history of the component.

$$Availability = \frac{\mu}{\lambda + \mu} \tag{1}$$

$$Unavailability = (1 - Availability) = \frac{\lambda}{\mu + \lambda} \tag{2}$$

The existing methods for the reliability assessment of composite power system are explained in the following chapters. The limitations and difficulties of those methods are also discussed.

5.1. Series-parallel approach

If two components are connected in series in a branch of the network and each component has its failure rate and repair rate as shown in **Figure 3**. The equivalent failure and repair rates for the branch are given in the Eqs. (3) and (4).

$$\lambda_{eq} = \lambda_1 + \lambda_2 \tag{3}$$

$$\mu_{eq} = \frac{\mu_1 \mu_2}{\mu_1 + \mu_2} \tag{4}$$

Similarly if two components are connected in parallel as shown in **Figure 4**, then the equivalent failure and repair rates are given in Eqs. (5) and (6).

$$\lambda_{eq} = \frac{\lambda_1 \lambda_2}{\lambda_1 + \lambda_2} \tag{5}$$

$$\mu_{eq} = \mu_1 + \mu_2 \tag{6}$$

Initially using this series-parallel approach, most of the simple power system network reliability was evaluated.

5.2. Star-delta approach

In the complex interconnected power systems, there exist a number of star and delta configurations, and series-parallel approach alone is not enough to reduce the network. During the evaluation of the availability, there will be a need for star-delta transformation for network

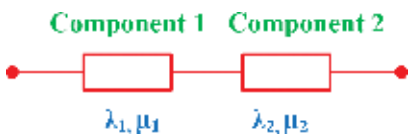

Figure 3. Components in series.

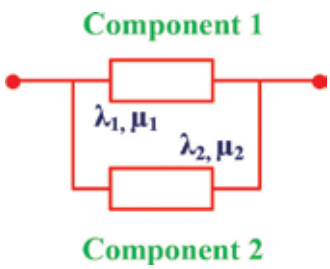

Figure 4. Components in parallel.

reduction. The equivalent failure and repair rate transformations from star to delta or vice versa are given in the following equations from Eqs. (7) to (12). The equivalents are based on the condition that the equivalent failure and repair rates for both the configuration should be same across any two terminals. The equivalent star-delta reliability models are shown in **Figures 5** and **6**.

The equivalent failure rates are given by

$$\lambda_{ab} = \frac{\lambda_1\lambda_2 + \lambda_2\lambda_3 + \lambda_3\lambda_1}{\lambda_3} \tag{7}$$

$$\lambda_{bc} = \frac{\lambda_1\lambda_2 + \lambda_2\lambda_3 + \lambda_3\lambda_1}{\lambda_1} \tag{8}$$

$$\lambda_{ac} = \frac{\lambda_1\lambda_2 + \lambda_2\lambda_3 + \lambda_3\lambda_1}{\lambda_2} \tag{9}$$

Equivalent repair rates are given in the equations from Eqs. (10) to (12) as follows

$$\mu_{ab} = \frac{\mu_1\mu_2}{\mu_1 + \mu_2 + \mu_3} \tag{10}$$

$$\mu_{bc} = \frac{\mu_2\mu_3}{\mu_1 + \mu_2 + \mu_3} \tag{11}$$

$$\mu_{ac} = \frac{\mu_1\mu_3}{\mu_1 + \mu_2 + \mu_3} \tag{12}$$

5.3. Delta-star approach

Similarly the conversion from star to delta is as follows. The equivalent failure rates are given by equations from Eqs. (13) to (18),

$$\lambda_1 = \frac{\lambda_{ab}\lambda_{ac}}{\lambda_{ab} + \lambda_{bc} + \lambda_{ca}} \tag{13}$$

$$\lambda_2 = \frac{\lambda_{ab}\lambda_{bc}}{\lambda_{ab} + \lambda_{bc} + \lambda_{ca}} \tag{14}$$

$$\lambda_3 = \frac{\lambda_{ac}\lambda_{bc}}{\lambda_{ab} + \lambda_{bc} + \lambda_{ca}} \tag{15}$$

Equivalent repair rates are given by

$$\mu_1 = \frac{\mu_{ab}\mu_{bc} + \mu_{bc}\mu_{ac} + \mu_{ab}\mu_{ac}}{\mu_{bc}} \tag{16}$$

$$\mu_2 = \frac{\mu_{ab}\mu_{bc} + \mu_{bc}\mu_{ac} + \mu_{ab}\mu_{ac}}{\mu_{ac}} \tag{17}$$

$$\mu_3 = \frac{\mu_{ab}\mu_{bc} + \mu_{bc}\mu_{ac} + \mu_{ab}\mu_{ac}}{\mu_{ab}} \tag{18}$$

The interconnected power system network (IEEE 6 bus reliability test system) used here consists of a number of circuit breakers, two generating units and four load points as shown in **Figure 7** [15]. In this IEEE 6 bus reliability test system, the failure and repair rates (λ and μ) of each component are given in [15]. The average probability of power availability at load bus is calculated by reducing the network by series-parallel and star-delta or delta-star conversion methods between the source node and the sink or load node. The equivalent reliability model of the IEEE 6 bus reliability test system is shown in **Figure 8**.

In the interconnected power system shown in **Figure 7**, the IEEE 6 bus reliability test system is reduced to simple delta connection, where it has two nodes of generating units and one node for load. The reduced reliability network is shown in **Figure 9**. Using the methodology explained above, equivalent λ and μ are obtained between generator nodes 1 and 2 and load node. From this, the probability of average power availability at the load is obtained using Eq. (1). The same procedure is used to find the probability of availability at all load points one by one. The probabilities of average power availability at each load are calculated using series-parallel and star-delta approach and are given in **Table 3**.

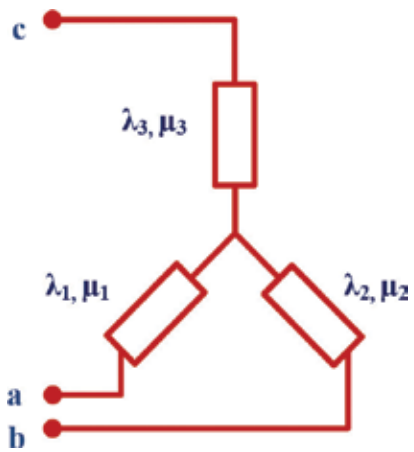

Figure 5. Equivalent star connected reliability model.

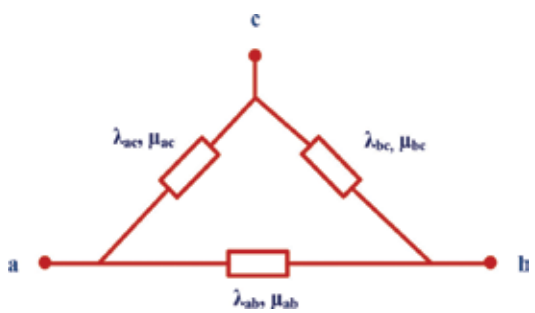

Figure 6. Equivalent delta connected reliability model.

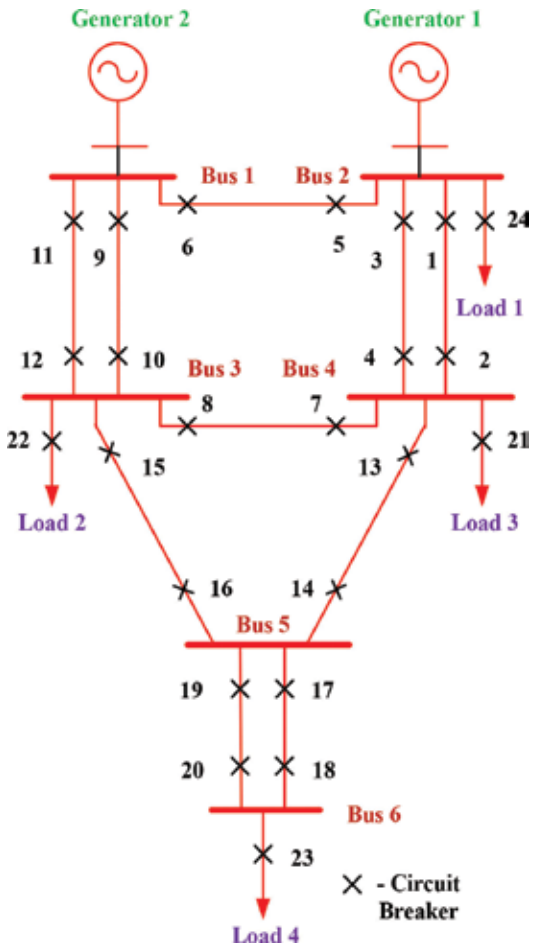

Figure 7. IEEE 6 bus reliability test system.

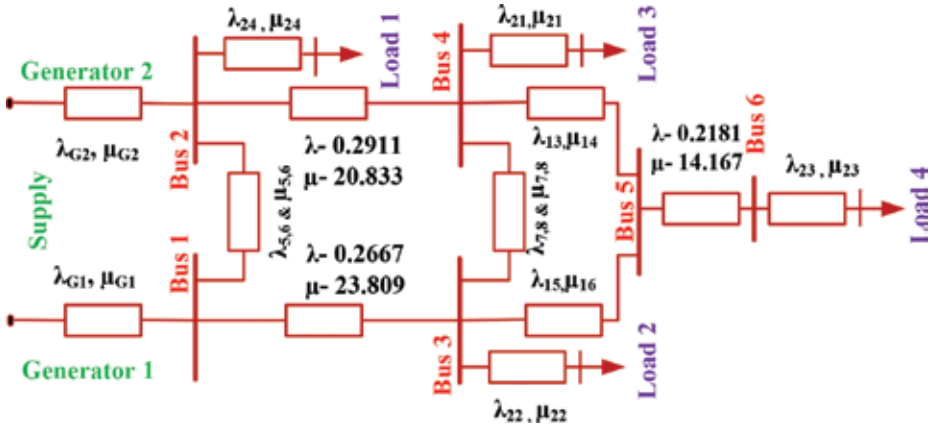

Figure 8. Equivalent reliability model of the IEEE 6 bus reliability test system.

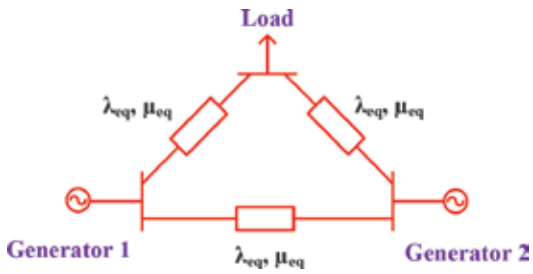

Figure 9. Reduced reliability network.

The evaluation of reliability in the interconnected power system is complex due to the large number of components connected and growing network topology. So far the reliability assessment in interconnected power system is obtained through tracing of the power flow paths [14]. Tracing of paths is time consuming in the case of large networks. Simple and more convenient method based on electrical circuit approach is presented in the following section.

5.4. Node elimination method

The interconnected power system (IEEE 6 bus reliability test system) consists of a number of components, and each component has its own failure and repair rates (λ and μ). From Eqs. (3), (4), (5) and (6), it can be observed the failure rate (λ) is similar to the resistance (R) and the repair rate (μ) is similar to the capacitance (C) in an equivalent electrical network. Hence the reliability model of interconnected power network shown in **Figure 8** can be replaced by an equivalent R-C network for reliability assessment. The classical node elimination method is a known technique. The classical node elimination method is used for power system analysis and has not been used so far for reliability studies. This is the first time the classical node elimination method for reliability assessment in interconnected power system is adapted. It is used to reduce the equivalent electrical network to calculate power availability at load bus.

The equivalent reliability model between generator nodes 1 and 2 and the load bus 4 is shown in **Figure 10**.

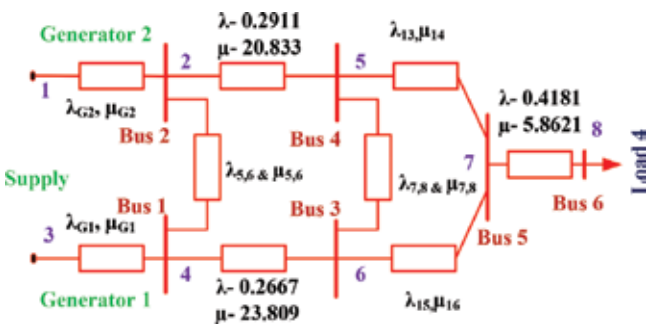

Figure 10. Equivalent reliability model for load 4.

In the analogous electrical model, this network is replaced by two networks where in the first one, all failure rates (λ) in each branch are represented by a resistance (equal to λ) and in the second one each branch is represented by a capacitance equal to μ. For reliability assessment, each of these equivalent electrical networks is reduced to a simplified network connecting the sources to the load nodes where the average power availability is required to be calculated. For simplification of the network, node elimination method is used as explained in the following paragraph.

The power system network consists of eight nodes. The power supply node is considered as a current injection node, and the load node where the availability is to be computed is treated as current sink. This reliability model is used to obtain the power availability at load bus 4 only. The other load nodes do not have any current injection. To reduce the network, the nodes in which the current does not enter or leave are eliminated. The equivalent electrical network is described by the nodal equation.

$$\begin{bmatrix} I_1 \\ I_2 \\ \vdots \\ \vdots \\ I_8 \end{bmatrix} = \begin{bmatrix} Y_{11} & Y_{12} & \dots & \dots & Y_{18} \\ Y_{21} & Y_{22} & \dots & \dots & Y_{28} \\ \vdots & \vdots & \dots & \dots & \vdots \\ \vdots & \vdots & \dots & \dots & \vdots \\ Y_{81} & Y_{82} & \dots & \dots & Y_{88} \end{bmatrix} \begin{bmatrix} V_1 \\ V_2 \\ \vdots \\ \vdots \\ V_8 \end{bmatrix} \tag{19}$$

5.5. Concept of conditional probability

The approach is used to evaluate the power availability in the composite power system, and it is based on conditional probability. A system/component is said to be connected if there exists a path between the source and the sink. The availability of power at the receiving end of a branch not only depends on the failure and repair rates of the components in that branch but also depends on the state of associated components of the branches. These branches can form a power flow path for the particular branch. In the literature, most of the methods are based on the tracing of power flow paths. For example, if a load bus is supplied by three paths a, b and c with power availability at the sending end of each path assumed to P_1, P_2 and P_3 and the probabilities of availability of paths a, b and c are P_a, P_b and P_c, then the probabilities of power unavailable at the ends of paths a, b and c are $(1 - P_1P_a)$, $(1 - P_2P_b)$ and $(1 - P_3P_c)$. Then net probability of average power available (P_L) at the receiving end load bus is given by

$$P_L = 1 - (1 - P_1P_a)(1 - P_2P_b)(1 - P_3P_c) \tag{20}$$

The sending end probabilities of each path are termed as conditional probabilities. The concept of conditional probability is explained with the example given in **Figure 11**. In this directed graph, the generators are connected at the buses 1, 2 and 4. The load buses are 2, 3, 5 and 7. The average power availabilities at the different buses are calculated using the concept of conditional probability as follows.

The availability of power injected into the system by generator G_1 at bus 1 is given by

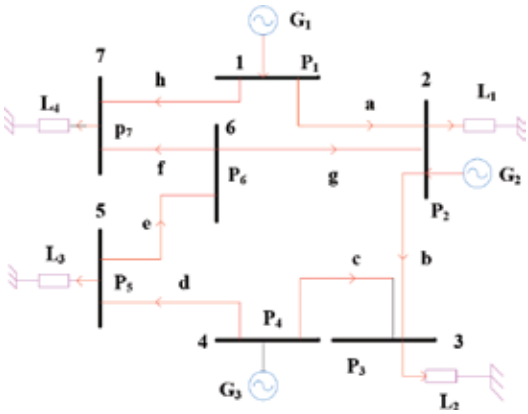

Figure 11. Interconnected power system.

$$P_1 = \frac{\mu_{G1}}{\lambda_{G1} + \mu_{G1}} \tag{21}$$

The incident paths for load L_1 are a and g in addition to path from generator G_2. The branch b is not incident on bus 2. The sending end probability of power availability of path a is P_1 and similarly for path g is P_6 and for generator branch is $\frac{\mu_{G2}}{\lambda_{G2}+\mu_{G2}}$.

So the power availability at bus 2 is given by

$$P_2 = 1 - \left[\left(1 - \frac{\mu_{G2}}{\lambda_{G2} + \mu_{G2}}\right)\left(1 - P_1\frac{\mu_{la}}{\lambda_{la} + \mu_{la}}\right)\left(1 - P_6\frac{\mu_{lg}}{\lambda_{lg} + \mu_{lg}}\right)\right] \tag{22}$$

Similarly the power availability at other buses is given by

$$P_3 = 1 - \left[\left(1 - P_4\frac{\mu_{lb}}{\lambda_{lb} + \mu_{lb}}\right)\left(1 - P_2\frac{\mu_{lc}}{\lambda_{lc} + \mu_{lc}}\right)\right] \tag{23}$$

$$P_4 = \frac{\mu_{G3}}{\lambda_{G3} + \mu_{G3}} \tag{24}$$

$$P_5 = P_4\frac{\mu_{ld}}{\lambda_{ld} + \mu_{ld}} \tag{25}$$

$$P_6 = P_5\frac{\mu_{le}}{\lambda_{le} + \mu_{le}} \tag{26}$$

$$P_7 = 1 - \left[\left(1 - P_6\frac{\mu_{lf}}{\lambda_{lf} + \mu_{lf}}\right)\left(1 - P_1\frac{\mu_{lh}}{\lambda_{lh} + \mu_{lh}}\right)\right] \tag{27}$$

where P_1, P_2, P_3, P_5, P_6 and P_7 are the probability of power available at respective buses; λ_{la}, λ_{lb}, λ_{lc}, λ_{ld}, λ_{le}, λ_{lf}, λ_{lg} and λ_{lh} are the failure rates of the respective branches; and μ_{la}, μ_{lb}, μ_{lc}, μ_{ld},

μ_{le}, μ_{lf}, μ_{lg} and μ_{lh} are the repair rates of the respective branches. Based on the generation availability, the direction of power can change in the network. Similarly another way to calculate the average power availability at the bus 2 is calculated by breaking the branch "b" at bus 2, and new node 2^{I} is created. The power availability at this node is $P_2^{\prime}$ equal to $P_3\left[\frac{\mu_b}{\mu_b+\lambda_b}\right]$. The new power availability at bus 2, when the branch "b" terminates on bus 2, is given by

$$P_2^{II} = 1 - \left(1 - P_2^{\prime}\right)(1 - P_2) \tag{28}$$

Knowing the probability of power availability at generators using their respective failure and repair rates, the probability of power availability at all load buses can be computed.

The matrix Y_{Bus} in the above Eq. (19) is the nodal admittance matrix using the concept of conditional probability, and I and V are the fictitious nodal injected current vector and voltage vector of the equivalent R-C network. To evaluate the equivalent failure rate, the nodal Y_{Bus} is made up of only the resistive component (λ) for each element, and for equivalent repair rate, the capacitance component (μ) is used for each element. From the equivalent reliability model shown in **Figure 10**, it is clear that currents I_1, I_3 and I_8 are injected currents and remaining currents are made zero for eliminating the corresponding nodes in the reduced network. Hence the name of this method is called node elimination method. Then Eq. (19) becomes as

$$\begin{bmatrix} I_A \\ I_B \end{bmatrix} = \begin{bmatrix} X & Y \\ Y^T & Z \end{bmatrix} \begin{bmatrix} V_A \\ V_B \end{bmatrix} \tag{29}$$

In Eq. (29), I_A is a vector containing the currents that are injected (I_1, I_3, I_8), I_B vector is a null vector (I_2, I_4, I_5, I_6, I_7), V_A is a vector containing the voltages at the injected currents (V_1, V_3, V_8), V_B is a vector of null vector (V_2, V_4, V_5, V_6, V_7) and Y_{Bus} is formed by the combination of matrices X, Y and Z.

From Eq. (29) the following variables are derived as.

$$\mathrm{I_A} = \mathrm{XV_A} + \mathrm{YV_B} \tag{30}$$

$$0 = \mathrm{I_B} = \mathrm{Y^T V_A} + \mathrm{ZV_B}$$

$$\mathrm{V_B} = -\mathrm{Z^{-1}Y^T V_A}$$

$$I_A = \left(X - Z^{-1}Y^T V_A\right)V_A \tag{31}$$

The reduced Y_{Bus} is given in Eq. (32), and with the help of this reduced Y_{Bus} matrix, we can draw the simple equivalent delta network as shown in **Figure 9**.

$$Y_{Bus}^{Reduced} = \left(X - Z^{-1}Y^T V_A\right) \tag{32}$$

From the above Eq. (32), the equivalent λ and μ between the source node and the load node are obtained. The reduced Y_{Bus} indicates the nodal equation of the simplified delta network shown

in **Figure 9**. The equivalent failure and repair rates are obtained from the reduced Y_{Bus} one at a time by assuming λ as resistance R and μ as capacitance C. Since the generator failure and repair rates are already considered in the Y_{Bus} formation, the nodes 1 and 2 of generators in the equivalent reliability model of the network shown in **Figure 9** have 1.0 availability and so can be combined together to evaluate the average availability of power at the load node. So the corresponding network elements between generator 1, generator 2 and load will be in parallel, and overall equivalent λ and μ are calculated. The same procedure is used if there are more than two generators in the power system network. The average power availability at the remaining load points is calculated by adapting the same procedure. The results obtained from this method are given in **Table 1**.

5.6. Modified minimal cut set algorithm

As discussed in previous sections, the composite power system reliability assessment becomes difficult in complex network because of the large number of equipment, components and integration of renewable power generation. Hence the calculation average power availability becomes complex in the modern power system. For power system reliability assessment, usually component failures are assumed to be independent, and reliability indices are calculated using traditional methods like series-parallel and star-delta equivalents of network connections. This section discusses one new evaluation algorithm for the estimation of average power availability based on modified minimal cut set method using conditional probability.

Due to the rapid growth in the power demand, environmental constraints and the competitive power market scenario, the transmission and distribution systems are frequently being operated under heavily loaded conditions, which tend to make the system less stable. The recent literature indicates that most of the blackouts took place due to overloaded transmission system. Further failure of components in the power system causes supply interruptions to connected loads. Statistically, the majority of the service interruptions are happening due to lack of proper planning and operation of power system [15–18]. Therefore complete reliability assessment in transmission and distribution systems (composite power system) is needed in planning of power system. For the above-stated reasons, there is a need for the reliability assessment of composite power systems. One of the objectives used for the evaluation of

S. no.	Cut set	Components in cut
1.	1	C
2.	2	a, b
3.	3	a, c
4.	4	a, b, c
5.	5	a, c

Table 1. Available cut sets.

composite power system reliability is power availability at load buses. Some assumptions made in the proposed algorithms are given below.

1. The failure and repair rates during the operating life of the component are assumed to be constants, and the probability distribution of the failure and repair states of the component is exponentially distributed.
2. Each component repair and failure rate is independent of the states of other components.

In literature there are several methods available for the calculation of network reliability. Monte Carlo simulation method has been used by many authors for the estimation of reliability indices including power availability. This method is very popular but takes large computational time. However, it is widely used for the testing of the new methods.

The proposed algorithm discussed in this chapter has the following advantages:

1. It is very efficient and easy to program.
2. The power availability at each bus can be computed easily without reducing actual network.
3. The proposed algorithm is applicable to any number of bus systems.
4. It takes less computation time compared to other methods.

The results obtained by the proposed step-by-step methods are validated by Monte Carlo simulation and also by classical node elimination method discussed in this chapter [64]. The steps for the methodology used in the proposed method are discussed in the following sections and are applied on practical example in [16]. Some of the relevant work regarding the reliability assessment of complex networks is available in [17, 18].

5.7. Introduction to minimal cut set method

The composite power system reliability assessment is generally based on minimal path or cut enumeration, tracing of power flow paths from which the related reliability indices are calculated. The minimal cut set is a popular method in the reliability assessment for simple and complex configurations. There are several methods available for the calculation of average power availability, which is one of the important reliability indices. Some of the popular methods used are minimal cut set, series-parallel, star-delta, tracing of power flow paths, node elimination method and step-by-step algorithm using conditional probability. Yong Liu et al. [13] have assumed that all the branches included in each cut set of order 1 are assumed to be in parallel, with the sending end of each branch in the cut set having the same probability of power availability which is not correct. This assumption is not used in the proposed method. The procedure adapted is explained in the following sections. The initial step in the cut set method is to figure out the minimal cut sets of the system. The identification of minimal cuts becomes more difficult in large complex systems. Some algorithms like node elimination method presented in [15] can be used to reduce this effort for identification. A step-by-step

procedure for a modified minimal cut set method is explained in the following sections using IEEE 6 bus, 14 bus and single-area IEEE RTS-96 system.

A system is said to be connected if there exists a path between the source (generator) and the sink (load). The removal of the cut set results in the separation of the system into two independent subsystems. One contains all generator nodes and the other system contains all load nodes. A cut set is a set of components or equipments whose failure will cause system failure [55–60]. The general cut set method is given in the following simple example where the cut sets for load in **Figure 12** are given in **Table 1**.

The definition of a minimal cut set as a cut set in which there is no other subset of components or equipments whose failure alone will cause the system to fail, implies that a normal cut set corresponds to more component failures than are required to cause system failure. The available minimal cut sets for the load in the given example are shown in **Table 2**. The order of the cut set is shown in **Figure 13**.

The concept of conditional probability is explained with the example given in **Figure 12**. In this system the generator is connected at the left side. The load bus is 3. The second-order cut set is supplied by two paths and has sending end power availability of P_1. The equivalent system is shown in **Figure 14**. λ and μ are the overall equivalent failure and repair rates of branches a and b in parallel and in series with branch c.

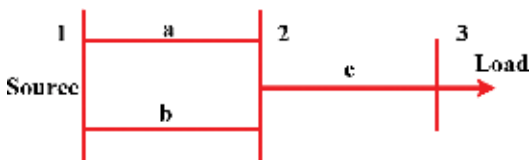

Figure 12. Simple power system to illustrate the concept of cut set.

S. no.	Cut set	Components in cut
1.	1	C
2.	2	a, b

Table 2. Minimal cut sets.

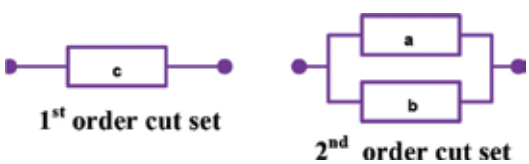

Figure 13. Minimal cut sets for example system.

Figure 14. Cut set branch.

Considering the probability of power availability at the source end, the equivalent failure, repair rates between source and load are given by

$$\lambda' = \frac{\lambda}{P_1} \tag{33}$$

$$\frac{1}{\mu'} = (1 - P_1)\frac{1}{\lambda} + \frac{P_1}{\mu}$$

$$\mu' = \frac{\lambda \times \mu}{(1 - P_1)\mu + P_1\lambda} \tag{34}$$

The net average power availability at the receiving end is given by

$$Average\ power\ availability = \frac{\mu'}{\mu' + \lambda'} \tag{35}$$

The proposed technique is used to find the average power availability at the consumer end in a composite power system and is based on the minimal cut sets.

The steps involved in the proposed algorithm are:

1. Draw the graph of the network.
2. Generators are connected to the network node through a branch toward that node.
3. Loads are directly connected to the bus called the load node.
4. All branches are represented by the reliability parameters failure and repair rates (λ and μ).
5. Choose a particular load node.

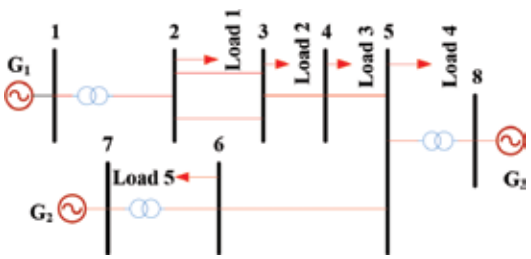

Figure 15. Practical example.

6. Obtain the cut set which isolates this node.

7. For those cut branches which are incident in this node, assume the probability of availability of power at the node at the other end of the branch.

8. Based on these probabilities (P), compute the probability of average power availability at the chosen load node.

9. Find the cut set which isolates all these above nodes identified in step 7.

10. Repeat steps 7 and 8 to find the power availabilities at these nodes assuming the probabilities at the other end of the branches in the cut set.

11. Using these probabilities, evaluate the probability of power availabilities at these cut nodes.

12. Repeat this exercise until all the nodes are covered including all generator nodes.

13. Using these probabilities works backwards to compute the probability of power availability at the chosen load node.

14. Repeat this exercise for all the load nodes.

15. Obtain the system overall average power availability from step 14.

The proposed algorithm is tested with the practical example taken from the Roy Billinton paper. The configuration of the practical example is shown in **Figure 15**. The system is connected to generators at the buses 1, 7 and 8 through interconnecting transformers. The failure and repair rates are assumed to be identical for all components throughout the system. This is only for convenience. If different failure and repair rates are specified for each component like generator, transformer, line, etc., the same can be used. There will be no change in the procedure steps 1 to 15 described above.

6. Results and discussions

The algorithms/methods presented in this chapter have been applied to practical example. In this practical example, all components are assumed to have identical reliability data ($\lambda = 0.1$; $\mu = 10$). The results are shown in **Table 3**. The proposed methodology is validated by the Monte Carlo simulation method, node elimination method [15] and step-by-step algorithm using conditional probability [16]. The algorithm developed in this chapter is also applied on IEEE suggested power system network to validate the results. The IEEE 6 bus reliability test system is shown in [15]. The reliability data of the system is given in [15]. The average power availability at the load buses is given in **Table 4**. To show the efficiency of the proposed method for reliability assessment of large systems, the IEEE 14 bus system and IEEE RTS-96 system are used. The IEEE 14 bus system is shown in [64]. The reliability data of the IEEE 14

S. no.	Load no.	Modified minimal cut set method	Node elimination method	Monte Carlo method	Step-by-step algorithm using conditional probability
1	Load 1	0.994	0.999	0.989	0.999
2	Load 2	0.984	0.985	0.974	0.992
3	Load 3	0.985	0.995	0.956	0.995
4	Load 4	0.991	0.998	0.985	0.998
5	Load 5	0.988	0.998	0.965	0.998

Table 3. Average power availability in practical example.

S. no.	Load no.	Modified minimal cut set method	Node elimination method	Monte Carlo method	Step-by-step algorithm using conditional probability
1	Load 1	0.994	0.994	0.92737	0.990
2	Load 2	0.964	0.967	0.89847	0.968
3	Load 3	0.935	0.939	0.90790	0.936
4	Load 4	0.883	0.884	0.85934	0.887

Table 4. Average power availability in IEEE 6 bus system.

S. no.	Load no.	Modified minimal cut set method	Node elimination method	Step-by-step algorithm using conditional probability
1	Load 1	0.956	0.967	0.967
2	Load 2	0.965	0.967	0.966
3	Load 3	0.967	0.967	0.966
4	Load 4	0.933	0.938	0.933
5	Load 5	0.911	0.914	0.914
6	Load 6	0.911	0.917	0.917
7	Load 7	0.942	0.951	0.950
8	Load 8	0.933	0.939	0.939

Table 5. Average power availability at different loads in IEEE 14 bus system.

bus system is given in [15]. The results obtained for the IEEE 14 bus system are shown in **Table 5**.

The proposed modified minimal cut set algorithm is also applied and tested on IEEE single-area RTS-96 system shown in [15]. The reliability data for IEEE single-area RTS-96 system is taken from [15]. The average power availability at the load buses for the system is shown in **Table 6**.

S. no.	Load no.	Modified minimal cut set method	Node elimination method	Step-by-step algorithm using conditional probability
1	Load 1	0.881	0.885	0.885
2	Load 2	0.822	0.819	0.812
3	Load 3	0.555	0.558	0.555
4	Load 4	0.852	0.846	0.852
5	Load 5	0.812	0.812	0.812
6	Load 6	0.813	0.812	0.813
7	Load 7	0.815	0.812	0.813
8	Load 8	0.833	0.836	0.833
9	Load 9	0.855	0.859	0.859
10	Load 10	0.854	0.857	0.854
11	Load 11	0.811	0.818	0.811
12	Load 12	0.836	0.832	0.836
13	Load 13	0.844	0.845	0.844
14	Load 14	0.786	0.788	0.788
15	Load 15	0.764	0.763	0.764
16	Load 16	0.862	0.868	0.864
17	Load 17	0.800	0.808	0.800

Table 6. Average power availability at different loads in IEEE single-area RTS-96 system.

7. Conclusions

In this chapter reliability modeling of power system components is analyzed by the node elimination method and modified minimal cut set method. The IEEE 6 bus system, IEEE 14 bus systems and single-area IEEE RTS-96 system are used to evaluate the reliability. The two methods gave similar results on average power availability at load bus. The series-parallel and star-delta method is quite difficult for the reduction of complex networks, whereas the node elimination method is easy even for large systems. The new methodologies proposed in this chapter are very useful for power system planners and utility consumers. The electrical circuit approach method is further useful to the power system operators to make decision on the future average power availability. The proposed method on minimal cut set is useful for the reliability assessment in the planning and operation of larger power system network.

Conflict of interest

There is no potential conflict of interest.

Author details

Thotakura Bharath Kumar*, M. Ramamoorty and O. Chandra Sekhar

*Address all correspondence to: tbkumar256@gmail.com

K L E F Deemed to be University, Guntur, India

References

[1] Billinton R. Bibliography on the application of probability methods in power system reliability assessment. IEEE Transactions on Power Apparatus and Systems. 1972;**91**:649-660

[2] Allan RN, Billinton R, Lee SH. Bibliography on the application of probability methods in power system reliability assessment: 1977-1982. IEEE Transactions on Power Apparatus and Systems. 1984;**103**:275-282

[3] Billinton R, Allan R. Reliability Assessment of Power Systems. 2nd ed. New York: Plenum Press; 1996

[4] Billinton R, Fotuhi-Firuzabad M, Bertling L. Bibliography on the application of probability methods in power system reliability assessment: 1996-1999. IEEE Transactions on Power Systems. 2001;**16**(4):595-602

[5] Carpignano A, Piccini M, Gargiulo M, Ponta A. Reliability and availability evaluation for highly meshed network systems: Status of the art and new perspectives. In: Proceeding Annual Reliability and Maintainability Symposium; 2002. pp. 104–111

[6] Sumper A, Sudria A, Ferrer F. International reliability assessment in distribution networks. In: Proceedings of the International Conference of Renewable Energies and Power Quality, Spain; 2004

[7] North American Electric Reliability Council Planning Standards. Available at: http://www.nerc.com (August 2007)

[8] Bae IS, Kim JO. Reliability assessment of customers in a microgrid. IEEE Transactions on Power Apparatus and Systems. 2008;**23**:1416-1422

[9] Yeh W-C, Lin Y-C, Chung YY, Chih M. A particle swarm optimization approach based on Monte Carlo simulation for solving the complex network reliability problem. IEEE Transactions on Reliability. 2010;**59**(1):212-221

[10] Malinowski RJ. A new efficient algorithm for generating all minimal tie-sets connecting selected nodes in a mesh-structured network. IEEE Transactions on Reliability. 2010;**59**(1):203-211

[11] Heydt GT. The next generation of power distribution systems. IEEE Transactions on Smart Grid. 2010;**1**(3):225-235

[12] Liu Y, Singh C. Reliability assessment of composite power systems using Markov cut-set method. IEEE Transactions on Power Systems. 2010;**25**(3):777-785

[13] Hashmi M, Hanninen S, and Maki K. Survey of smart grid concepts, architectures, and technological demonstrations worldwide. In: Proceedings IEEE PES Conference Innovative Smart Grid Technologies (ISGT Latin America); 2011

[14] Al-Muhaini M, Heydt G. Minimal cut sets, Petri nets, and prime number encoding in distribution system reliability assessment. In: Proceedings 2012 IEEE Power and Energy Society T&D Conference; 2012

[15] Bharath Kumar T, Chandra Sekhar O, Ramamoorty M. Reliability modelling of power system components through electrical circuit approach. Journal of Electrical Engineering (JEE). 2016;**16**(3):232-239

[16] Bharath Kumar T, Chandra Sekhar O, Ramamoorty M. Composite Power system Reliability assessment using modified minimal cut set approach. In: Alexandria Engineering Journal – Elsevier; 2017 (Accepted- Production house & Available in Early access)

[17] Bharath Kumar T, Chandra Sekhar O, Ramamoorty M, Lalitha SVNL. Evaluation of power capacity availability at load bus in a composite power system. IEEE Journal of Emerging and selected topics in Power Electronics (JESTPE). 2016;**4**(4):1324-1331

[18] Bharath Kumar T, Chandra Sekhar O, Ramamoorty M. Evaluation of average power availability at load buses for an interconnected composite power system using step by step method with conditional probability. In: Proceedings of IEI Sustainable Development in Indian Power Sector for the Next Decade, Pune, November 2016

Chapter 7

The EU Research Project PLANET

Andrea Schröder, Christoph Kahlen,
Mariapia Martino and Antonis Papanikolaou

Additional information is available at the end of the chapter

http://dx.doi.org/10.5772/intechopen.78563

Abstract

Renewable energy sources offer unprecedented opportunities to reduce greenhouse gas emissions. But some challenges remain to be solved before their full benefits can be reaped. The main one relates to the intermittency of their electricity supply which can lead to grid problems such as congestion and imbalance between generation and demand. Energy conversion and storage has been touted as a very promising solution to all aforementioned issues. PLANET will develop a holistic decision support system for the optimal orchestration of the different energy networks for aggregators and balance responsible parties, policy makers and network operators. It will aid them to leverage innovative energy conversion in alternative carriers and storage technologies in order to explore, identify, evaluate and quantitatively assess optimal grid planning and management strategies for future energy scenarios targetting full energy system decarbonization. Moreover, an analysis of the possible synergies between electricity, gas and heat networks will be carried out by creating simulation models for the integration between energy networks and conversion/storage technologies, for example power-to-gas, power-to-heat and virtual thermal energy storage. Application of the developed tools in two different test cases in Italy and France will showcase their benefits and reveal potential grid stability issues and effective countermeasures.

Keywords: smart grids, synergies between networks, electricity, district heating, natural gas, power-to-gas, power-to-heat, virtual energy storage, network planning tools, grid operation ICT tools

1. Introduction

1.1. The problem and the need

The motivation for this research project stems from the ambitious target setting of the European Commission (EC) to reduce carbon dioxide. Its energy roadmap 2050 [1] suggests that by 2050, the European Union (EU) should cut greenhouse gas emissions to 80% below 1990 levels. Although all sectors—power generation, industry, transport, buildings, construction and agriculture—need to contribute to the low-carbon transition according to their technological and economic potential, the power sector has been identified to have the biggest potential for cutting emissions.

It can almost totally eliminate CO_2 emissions by 2050 (see **Figure 1**) [2]. To meet these aspiring aims, more renewable energy generation (wind, solar, water and biomass or other low-emission sources) is needed. As some of these resources are intermittent like wind and solar, their integration into the power grid calls for apt measures in order not to endanger system stability and reliability.

To accomplish the integration of renewables, there are three measures at hand:

- Enhancement of the grid

  By establishing new power lines and enhancing existing ones, excess electrical energy can be transported from the centres of generation to the centres of demand avoiding bottlenecks.

- Provision and use of flexibility

  Some decentralised energy resources (DER) such as combined heat and power plants (CHP) or an aggregation of them like photovoltaic (PV) systems with batteries and electric vehicles (EV) can provide flexibility to the grid, allowing for balancing generation and demand. By using flexibility of aggregated DER, curtailment of renewables can be avoided, and ancillary services (e.g. frequency and voltage support) can be provided.

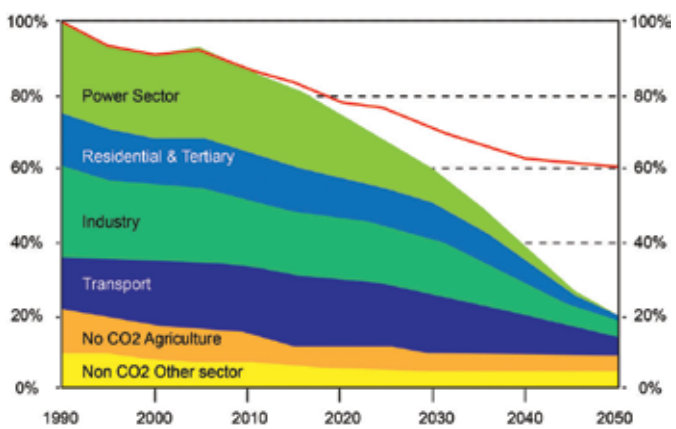

Figure 1. Possible 80% cut in greenhouse gas emissions in the EU (100% = 1990).

- Storage and conversion of electrical energy

  The current modus operandi of the decoupled electricity/gas/heating networks must be changed in order to allow synergies between the energy networks. Excess electrical energy can be converted into gas or heat and be stored in the respective gas and heat networks. From there it can be used for the purpose of the respective energy network (generation/provision of heat) or be reconverted in electric energy.

The PLANET project primarily focuses on the conversion of electrical energy and its storage in networks of other energy carriers. By doing so, it will also provide flexibility to the grid. This flexibility can be used for balancing purposes or for offering ancillary services to the grid. Furthermore, PLANET will provide the necessary ICT tools for policy makers and grid planners to guide future network expansion activities by allowing to evaluate if an investment in grid enhancement or conversion technologies or a combination of both is the best solution for today's and future grid challenges.

1.2. The PLANET solution

PLANET will facilitate the grid integration of a broad portfolio of decentralised storage/conversion solutions capable of providing different grid services via a unified and holistic framework for distribution grid planning, operation and management optimization. This solution contributes towards full integration of clean renewable energy resources by exploiting the potential of interconnections and synergies between different energy networks to increase flexibility of electricity demand and to align it with intermittent generation inherent to renewable energy resources. By doing so, it will add to the realisation of the fully integrated EU internal energy market and is of course also apt of being utilised outside the EU.

A functional scheme of this integration is shown in **Figure 2**. It depicts models of the electric grid, the gas network and the district heating (DH) network interconnected by the following conversion technology models:

- power to gas (P2G),
- combined heat and power (CHP), and
- power to heat (P2H) including
  - centralised power to heat (CP2H),
  - local power to heat (LP2H),
  - power to heat (P2H), and
- virtual energy storage (VES).

CP2H refers to heat pumps (or other P2H equipment such as boilers) that are installed at the premises of the DH operator in order to heat the water that goes into the DH grid. LP2H refers to heat pumps that are installed in the premises of customers of the DH grid. Their operation can relieve the DH grid of some heat demand. Although it is in principle possible for LP2H to affect the temperature of the water of the DH grid, it is not intended in the project. Instead, the heat is consumed at the customer premises. VES implies the conversion to heat

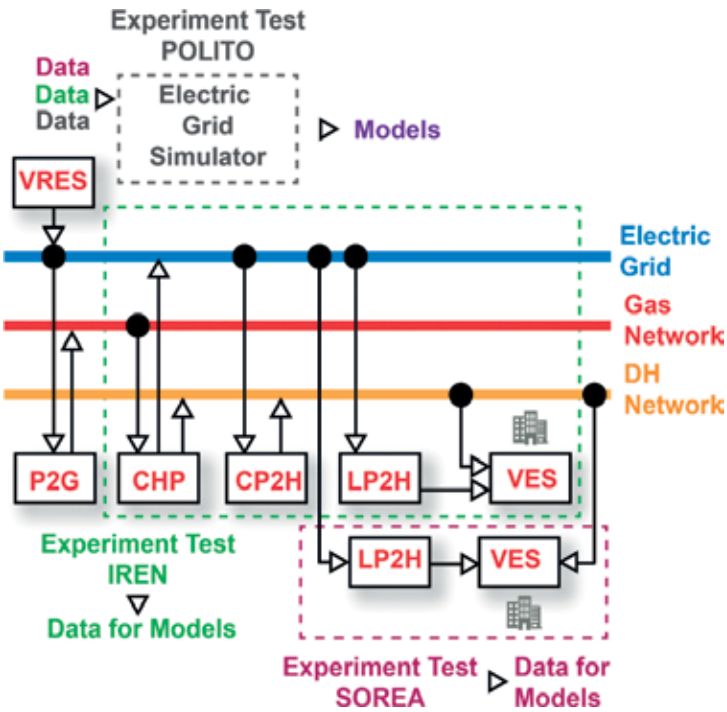

Figure 2. The PLANET energy flows, grid integration and energy conversions.

by means of human-centric thermal management. It leverages the thermal inertia of buildings and installed heating and cooling equipment for the maximum human comfort. Variable and intermittent renewable energy sources (VRES) feed energy into the electric grid. From there, electric energy is converted with one of the conversion technologies, and the transformed energy is fed either into the gas network, the electric grid, or the DH network (indicated by the arrows). In case of CHPs, it is assumed that they are gas-driven and that hence their input energy comes from the gas network. The cogeneration technology allows CHPs to bring synergies among networks as they simultaneously generate heat and electric power that can then be fed into the corresponding heat network and electric grid. Besides, **Figure 2** shows the experimental test sites and their coverage of conversion technology models. These test sites will provide real data for conversion model verification and calibration. Data from the IREN [Italian distribution system operator (DSO)] and SOREA (French DSO) test sites are provided for the Electric Grid Simulator of POLITO (Italian university) which derives models for the networks out of it. The PLANET solution is based on the following four core activity lines:

1. **The modelling of conversion/storage technologies** in order to enable planning, management and operation tools to properly account for their expected impact upon real deployment in the field. These technologies include P2G (high purity methane for direct injection to the gas grid), P2H (including CP2H, LP2H and VES) and CHP (cp. **Figure 2**).
2. **The simulation of the integration between electricity, gas and heat networks models, together with conversion/storage technologies models**, in order to understand how these conversions can affect network stability, reliability and responsiveness.

3. **The development of a holistic decision support system** (DSS) that enables multi-grid operational planning and management taking into account synergies and energy flows between the electricity, gas and heat networks. The purpose is to identify and evaluate optimal strategies to deploy and operate conversion/storage systems on the distribution grids within boundary constraints of real deployments outlined in the future energy system scenarios.
4. **Policy and market model impact assessment and exploration** to evaluate the current regulatory landscape for the deployment of P2G and P2H storage/conversion solutions, as well as policy/market reform recommendations in order to pave the way for their deployment in a technology-neutral manner that ensures maximum benefits to society and the environment. Moreover, an activity of exploration and investigation of novel roles and business models in the energy market will be carried out to pave the way for the commercial exploitation of project results within the opportunities that arise from the existence of PLANET products.

In addition to the aforementioned core PLANET activities, a number of complementary activities will be carried out to investigate and facilitate the adoption and replication of the developed solutions. They include:

1. **Preliminary business planning** to set out initial revenue models and go-to-market strategies for the innovative market actors that will assume the risk of bringing the PLANET solutions to the market through a long maturation process and cost structure improvement, building acceptance in society, establishing appropriate business models and go-to-market strategies and finally developing new products/services.
2. **Pre-design of ICT interfaces to the energy networks and devices** that will deliver grid services (P2G and P2H units, storage units, PCM, CHP units) in order to facilitate their effective operation within the electricity distribution grid in a coordinated manner that will enable the appropriate business actor to deliver valuable grid services.
3. **Definition and promotion of proposals for standardisation bodies** based on the aforementioned interfaces to strive for industrial consensus and to speedier and frictionless adoption by the entire energy system ecosystem, including network operators, equipment vendors, energy retailers, actor marketing conversion/storage solutions, and so on.

2. The PLANET approach

2.1. Concept

Recently, the EU roadmaps outlined the requirement of a slew of technologies and solutions for maximising the capability of the electrical grid to safely host variable and intermittent renewable energy sources (VRES) generation in future energy systems. Actually, the majority of VRES generation in Europe is made available by large, centralised plants (mostly off-shore wind farms) connected to the transmission grid. In the mid-term future, though, the expected proliferation of distributed, variable, small-scale RES systems, aided by extensive policy incentives, can

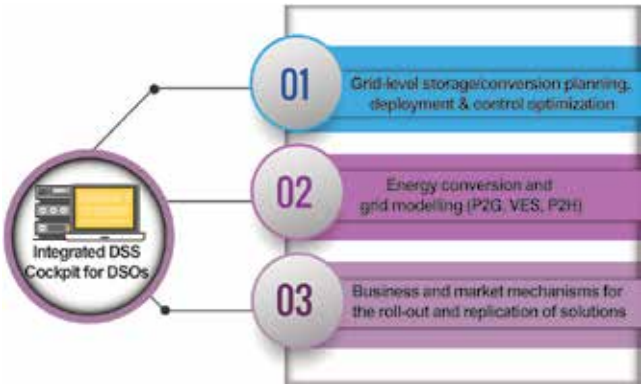

Figure 3. The PLANET concept.

create concern for the distribution grid. Their generation patterns depend directly on weather conditions which tend to be homogeneous across restricted geographical areas. This results in amplification effects that can hamper grid stability and balance. For example, solar irradiance variations in a neighbourhood can be homogeneous resulting in synchronised energy injection in the grid by multiple PV systems hampering grid balance and stability on a very local scale. This example demonstrates the need for decentralised mitigation means. Moreover, significant benefits stem from placing the mitigation means as close as possible to the instability sources in the grid topology. Matching (in terms of proximity in the grid topology) intermittent generation to conversion/storage facility reduces the jeopardised sub-grid area which in turn improves the effectiveness of ancillary services (e.g. reactive power) and DSO grid operation management.

The PLANET project aims at developing a comprehensive solution for the mitigation of critical situations due to decentralised VRES deployment in the distribution grid, towards enabling the elimination of their curtailment and ultimately, the integration of large shares of renewables into the electricity system to achieve the EU energy and environmental objectives for decarbonising the electricity grid and establishing the EU Internal Energy Market. As depicted in **Figure 3**, the PLANET concept consists of the following components:

1. Grid-level storage/conversion planning, deployment and control optimization

PLANET will set up a decision support system that will enable the introduction of storage/conversion solutions in energy system level assessment and evaluation scenarios by authorised energy system actors for network planning, operation and optimization in an integrated and holistic manner. To enhance the representativeness and applicability of the DSS outputs on the actual energy system, real grid constraints will be introduced via a hardware-in-the-loop simulation engine. The heart of this framework is a multi-purpose, district-level optimization software suite with holistic visibility over electricity supply and demand on the grid as well as on the availability and diverse flexibility characteristics of storage/conversion solutions. This suite can be used by network operators to coordinate/orchestrate available flexibility sources (P2H, P2G, VES) for optimal grid operation or by policy makers to evaluate and assess incentives and instruments for maximisation of social welfare and acceleration of policy implementation. Optimization approaches that will be applied include conventional deterministic optimization as well as efficient handling of uncertainty.

2. Energy conversion and grid modelling (P2G, VES, P2H)

The three conversion/storage technologies that are in the heart of PLANET activities are already quite mature, ranging from validated research work (VES and P2G) to established technology deployed in the field for decades (P2H). To enable their incorporation in the aforementioned DSS, PLANET will create novel simulation models of these technologies that can be used for fast what-if scenario analysis without compromising on their accuracy for the intended purpose. For P2G conversion, the model will be a high-level abstraction of the detailed simulation process focusing on the electrical interfaces of the conversion infrastructure in order to accurately represent grid interfaces and interactions. For the VES and P2H solutions, the simulation models will be based on the emulation of the actual system working on experimental data collected over a series of demonstration and validation activities that will take place within the project. Again, special emphasis will be given both to the electrical response of the associated devices as well as to the preservation of comfort and indoor healthy conditions. The P2H conversion technologies that will be analysed and modelled will take into account centralised power to heat and local power to heat. CP2H are P2H technologies that can be employed in district heating applications with large-scale thermal storages while LP2H are P2H technologies that can be exploited for the conversion of electricity in thermal energy in decentralised applications where traditional, phase change material (PCM) or VES solutions thermal storage can be applied for the heat conservation.

3. Business and market mechanisms for the roll-out and replication of the PLANET solutions

The implementation of the PLANET approach calls for large capital expenditures and new business models to be implemented. Moreover, the implementation of such innovative model needs national regulatory authorities to adopt a new set of rules on energy grids which are intended, on the one hand, to enhance market efficiency and coordination, and, on the other hand, to provide enough incentives to invest to all actors. This part of the project will, therefore, first evaluate business models according to the different possibilities that the regulatory scenario will generate. Each business model will be evaluated using the standard strengths, weaknesses, opportunities and threats (SWOT) analysis. For the business model that will emerge as marketable, we will provide a quantitative assessment using the cost-benefit analysis approach, quantifying the cost of its implementation and the (expected) revenues that it will generate. The second part will be devoted to an institutional comparison between regulatory rules in different EU regions and for different energy services (electricity, gas and heating) with the aim of defining a common regulatory setting and common innovative rules to foster grid investments. This part will involve national regulators, possibly through a questionnaire, and defining a new regulatory approach, which combines two regulatory tools: the first is the engineering-based simulation model developed in PLANET to define ex ante an efficient total network expenditures. The second tool is an incentive-compatible regulatory scheme that should provide ad hoc incentives.

2.2. Methodology

All smart grid actors and stakeholders (network planners and operators, market operators, policy makers, conversion equipment manufacturers and vendors, building managers, citizens, etc.) are collectively placed at the centre of different activities of the PLANET project, which

Figure 4. The PLANET user-driven innovation approach.

will adopt a user-driven innovation approach (see **Figure 4**) towards addressing emerging grid, end user and market needs, critical for the successful project implementation and the impacts realization. This user-driven innovation approach intends to involve its stakeholders as active constituents of virtual thermal storage systems as key enablers of the PLANET innovation process and encourages active and collaborative contributions in the development of technological solutions as well as the unique ICT framework for their assessment and grid deployment planning. Agile IT implementation methodologies in conjunction with early validation and verification protocols will be incorporated in the user-driven innovation approach to manage cross-functional teams and facilitate the efficient and proactive communication exchange. Continuous interactions between stakeholders, end users and developers will be encouraged in order to minimise deviations between end users expectations and final outcomes and guarantee the delivery of significant added value both at the level of individual project results (novel storage/conversion technologies, ICT framework) as well as at the level of the unified system which will be ready for use by network operators and policy makers. The proposed **user-driven innovation methodology/approach and activities** will effectively provide an excellent environment for experience sharing and exchange towards user-driven open innovation of products and services. The activities to be carried out will be oriented towards fulfilling the following objectives:

- Disseminate the project outcomes towards end users and various stakeholders to generate a broad awareness and involvement in the project activities.
- Create opportunities for further exploitation and replication of the project results after its official completion in both research and innovation activities.
- Obtain feedback from the end users and interested stakeholders throughout the entire project implementation duration and optimise all project developments, so as to directly address critical needs of end users (network operators, policy makers, etc.) and relevant stakeholders.

To achieve this degree of collaboration, the project will establish a complete awareness and communication framework with all aforementioned end users and stakeholders, including

also project partners as main drivers of communication activities. They will be actively involved from the very beginning of concept creation, spurring the motivation to share and discuss their experiences and requirements. This collaborative environment where all the stakeholders co-create the solutions will lead to a natural acceptance by the users who will be empowered not only to test, evaluate and report their own experience with the PLANET technologies and ICT framework, but mainly to start preparing for its adoption in their further research and business activities.

2.3. The PLANET system architecture

Figure 5 depicts the PLANET system architecture. It contains four main functional constituents:

1. Electricity supply module, uncontrollable demand module, virtual energy storage module and power-to-gas conversion module (middle);
2. PLANET SCCE (storage/conversion management and coordination engine) module (top);
3. PLANET IDOC (integrated DSS and orchestration cockpit) (left);
4. Dynamic grid simulation environment including the simulation model generator/integrator (bottom, yellow circle) and the eMEGAsim grid simulation environment (bottom, green circles).

The modules at the middle of the architecture diagram (supply, demand, VES, power-to-gas/heat) are of special importance since they link the PLANET optimization framework with the grid simulator that will validate the project results. Essentially these modules substitute the physical systems for electricity supply, demand, virtual energy storage and conversion systems (P2G, P2H) that will interface with future electricity

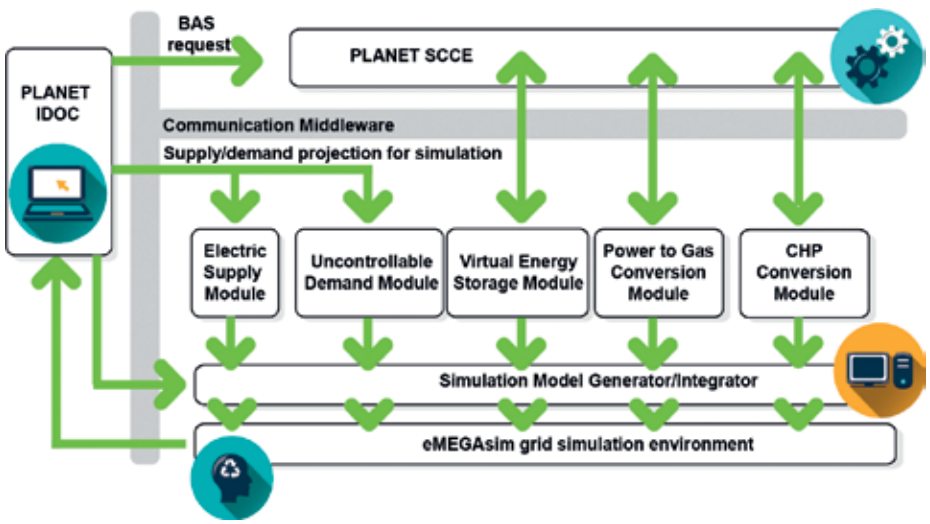

Figure 5. High level system architecture. BAS: balancing/ancillary services for the grid. IDOC: integrated DSS and orchestration cockpit; ISM: instantiated simulation model; M&(O&) C: monitoring and (optimization &) control; SCCE: storage/conversion management and coordination engine; VES: virtual energy storage.

distribution grids. Along with the grid simulator they represent the "physical world" with which the PLANET ICT system (IDOC, SCCE and middleware components) will interact. In order to adequately fulfil this intermediary role, their interfaces need to be very carefully defined. The interfaces towards the grid simulation environment will comprise high-level models of the electrical response of each system, which will then be translated into a simulation model by the generator (e.g. automatically generated Simulink models appropriately configured to exhibit their exact electrical supply/demand response during simulation). The interfaces towards the other system components depend on the nature of the modules.

The "electricity supply" and "uncontrollable demand" modules are the main levers of the PLANET ICT system for setting up the simulation environment with the expected supply/demand characteristics in the selected future energy system scenarios.

The main functional constituents of the PLANET high-level system architecture are described in more detail in the following lines:

1. The **electricity supply module** provides the entire electricity generation perspective to the simulation environment with special emphasis on the modelling of the electricity supply from intermittent VRES and especially small-scale ones. The models will help to understand the real scale of problems to be expected in the coming decades. They will also include the necessary abstract statistical models to forecast generation based on weather forecasts.

   The **uncontrollable demand module** models the expected demand that cannot be directly controlled by the PLANET ICT system, that is, any demand apart from power-to-heat/gas systems. Contrasting this demand with the supply forecast enables the quantification of "excess" supply that should be flexibly consumed/converted by the P2G, P2H and VES systems. Even more importantly, this contrast will also reveal the grid requirements for balancing/ancillary services.

   The **virtual energy storage module** will include a complete, unified representation of the equipment (VES unit) offering thermal storage as well as the building-level control system that will manage it. The latter will be responsible for extracting and aggregating the available demand flexibility of the building as well as the optimal coordination of the equipment based on control commands coming from the SCCE in order to deliver the agreed services to the grid. Moreover, this module contains the high-level VES model that encapsulates the interface behaviour of the VES producing the appropriate electrical response for the provided configuration settings.

   The **power-to-gas/heat conversion module** will perform similar functionality for the power-to-gas/power-to-heat system. Its control system will expose a standards-based interface to the SCCE component in order to receive instructions on how to instantiate energy conversion systems on the simulated grid as well as their operation setpoint for their control. The high-level models for P2G and P2H will encapsulate the interface behaviour of the P2G and P2H systems, respectively, producing the appropriate electrical response for the provided configuration settings.

2. **PLANET SCCE**: the SCCE component receives the grid needs for balancing and ancillary services and performs a holistic management and coordination across all available conversion/storage options in order to identify how to fulfil the service requests in an optimal manner. The SCCE is divided into the following three functional components:

   BAS request analysis and decomposition module

   This module analyses the grid needs formulated and communicated as a balancing/ancillary service (BAS) request and decomposes them as far as service type, location, time is concerned in order to generate the optimization objectives for the subsequent steps/modules. The decomposition step will perform flexibility allocation to the energy conversion/storage types based on technical and economic efficiency constraints.

   BAS from VES

   This module is in charge of optimally aggregating the available thermal storage capacity to satisfy grid needs in a fashion that is very similar to VPP aggregation and management.

   Energy conversion selection and deployment optimization

   The purpose of this module is to find the optimal way to convert excess electricity that is not used for thermal storage into another energy carrier using the power-to-gas technologies by virtually allocating such systems throughout the distribution grid and coordinating their operation.

3. **PLANET IDOC**: the IDOC component effectively represents the electricity distribution network operator in the PLANET ICT system. It has a complete view on the grid and can directly evaluate and pinpoint potential problems on the grid and subsequently issue requests for balancing/ancillary services. Additionally, it acts as the main user interface to the entire system. It consists of the following five components:

   Grid topology instantiation module

   This module specifies the inputs required for the grid simulation, including the grid topology instance, the detailed scenario regarding intermittent/conventional generation deployment and uncontrollable demand, the sizing and deployment of P2H systems and their connection to the grid, and so on. This information is used to instantiate.

   Simulation results analysis module

   This module interfaces directly with the dynamic grid simulation environment and receives the fine-grain (temporally/spatially on the grid) simulation results for analysis and insights on whether grid stability/imbalance problems (e.g. congestion, frequency deviations) may arise given specific supply and uncontrollable demand sources.

   BAS request generation module

   This module is responsible for generating a request for balancing/ancillary services that is compliant to the communication standard among the IDOC and SCCE component based on the findings of the simulation results analysis.

Process orchestration module

This module's responsibility includes the proper orchestration of all necessary activities for the meaningful and relevant execution of the PLANET ICT system, as specified in the process steps. To achieve this goal, it triggers the remaining system components with appropriate information and oversees the proper functioning of the system.

GUI and visual analytics module

This module comprises the front-end of the PLANET ICT system towards the user. Its feature set allows diverse user types to extract value out the system. For example, a network operator will be able to use the system to evaluate grid reinforcement needs assuming certain penetration of power-to-heat/gas systems in his grid. A policy maker may use it to establish policy instruments to subsidise storage/conversion technology deployment to defer grid reinforcements.

4. The **simulation model generator** component implements an automated method for the coupling of the high-level models of storage/conversion technologies to the dynamic grid simulation environment. Its interface towards the high-level models includes all the necessary information for the instantiation of appropriate models in the simulation framework. This ranges from the number of components and their grid connection location to their electrical response characteristics. This automatic model generation will be based on pre-defined templates for the storage equipment and conversion plants. They will be calibrated using the data provided by the high-level models and instantiated accordingly by generating Simulink components and plugging them in the simulation testbed.

   The **eMEGAsim grid simulation environment** is a real-time, hardware-in-the-loop simulator able to simulate grids at fine-grain time steps.

All communications among PLANET components will be handled by the **Communication Middleware** (grey bar), which will provide the necessary scalability and modularity to the system architecture. It will provide crucial functionalities on top of message routing, such as mediation, service orchestration, protocol conversion, and so on and enhance the interoperability between PLANET components. The middleware will comply with the interfaces to be specified in the project for standardisation purposes and will provide interoperability between them. Furthermore, the middleware will embed data protection and information (cyber-)security measures.

2.4. Models

As described in the PLANET architecture section the modules for electric supply, uncontrollable demand, VES, P2G conversion and P2H conversion comprise high-level models, among them those for P2G, P2H and VES. These models are explained in more detail in this section.

2.4.1. Power-to-gas model

The use of synthetic gases as carriers for excess renewable electricity, known as P2G, offers a solution to manage fluctuating output of renewable energy and mitigating CO_2 emissions at

the same time. The storage concept links power and gas networks by the conversion of power into gas by two major steps: hydrogen (H_2) production by water electrolysis and the following conversion of H_2 and carbon dioxide (CO_2) into methane (CH_4) in the Sabatier reaction. Production of synthetic or substitute natural gas (SNG) from CO_2 and H_2 is the advantageous option regarding thermodynamics, which has been demonstrated on an industrial scale at the Audi motor company "e-gas" facility in Werlte (Germany) of 1000 metric tons/year production of SNG from concentrated CO_2 obtained from a nearby biogas plant [3].

The electrochemical analysis will be exploited to develop a simplified high-fidelity model able to investigate optimization options to improve the value of power-to-gas systems to the distribution grid by enabling deployment in proximity to the distributed intermittent generation. During integration optimization, the availability of intermediate outputs and their condition (temperature, pressure) will be explored in order to improve the plant-level conversion efficiency and cost structure. Furthermore, this integration will take into account the energy system boundary conditions for the plant, such as CO_2 availability conditions, electrical supply characteristics and transport capability for SNG in order to optimise the electrolyser capacity. Different electrolysis technologies will be explored, for example, solid oxide electrolysis cells (characterised by high efficiencies, around 90%, but low H_2 production capacities), and Alkaline Electrolyser Cells (which have lower efficiencies, e.g. 75%, but higher H_2 production capacities). The modularity of both electrolysers and methanation reactors, which is necessary to adapt the P2G system throughput to the PLANET requirements, is particularly challenging, given the degree of integration that such two modules could benefit from. Therefore, proper process modelling of the integrated plant, together with reliable dynamic models for the coupling of the electrolyser with the electrical grid, is crucial for the success of the power-to-gas concept.

In particular, the best configuration of electrolysis and methanation coupling will be devised in terms of system efficiency as well as plant size (from 100 kW to 1 MW) and flexibility. Individual component modelling, namely the electrolyser, methanation reactor, heat exchanger network and balance of plant equipment will be simulated using numerical tools (e.g. Apros, Matlab and/or Simulink platform) to perform such integration, and the most suitable technologies will be selected: electrolysers (polymer electrolyte membrane (PEM), solid oxide electrolyser cell (SOEC), alkaline) and methanation (multistage adiabatic and/or isothermal reactors) modules will be investigated in order to resort to the optimal size and efficiency of the power-to-gas plant, selected based on technoeconomic criteria applied to the aforementioned simulated system.

2.4.2. Power-to-heat model

District heating has its roots in the late 1800s with steam-based systems and high temperatures (>200°C). This first-generation system has evolved through two more generations (second and third) characterised with use of pressurised hot water and lower supply temperatures. The discussion of fourth generation district heating grid [1] has raised issues such as new energy sources (e.g. solar, biomass, surplus energy), local production, using buildings as heat storages [4], cooling, heat pumps and ever lower temperature levels (<50–60°C). This evermore complex system poses challenges to its design and operation and in addition, coupling the heating

network with gas and electrical grids makes analysis and optimization of the system even more complex. Allegrini et al. [4] reviewed 20 modelling software solutions related to district-scale energy systems and their interactions with focus not only on district heat but also on renewable energy and urban microclimate. They concluded the simulation tools in this field are diverse in terms of data requirements, robustness, accuracy, speed, applicability and ease of use and the no on tools seems to fit all needs. Thus, a two-stage modelling approach combined with data from the pilot site are and ideal combination to be used in the P2H and DH modelling of the project. More precisely, data from the pilot site will aid in the conversion modelling whereas utilisation of a high-fidelity district heating system model (based on Apros [5]) will aid in the DH area.

Furthermore, until now, no integration of power-to-gas solutions with heat grid planning and operation optimization has been done. This area will be advanced in the project, bridging renewable power simultaneously to the gas and heat grids. Two possible power-to-heat conversion applications will be modelled: centralised power-to-heat (CP2H) applications and local power-to-heat (LP2H) applications.

2.4.3. Virtual energy storage model

Virtual energy storage is fundamentally different than the conversion solutions investigated in the project. It represents electricity demand that will fulfil actual human cooling/heating needs that are not bound by energy supply availability. The inherent building thermal inertia—ability to preserve indoor temperature conditions over time—and the availability of electrical heating/cooling equipment with thermal storage capacity (e.g. electrical boilers, heat pumps) provide the leverage to shape the time profile of electricity demand in both magnitude (load turn-up/shedding) and time (load shifting) without sudden and noticeable changes in the occupant ambience. This comfort-preserving flexibility can be almost instantaneously invoked and can reach very large magnitudes, if aggregated over several buildings, offering unique benefits for mitigation of grid instability, and secondarily imbalance. The virtual energy storage module models this flexibility to bridge the gap between the SCCE and the simulation model generator. Since the VES module should provide instances of high-level models of representative buildings—and their aggregated electrical response based on the configuration provided by the SCCE—most internal modelling in the VES module will be performed statistically to enable generation of multiple different, yet representative building instantiations.

The VES module is internally sub-divided into four distinct functionalities. The human-centric comfort preferences modelling component aims to understand and model how building occupants use the facilities and how their thermal comfort is affected by the building characteristics (natural light availability, insulation, etc.) as well as external factors (e.g. seasonal and weather patterns). The main goal of this component is to create user profiles that model thermal comfort by explicitly linking space temperature and comfort (using metrics like comfort elasticity) enabling optimization components to make educated decisions. In addition, it will identify and quantify temperature ranges where humans feel at maximum comfort, hence defining the user comfort flexibility. These models will be calibrated and trained using data that will be captured from real-life (residential/tertiary) buildings offered

by SOREA under normal operating conditions. In parallel, another component will undertake the modelling of the energy storage elements in terms of thermal and electrical properties. Its purpose is to quantify the thermal capacity and characteristics of buildings including the relevant equipment they host. To achieve this, the dynamic thermal and electrical characteristics of equipment with heat storage properties will be modelled to quantify the effective storage characteristics—for example, thermal capacity and associated electricity consumption, "discharge rate"—given specific environmental conditions. Apart from equipment, dynamic models of the building thermal inertia will also be developed to provide information on the operational context of the equipment. Subsequently these models will be merged to provide thermal storage models for specific building spaces—for example, apartments—that incorporate the properties of the equipment and the host building to yield the combined view on how electricity consumption patterns affect indoor temperature.

By merging the results of the two aforementioned components, the demand flexibility modelling component will calculate the actual acceptable variations in electricity demand that comply with the comfort preferences of building occupants or prespecified allowable comfort degradation. This demand flexibility is completely personalised to the individual user and customised to the specific characteristics of the space he resides in. Alternative user comfort profile templates will be combined with representative building space/amenities combinations in order to generate several possible configurations of context-aware flexibility and cover the diversity of real people living in actual buildings. Finally, the building-level VES optimization component will collect the human-centric flexibility configurations and perform three tasks:

- instantiate a certain building configuration and based on space-level flexibilities assemble the entire suite of flexibility offerings (alternative permissible combinations of demand shifting/shedding/turn-up based on space level demand flexibility) at the building level;
- provide these flexibility options to the SCCE component, which will select one and exercise this configuration option; and
- based on this configuration create the corresponding high-level models with the appropriate building-level electrical response that will be handed over to the simulation model generator component.

2.5. Solution operation steps

To assess conversion/storage at grid level, the following steps are performed between the components of the PLANET system architecture as laid out in the flow chart of **Figure 6**:

1. Step 1: initialization and configuration
2. Step 2: system simulation and imbalance identification
3. Step 3: flexibility dispatch optimization
4. Step 4: real-time monitoring and iterative "on-the-loop" optimization

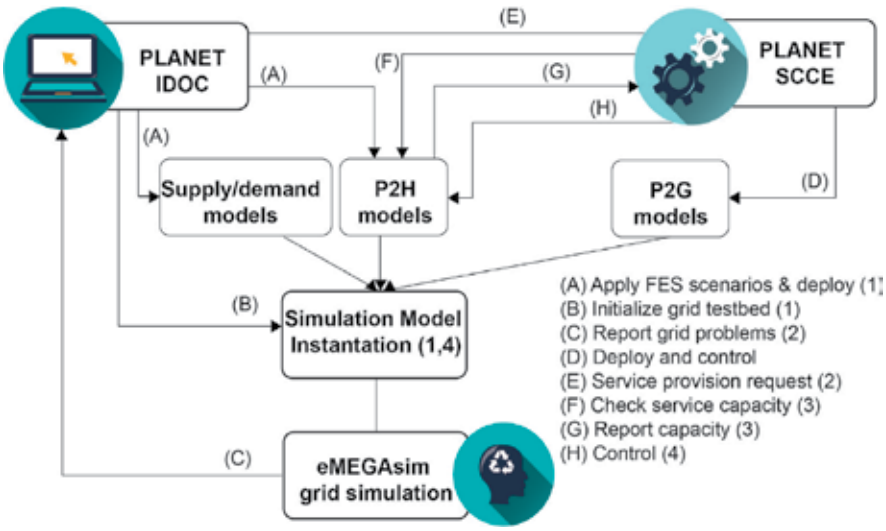

Figure 6. Flow chart of the conversion/storage assessment.

2.5.1. Step 1: initialization and configuration

The ICT system will allow end users (e.g. DSOs), as a first step to select a future energy system (FES) scenario and a network template that will be used for the simulation (A). Based on this information, the IDOC instantiates the simulation testbed with all necessary information including the grid topology and generation, load, storage simulation models (B). The latter can interface directly with the grid simulator and expose the time profile of the electrical behaviour of these devices to the grid including about the location and connection points of these generators/loads on the grid topology. These models include:

- **Conventional and intermittent RES generation facilities**: this model corresponds to the installed RES base according to the FES scenario that is being explored and incorporates all the necessary functionality.
- **Uncontrollable load**: this model corresponds to the electricity loads of the network excluding buildings assumed to be equipped with virtual energy storage capabilities, including conventional buildings, transport-related loads (e.g. EVs), industry/agricultural/commercial loads as applicable to the grid template.
- **Forecasted controllable load of P2H facilities (buildings)**: this corresponds to the intended/forecasted load of the power-to-heat equipped buildings if no grid service provision was required. This will encapsulate human/occupant behaviour and preferences as well as building amenities/equipment.

These last two load models constitute the total load on the grid and they are separated this way to enable the independent modelling of the controllable and uncontrollable loads in the PLANET context. The grid simulator performs a baseline simulation whereby the time profile of energy flows on grid nodes is analysed using power-flow calculations and potential grid issues (congestion, instability and unbalance) are identified and quantified (C).

2.5.2. Step 2: system simulation and imbalance identification

The information about grid problems is returned from the simulation environment to the IDOC detailing potential imbalances on individual grid nodes/strings. Based on this information, the IDOC generates a request for service delivery by the "flexibility providers" who control storage/conversion facilities on the network topology. This request can be structured upon the template of the FlexRequest of the Universal Smart Energy Framework (USEF) [6] including extensions to incorporate other services additional to the active power flexibility currently covered by USEF.

2.5.3. Step 3: flexibility dispatch optimization

The SCCE module analyses the service request of the IDOC (E) and performs a two-step optimization approach. Initially, the demand flexibility of the power-to-heat is queried from the building-level coordinating modules to establish the amount of services that can be offered (F). Based on the collected information (G), the optimiser performs a fast estimation about remaining service needs and instantiates/allocates power-to-gas units to the grid topology in order to cover the DSO needs entirely. This optimal allocation takes into account a number of relevant constraints, like gas grid proximity, CO_2 availability, proximity to sensitive electricity node (especially important to suppress frequency problems), and so on.

2.5.4. Step 4: real-time monitoring and iterative "on-the-loop" optimization

After the final allocation and usage of P2H and P2G systems is finalised, and it is compliant to the IDOC service request, the optimiser generates the necessary control signals (in function of time to match the service request time schedule) for these systems so that during operation/simulation they offer exactly the required grid services (D, H). The simulation testbed will be updated accordingly, and the IDOC will launch a second simulation round to validate grid stability and balance. During this simulation run, all the simulation models instantiated during initialization and the previous step provide their expected electrical behaviour to the grid so that the new power flow calculations verify that grid problems have been alleviated using these services.

The aforementioned steps largely correspond to standard grid operation planning activities that transcend current energy market/network operations. They are typically performed both day-ahead (based on supply and load forecast models to resolve expected grid imbalances) as well as intra-day (based on the actual demand and supply encountered by the grid to resolve imbalance and/or instability) to counter planning inadequacies in real-time. This incremental grid optimization that is commonplace in grid operations is also inherently supported by the PLANET ICT solution via repetition of the step sequence.

2.6. Market analysis and policy implications

Storage/conversion technologies and dispersed energy generators call for a deep rethinking of current regulatory instruments used to encourage the widespread deployment of green energy generation means. The new policy design must have clear targets and objectives that mix policy solutions to stimulate innovation, environmental sustainability and energy efficiency and provide societal benefits by encouraging unbiased technology deployment, based

purely on merits and benefits. Should VES prove technically efficient and cost-effective in mitigating the problems of VRES, policy makers will face significant challenges to design adequate regulatory instruments to incentivise the improvement of the building stock for VES proliferation. The pricing methods and, therefore, the remuneration of DSOs in the presence of demand flexibility is currently a hotly contested topic in the current regulatory debate, but its financial benefits for building owners are expected to be too small to mobilise capital investments. Converting power to gas, on the other hand, effectively shifts the massive decentralised energy generation paradigm from the electricity grid to the gas grid, where it is currently very limited. Policy makers should revisit existing instruments, such as feed-in tariffs for electricity, in light of this shift and investigate whether they should incentivise green electricity generation, carbon-free gas generation or both. Another market/policy side effect of conversion technologies is that they close the loop between the electricity and the natural gas grids and markets. Gas to electricity conversion has long been available, gas-fired plants are widespread.

The emerging ability to purchase electricity and transform it to gas to be sold on the market enables two-way transactions. The relative price of energy carriers (and their volatilities), the conversion efficiency and potential supply security issues are critical factors on how conversion outputs can be used in the energy markets; the structure of the respective markets needs to be examined to verify that they can enforce prevailing regulations given this new capability. Securing funding for policy implementation is another major aspect. There is a stark contrast between the investment structure for grid expansion and storage/conversion system deployment in the grid. The former are financed using funds (indirectly through electricity bills) mostly defined by regulatory bodies since electricity grids provide public utility service. The latter would likely be deployed by private companies through market mechanisms and therefore for profit. Deferred investments on public money cannot directly fund private ventures without skewing competition and violating EU legislation.

To overcome such issues, PLANET will investigate alternative market models/structures as well as regulatory policies for maximising social welfare. It will design and propose a coherent reform recommendation package touching upon both the energy market structure and the necessary regulatory policy instruments to achieve a decarbonised energy system by 2050. The objective of this package will focus on the market integration of VRES generation and storage/conversion technology under fair terms with the ultimate goal to support achievement of the Energy Union targets. This activity will be complemented by an investigation of extensions to market roles and business models that will be required to facilitate the commercial exploitation of the conversion/technology.

3. Results and outlook

The project is at a beginning state, and this means that the consortium is actually working on the elaboration of the potential business cases for the deployment of energy conversion/storage technologies in the European grids, on the investigation of necessary business roles for the successful proliferation of technologies and in identification of PLANET system requirements as an initial step for implementation.

The successful deployment of the global and local level coordination system for power-to-heat and power-to-gas resources depends on seamless information exchange between all actors. This task aims to define the requirements for effective communication and grid interfaces throughout the various system architecture layers to ensure that all necessary information is properly collected and transmitted.

The functional behaviour of the entire system will be finalised and decomposed into the component/module functionalities. Detailed functional decomposition and sequence diagrams will be developed to ensure full interoperability between components. Information exchange and interfaces among (and within functionalities of) components/modules as well as to the outside world will be defined.

Another purpose is to set the requirements and targets that power-to-gas/heat systems should meet so that their decentralised deployment becomes a viable value and business proposition in the future energy systems is fulfilled. PLANET will utilise controllable conversion/storage as flexibility sources for grid balance and stability. To simulate and validate this claim, models of uncontrollable source of electricity demand and supply must be developed as well as projections of heat, gas demand and supply. This to produce the necessary models for energy supply—including conventional generation and variable RES—and uncontrollable demand forecasting in the future energy system scenarios.

4. Conclusions

During the project, PLANET will be also in charge to move the application of the decision support system from a specific network topology towards a more generic network topology. Flexibility in the instantiation of network topologies, selection of conversion and storage options as well as other available infrastructure will ensure the applicability of the tool to very diverse environments and situations that reflect the particularities of grids across Europe. In terms of socio-economics, the ultimate aim of the DSS deployment in real-life scenarios brings opportunities for the further integration of RES-E generation on the electricity grid as well as feeding the gas and heat networks from their oversupply. Long-term side effects of this may include the cost reduction of energy (regardless of carrier), increased security of supply since all generation will be local as well as a significant improvement of social welfare as a direct consequence of these.

Renewable energy sources hold the promise to decarbonise the entire system, including the electricity, heating, gas and transport systems with the use of appropriate conversion and storage technologies. Optimal use of the latter becomes critical in order to achieve the ambitious EU policy objectives of the Energy Union. The PLANET solution will comprise a valuable tool in the arsenal of policy makers and network planners for the coordinated design of networks and compatible policy instruments for the stimulation of the most appropriate technology deployments that can achieve the aforementioned objectives.

Since the annual expected curtailment of solar and onshore wind sources is expected to grow significantly from 29 TWh of electricity in 2030 to 217 TWh curtailed in 2050, the distribution grid should be modified to operate with a higher degree of flexibility. Flexibility sources are required not only for balancing demand and supply, but also for enhancing stability and

reliability through voltage/frequency regulation and other ancillary services. Key requirements to achieve proper grid operation include smarter energy grids and enhanced flexibility provided by a wide range of technologies and solutions, such as energy storage, energy conversion and network interconnection, along with demand response.

These solutions will permit a lower use of curtailments, increasing the benefits of RES on the environment. The impact of PLANET outcomes of market transformation will be multifold: initially, the deployment of conversion and storage solutions can reduce the impact of RES generation unpredictability of existing wholesale markets and can relax the necessity for real-time markets giving time to policy makers and the energy system to respond to the new grid challenges. Furthermore, PLANET will provide solutions to encourage and stimulate self-consumption of locally produced electricity in order to isolate intermittency before it becomes a grid problem through a novel human-centric virtual energy storage system that transforms conventional heating/cooling systems into flexible energy resources that respond to local generation or market/grid conditions. The same solution can also become an enabler for the active participation of buildings in energy markets through energy cost optimization or even service provision for grid or energy balancing.

Finally, PLANET facilitates the absorption of electricity exceeding demand from intermittent RES through conversion to alternative energy carriers, such as natural gas or heat/cold, and injection in the respective distribution networks for short-term or even seasonal storage. The PLANET tools enable market actors and regulators to optimally plan, install, commission and dispatch energy conversion units along the electricity distribution grid in order to ensure maximum absorption of excess RES generation and immediate consumption or conversion into alternative carriers.

Acknowledgements

This project has received funding from the European Union's Horizon 2020 research programme under Grant Agreement No. 773839.

Author details

Andrea Schröder[1]*, Christoph Kahlen[1], Mariapia Martino[2] and Antonis Papanikolaou[3]

*Address all correspondence to: andrea.schroeder@fgh-ma.de

1 FGH e.V, Mannheim, Germany

2 Politecnico di Torino, Turin, Italy

3 Hypertech, Athens, Greece

References

[1] European Commission. Energy Roadmap 2050. Publications Office of the European Union. 2012. DOI: 10.2833/10759

[2] European Commission. 2050 Low-Carbon Economy [Internet]. Available from: https://ec.europa.eu/clima/policies/strategies/2050_en#tab-0-0 [Accessed: April 10, 2018]

[3] Weiss R et al. Optimal scheduling of a P2G plant in dynamic power, regulation and gas markets. In: 10th International Renewable Energy Storage Conference (IRES 2016); Düsseldorf, Germany; 2016

[4] CEN-CENELEC-ETSI Smart Grid Coordination Group (SG-CG). CEN-CENELEC-ETSI Smart Grid Coordination Group—Framework Document. November 2012. Available from: ftp://ftp.cen.eu/EN/EuropeanStandardization/HotTopics/SmartGrids/Framework%20Document.pdf [Accessed: April 25, 2018]

[5] Allegrini J, Orehounig K, Mavromatidis G, Ruesch F, Dorer V, Evins R. A review of modelling approaches and tools for the simulation of district-scale energy systems. Renewable and Sustainable Energy Reviews. 2015;**52**:1391-1404

[6] Papanikolaou A, Malavazos C, Broekmans M, van den Berge M, Derksen B. Flexibility provision in the Smart Grid era using USEF and OS4ES. In: IEEE International Energy Conference (ENERGYCON); Leuven, Belgium; 2016

Edited by Majid Nayeripour, Eberhard Waffenschmidt and Mostafa Kheshti

Public support and feed-in tariff as a nonvariable compensation for the electric power production of energy have suppressed the risky investment of distributed generators (DGs) in smart distribution systems (SDSs). Although the using renewable energy technologies and the incorporation of plug-in DGs into SDS may have positive effects on congestion management, power loss reduction, and sustainability, they may create some difficulties relating to manage the system optimally by considering the intermittency of renewable resources in power production and uncertainties. Many researches have been carried out to deliver the high-quality power to the end-users with acceptable reliability. This book aims to present the recent materials related to the smart microgrids and the management of intermittent renewable energy sources that organized into seven chapters.

Published in London, UK

IntechOpen

ISBN 978-1-83881-653-7